UNIVERSITÀ DI PARMA

UNIVERSITA' DEGLI STUDI DI PARMA

DOTTORATO DI RICERCA IN
"Scienze Mediche e Chirurgiche Traslazionali"

CICLO XXXIV

New therapeutic approaches for the treatment of malignant pleural mesothelioma

Coordinatore:
Chiar.mo Prof. Nicola Sverzellati

Tutor:
Chiar.ma Prof.ssa Roberta Alfieri

Dottoranda: Rita Terenziani

Anni Accademici 2018/2019-2020/2021

A mio nonno Vittorino

Abstract

Malignant pleural mesothelioma (MPM) is an aggressive malignancy of the pleura, characterized by poor prognosis. The current therapeutic actions against this disease are limited due to the late stage at which most patients are diagnosed and to the intrinsic chemo-resistance of the tumor. Currently, the recommended systemic therapy for MPM is cisplatin/pemetrexed. Following the results of the CheckMate 743 study, the combination of nivolumab with ipilimumab has been recently approved by FDA as first line treatment in patients with unresectable MPM. However, the prognosis remains poor with a mean overall survival of about 12-14 months for patients treated with chemotherapy and around 18 months for those treated with immunotherapy. Therefore, novel therapeutic approaches are urgently needed. Carcinogenesis of MPM is predominantly associated with loss of *CDKN2A/ARF*, a tumor suppressor gene encoding for the cell cycle inhibitors $p16^{INK4a}$ and $p14^{ARF}$. In particular, $p16^{INK4a}$ by inhibiting the CDK4/6-cyclin D1 complex prevents Rb release from the E2F transcription factor. Therefore, *CDKN2A/ARF* loss drives cell cycle progression through the upregulation of the Rb/E2F/myc pathway.

This study aims to investigate new therapeutic approaches for the treatment of MPM, based on targeted therapy with CDK4/6 inhibitors (palbociclib and abemaciclib). First of all, this study investigates the effects of the CDK4/6 inhibitor palbociclib in association with PI3K inhibitors (NVP-BEZ235 or NVP-BYL719) on glucose metabolism in human MPM cell lines. In this case, palbociclib combined with PI3K inhibitors (NVP-BEZ235 or NVP-BYL719) significantly reduces both glycolytic activity and mitochondrial respiration compared to the treatments with drugs used alone in MPM cell lines. Moreover, the combined treatment

(palbociclib in association with NVP-BEZ235 or NVP-BYL719) prevents the glucose consumption in both normoxia and hypoxia. In addition, a strong reduction of glucose uptake is observed in MPM cells treated with palbociclib combined with NVP-BEZ235 in hypoxia. In fact, the expression of GLUT-1 is strongly reduced by the association of palbociclib with NVP-BEZ235 or NVP-BYL719 in MPM cell lines in hypoxia.

Subsequently, this study aims to evaluate the efficacy of the CDK4/6 inhibitor abemaciclib in combination with the standard chemotherapy used as first line treatment in MPM patients, using different schedules of treatment (simultaneous or sequential). The simultaneous treatment of abemaciclib combined with cisplatin and pemetrexed has a greater antiproliferative effect than the combination of cisplatin with pemetrexed in MPM cell lines. Moreover, this simultaneous treatment shows cytostatic effects in MSTO-211H cells, causing senescence. By contrast, an autophagic cell death is observed in H28 cells treated with abemaciclib in association with cisplatin and pemetrexed. Interestingly, the effect of such a combination is irreversible, and after drug withdrawal, we fail to observe a resumption in tumor cell proliferation.

Finally, this study for the first time investigates the anticancer effects of a new molecule, called VS2-370, a double inhibitor of CDK4/6 and CDK9, in MPM cell lines. VS2-370 is more potent in inhibiting cell proliferation respect to approved CDK4/6 inhibitors and its efficacy is associated with cell death induction via MCL-1 downregulation.

Taken together, these data suggest that a therapeutic strategy, based on target therapy, may represent a new therapeutic option for the treatment of MPM.

1. Introduction

1.1 Malignant pleural mesothelioma

Malignant mesotheliomas (MMs) are rare tumors of the mesothelial cells lining the pleura, peritoneum, pericardium and tunica vaginalis. Most cases of MMs are represented by malignant pleural mesothelioma (MPM) developing from the pleura (Delgermaa V. et al., 2011). MPM has three histologic subtypes: epithelioid, sarcomatoid and biphasic (Fig 1). Morphologically, MPM subtypes are identified by standard hematoxylin-eosin staining. About 50 to 70 % of MPM patients have the epitheliod subtype (Bonelli M. A. et al., 2017), characterized by polyhedral shaped cells (Beasley M. B. et al., 2021). Recently, the epitheliod subtype is further classified on the basis of architectural, cytologic and stromal characteristics (Nicholson A.G. et al., 2020; Beasley M. B. et al., 2021). The sarcomatoid subtype is diagnosed in approximately 10-15% of MPM patients (Odisio E. G. et al., 2017) and it is characterized by spindle cells with nuclear atypia, areas of necrosis and aberrant mitosis (Beasley M. B. et al., 2021). Due to its morphological heterogeneity, the sarcomatoid subtype has a variant called desmoplastic mesothelioma and two cytologic features: pleomorphic and transitional (Beasley M. B. et al., 2021). 20 to 35% of MPM cases are represented by the biphasic subtype, having both epithelial and sarcomatoid features (Bonelli M. A. et al., 2017).

The MPM histologic classification has prognostic value: 12-27 months for the biphasic subtype, showing the longest survival; 7-18 months for the sarcomatoid subtype, having the shortest survival and finally 8-21 months for the biphasic subtype (Yap T. A. et al., 2017).

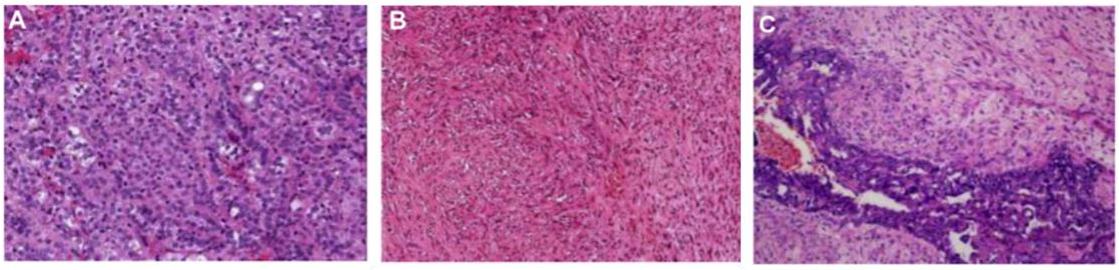

Figure 1. Histological subtypes of MPM: epithelioid (A), sarcomatoid (B) and biphasic (C). (Nicholson A.G. et al., 2020).

MPM patients show nonspecific signs and symptoms, depending on tumor progression (Huang Y. P. et al., 2020). At diagnosis, MPM patients usually have pleural effusion, shortness of breath and chest pain, as the main clinical symptoms (Odisio E. G. et al., 2017).

The imaging modalities usually used for MPM diagnosis, staging and treatment planning are: chest radiography, computed tomography (CT), positron emission tomography (PET/CT) and magnetic resonance imaging (MRI) (Odisio E.G. et al., 2017; Kindler H. L. et al., 2018; Carbone M. et al., 2019). Chest radiography identifies abnormalities affecting the pleura. Chest and upper abdomen CT, with intravenous contrast, is the standard imaging tool, showing the extent of the tumor, the enlargement of the hilar and mediastinal nodes and the presence of mestastasis (Kindler H. L. et al., 2018; Carbone M. et al., 2019). PET/CT, with intravenous administration of the fluorodeoxyglucose (FDG), is a complementary test to CT for differentiating benign from malignant pleural diseases and for identifing metastasis (Kindler H. L. et al., 2018). Both CT and PET/CT can be used to assess tumor response after therapy (Odisio E.G. et al., 2017; Kindler H. L. et al., 2018). Thoracic MRI, with intravenous contrast, is used only in specific

MPM cases that need a more detailed evaluation to complete the information obtained with CT (Odisio E.G. et al., 2017).

These imaging tools may be associated with some invasive techniques as, thorascopy, mediastinoscopy, laparoscopy and endobronchial ultrasound in order to provide detailed features for MPM staging (Kindler H. L. et al., 2018).

The staging system for MPM, based on TNM descriptors, was born in the mid-90s due to the rarity of the tumor, the difficult of diagnosis and the lack of clinical data (Euhus C. J. Et al., 2020). In 2016, the International Association for the Study of Lung Cancer (IASLC) published the eighth edition of staging system for MPM based exclusively on data obtained from MPM patients (Pass H., et al., 2016).

1.2 Risk factors associated with malignant pleural mesothelioma

The correlation between MPM and asbestos is well documented. Inhalation of asbestos fibers represents one of the major risk factors for the development of MPM (Fig. 2). A group of six silicate minerals, including both the serpentine class (chrysolite) and the amphibole class (riebeckite, grunerite, anthophyllite, tremolite and actinolite) subjected to regulatory control due to their carcinogenic properties, is called asbestos. In fact, tumors of the pleura, lung, ovary and larynx are asbestos related (Fazzo L. et al., 2018). All forms of asbestos are classified as occupational carcinogens. However, there is also environmental exposure to asbestos, which is also related to the development of cancers (Carbone M. et al., 2019).

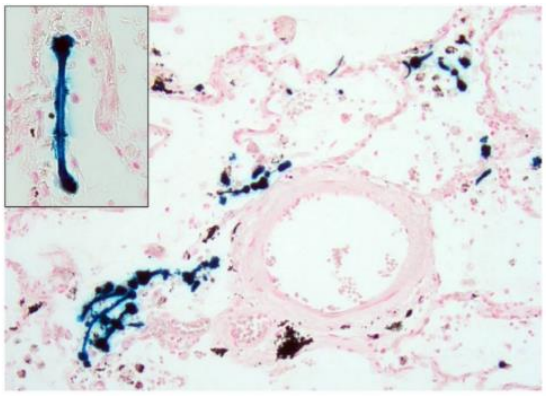

Figure 2. Human MPM biopsy shows asbestos fibers in the lung alveoli (Carbone M. et al., 2019).

Other natural minerals, called NOA (naturally occurring asbestos), are: erionite, fluoro-edenite, winchite, antigorite and richterite (Baumann F. et al., 2013). This group of minerals is not currently regulated and it is not included in the group called asbestos (Yap T. A. et al, 2017). However, erionite and fluoro-edenite are recognized as carcinogens. Erionite is considered to be responsible for the

mesothelioma epidemic in the Cappadocia region of Turkey (Carbone M. et al., 2019). An Italian study first shows the development of MPM and peritoneal mesothelioma after local administration into the pleura and peritoneum of fluoro-edenite fibers in rats (Soffritti M. et al., 2004).

The role of the simian virus 40 (SV40), a DNA polyomavirus of rhesus monkey, in developing human cancers, including MPM, is still controversial (Attanoos R. L. et al., 2018; Carbone M. et al., 2020). In the last century, many stocks of human poliovaccines were contaminated with SV40 all over the world, causing accidental human exposure to the virus (Carbone M. et al, 2020). In fact, Sabin's and Salk's vaccines were prepared by growing the poliovirus in rhesus monkey kidney cell cultures (Carbone M. et al, 2020). Although it is difficult to establish a correlation between the administration of the vaccine containing the virus and the development of human tumors, SV40 is considered a carcinogenic virus. The oncogenic effects of SV40 are caused by the SV40 Tag protein, which inactivates proteins involved in the cell cycle regulation (Carbone M. et al., 1997; De Luca A. et al., 1997). Several studies in rodents show that SV40 causes cancer at the injection site, including MPM (Cicala C. et al., 1993). Subsequently, another study observed the development of mesothelioma in both rodents and human mesothelial cells exposed simultaneously to asbestos and SV40 (Kroczynska B. et al., 2006). SV40 DNA sequences have been found in some brain tumors (Bergsagel D. J. et al., 1992), in some osteosarcomas (Carbone M. et al., 1996) and in MPM (Carbone M. et al., 1994), showing a possible role of the virus in developing of certain types of human cancers. Based on these results, SV40 can be considered an exogenous risk factor for the development of MPM. On the other hand, some studies show that in some human brain tumors (Engels E. A.

et al., 2002) and in some forms of human mesothelioma (Lòpez-Rìos F. et al., 2004) the presence of SV40 DNA sequences is not detected. Further investigation is needed to determine the correlation between SV40 and human tumors.

Germline mutations of tumor suppressor genes can cause a hereditary predisposition for the development of various types of cancer, including mesotheliomas (Pastorino S. et a., 2018). One of the most studied tumor suppressor genes is *BAP1*, involved in the regulation of DNA repair and replication, cell death and metabolism (Carbone M. et al., 2020). Heterozygous germline-inactivating mutations of *BAP1* gene caused “BAP1 cancer syndrome” that predisposes to the development of some tumors, including mesothelioma (Carbone M. et al., 2012). Exposure to carcinogenic fibers, including asbestos, increases the incidence of mesothelioma in case of *BAP1* mutations. In fact, the mesothelioma epidemic in Cappadocia is also caused by the presence of *BAP1* germline mutations in the population, showing a strong correlation between exposure to erionite and inactivation of *BAP1* (Roushdy-Hammady I. et al., 2001). A few years later, a study shows that exposure to asbestos causes mesothelioma in $BAP1^{+/-}$ mice while unexposed $BAP1^{+/-}$ mice do not develop tumor (Xu J. et al., 2014). Subsequently, in another study $BAP1^{+/-}$ mice developed mesothelioma after exposure to low levels of asbestos, while very high doses of asbestos caused mesothelioma in *BAP1* wild-type mice (Napolitano A. et al., 2016).

All forms of mesothelioma, including MPM, can also be caused by radiotherapy used for the treatment of various types of cancer (Attanoos R. L. et al., 2018).

1.3 Epidemiology of malignant pleural mesothelioma in Italy

Asbestos played an important role in the industrialization of Italy for most of the twentieth century, due to its chemical-physical properties. On the other hand, the health effects caused by chronic exposure to asbestos had a strong impact on the Italian population.

In the Piedmont region, there were the chrysotile quarry in Balangero and the manufacturing industry for the processing of asbestos in Casale Monferrato. The quarry was used from about 1917 to 1990 and the factory, called Eternit, was active from 1907 to 1985 (Comba P. et al., 2018). Asbestos affected both those who worked this mineral and those who lived in the areas of its extraction and processing.

The first epidemiological study on asbestos-related tumors begins in 1986 and covers the period from 1950 to 2003, involving 3434 workers from the Eternit industry, including 777 women (Comba P. et al., 2018). 497 deaths occurred between 1965 and 2003 and from 1990 to 2003 there were 49 cases of MPM and 23 cases of peritoneal mesothelioma. Subsequently, a study of 1780 married women to asbestos workers showed 146 cases of malignant tumors, including 21 cases of MPM, between 1965 and 2003 (Ferrante D. et al., 2007). From the mid-80s of the last century, several studies were conducted in Casale Monferrato to measure the concentration of asbestos in various points of the city and to identify mineral fibers (Comba P. et al., 2018). In 1984, the first study shows asbestos fibers at a concentration between 0.4 and 19.1 f/l (fiber counts per litre) and the mineral fiber was crysolite (15 to 30%) (Marconi A. et al., 1989). Since 1999 the concentration of asbestos fibers has been monitored regularly both in Casale

Monferrato and in the nearby areas. The current mean concentration of asbestos is lower than 0.2 f/l, showing a progressive decrease (Comba P. et al., 2018).

Epidemiological studies in Casale Monferrato have highlighted for the first time the correlation between asbestos and MPM in Italy. Since 1992, Italy has prohibited the extraction, processing and use of asbestos (Marsili D. et al., 2017). However, the effects of asbestos on cancer development are currently present due to the long latency period (30 to 40 years). For example, 121 cases of MPM occurred in Casale Monferrato from 2010 to 2014 (Comba P. et al., 2018). Moreover, since 2002 a system of epidemiological surveillance of MPM called ReNaM (Registro Nazionale dei Mesoteliomi) has been organized in Italy.

The Piedmont region is not the only one to be severely affected by asbestos-related cancers. In fact, in the Lombardy region, an asbestos processing industry was active from 1932 until 1993 in the city of Broni. Mortality from MPM in Broni is currently 20-fold higher than in the entire Lombardy region (Comba P. et al., 2017). The Sicily region is also affected by a high mortality from MPM due to a fluoro-edenite quarry near the city of Biancavilla (Comba P. et al., 2003). An epidemiological study, collecting 26 cases of MPM (13 men and 13 women) from 1998 to 2011, shows an incidence of this tumor 20-fold higher in patients under 50 than in the entire region (Bruno C. et al., 2014).

Asbestos has been used in various working sector, thus exposing also other workers to the risk of cancer. For example, 70% of mesothelioma cases were caused by occupational exposure in the region of Friuli Venezia Giulia, between 1995 and 2015 and the highest number of cases occurred among shipbuilders (D'Agostin F. et al., 2017). In the Lazio region, data from 2001 to 2009 show that 54% of pleura and peritoneum mesothelioma cases are caused by occupational

exposure and construction workers are the most affected (Romeo E. et al., 2013). Also in the Puglia region, 178 cases of mesothelioma (96,06 % MPM) occurred between 1993 and 2018 and all are men employed in the construction (Vimercati L. et al., 2019).

The latest report on MPM mortality in Italy, collecting data from 2003 to 2014, shows 13051 deaths of which 9397 men and 3654 women (Comba P. et al., 2018). In Italy, an increase of about 7000 cases of MPM is expected from 2020 to 2024 (Oddone E. et al., 2020).

1.4 The mechanisms of asbestos carcinogenesis

The deposition of asbestos and other mineral fibers in the pleura causes a chronic inflammatory process, leading to MPM development after 30-40 years. Inflammation, considered a hallmark of asbestos-related cancers, is caused by the high mobility group box 1 (HMGB1) protein and the nod-like receptor family member containing a pyrin domain 3 (Nalp3) inflammosome (Carbone M. et al., 2012).

Asbestos exposure induces apoptosis (Broaddus V. C. et al., 1996; Jiménez L. A. et al., 1997) and programmed necrosis (Yang H. et al., 2010) in rabbit, rat and human mesothelial cells. HMGB1 protein, released by necrotic mesothelial cells, is involved in both the chronic inflammatory process (Yang H. et al., 2010) and the MPM progression (Jube S. et al., 2012). In physiological conditions, HMGB1 is a nuclear protein acting as a DNA chaperone (Bianchi M. E. et al., 2017). In response to cellular stress, HMGB1 acts as a damage-associated molecular pattern (DAMP), having a key role in inflammation and tissue repair (Bianchi M. E. et al., 2017). In MPM, secreted HMGB1 favors the formation of a tumor microenvironment, causing the recruitment and activation of macrophages that release mutagenic molecules: reactive oxygen (ROS) and nitrogen (iNOS) species, both involved in the mesothelial cells' transformation (Choe N. et al., 1998; Xu A. et al., 2007). Moreover, macrophages also release TNF-α, involved in both the inflammatory process and the carcinogenesis process. In fact, a study showed that TNF-α induced cell survival by activating NF-kB pathway, having a critical role for asbestos carcinogenesis (Yang H. et al., 2006). In epithelioid MPM, the high percentage of M2 macrophages in the tumor microenvironment correlates with a worse prognosis (Cornelissen R. et al., 2014).

Recently, a preclinical study shows that HMGB1 induces autophagy in mesothelial cells due to exposure to asbestos, highlighting another possible mechanism of carcinogenesis (Xue J. et al., 2020). In this case, autophagy could protect cells from asbestos cytotoxicity, promoting the proliferation of mesothelial cells with damaged DNA and the development of MPM (Xue J. et al., 2020).

HMGB1 protein also causes the activation of Nalp3 inflammosome, which in turn releases IL-1β, favoring chronic inflammation in asbestos-related diseases (Cassel S. L. et al., 2008; Dostert C et al., 2008).

1.5 Genomic background of malignant pleural mesothelioma

Carcinogenesis is due to the accumulation of genetic aberrations that favor neoplastic transformation. The study of the genomic background of a tumor aims to understand the biological processes of the tumor in order to identify possible therapeutic targets.

Recently, a genomic study of 74 MPM patients confirms that MPM development is mainly characterized by loss of tumor suppressor genes (Hmeljak J. et al., 2018). The most common loss of function aberrations in MPM involve the *CDKN2A/ARF* locus, the *BAP1* (BRCA1-associated protein 1) gene and the *NF2* (neurofibromatosis type 2) gene.

The *CDKN2A/ARF* gene encodes for two tumor suppressor proteins involved in the cell cycle regulation: $p16^{INK4A}$ and $p14^{ARF}$. *Cdkn2a* and *arf* genes are transcribed by alternative reading frame, having each their own promoter and a different first exon (Ruas M. et al., 1998). $p16^{INK4A}$ binds to CDK4/6, avoiding the formation of the cyclin D-CDK4/6 complexes. As a result, retinoblastoma protein (Rb) is not phosphorylated and the cell remains in the G1 phase of the cell cycle. $p14^{ARF}$ binds mouse double minute 2 protein (MDM2), avoiding the degradation of p53. Hence, the loss of the *CDKN2A/ARF* locus causes both the progression of the cell cycle and the lack of apoptosis, resulting in the immortalization of the cell. Deletions of *CDKN2A/ARF* gene are observed in approximately 70% and 100% of MPM cases, respectively with epithelioid and sarcomatoid histotype (Sekido Y., 2013). A recent study shows that 49% of MPM patients lost both copies of *CDKN2A* gene and 7% had only one copy while a co-deletion of *CDKN2A* and *MTAP* is observed in 27 % of samples (Hmeljak J. et al., 2018). In fact, *MTAP* gene is adjacent to the *CDKN2A/ARF* locus and it encodes

methylthioadenosine phosphorylase (MTAP), an enzyme that cleaves methylthioadenosine (MTA) to generate precursors acting as substrates for methionine and adenine pathways. Consequently, the loss of *MTAP* gene impairs the metabolism of methionine and adenine (Kryukov G. V. et al.,2016). MTAP is deleted in other tumors, including melanomas, pancreatic adenocarcinomas, urothelial carcinomas, glioblastomas and non-small cell lung carcinomas (Cerami E. et al., 2012).

BAP1 protein belongs to the deubiquitylase family of enzymes (Carbone M. et al., 2020). In fact, BAP1 removes ubiquitin tags from various types of cytoplasmic and nuclear proteins, with an ubiquitin carboxy-terminal hydrolase domain (Cakiroglu E. et al., 2020). In the nucleus, BAP1 has an important role during DNA synthesis under both physiological and stress conditions, interacting with the INO80 chromatin-remodeling complex (Lee H. S. et al., 2014; Lee H. S. et al., 2019). Furthermore, BAP1 regulates cell growth by deubiquitylating HCF-1 (host cell factor-1), a cell cycle regulator (Machida Y. J. et al., 2009). Subsequently, an *in vitro* study shows that BAP1 forms a multiprotein complex with HCF-1 and the transcription factor Yin Yang 1 (YY1), regulating the activity of genes involved in many cellular processes (Yu H. et al., 2010). BAP1 also induces double-strand DNA repair, favoring homologous recombination, in order to prevent DNA damage (Yu H. et al., 2014). In the cytoplasm, BAP1 regulates apoptosis by deubiquitylating the type 3 inositol-1,4,5 trisphosphate receptor (IP3R3), inducing the release of Ca^{2+} in the mitochondria (Bononi A. et al., 2017). A recently *in vitro* study shows that BAP1 also induces ferroptosis, a regulated form of non-apoptotic cell death induced by metabolic stress conditions (Zhang Y. et al., 2018). In fact, BAP1 causes a downregulation of the *SLC7A11* gene, encoding

for solute carrier family 7 member 11, an antiporter involved in the up-take of cystine. Consequently, the synthesis of reduced glutathione decreased, favoring ferroptosis (Zhang Y. et al., 2018). Therefore, *BAP1* acts as a tumor suppressor gene and it is deleted in many human cancers. Truncating *BAP1* germline mutations favor the development of various type of tumors such as, MPM, uveal and cutaneous melanoma (Carbone M. et al., 2012) and clear-cell renal cell carcinoma (cc-RCC) (Farley M. N. et al., 2013). In addition, somatic BAP1 mutations are involved in the development of many cancers, including MPM. In fact, uveal melanoma (45%), mesothelioma (60-70%), cc-RCC (15%), thymic carcinoma (13%), cholangiocarcinoma (7%), cutaneous melanoma (5%) and basal cell carcinoma (4%) show loss of *BAP1* (Carbone M. et al., 2020). A genomic study on MPM biopsies shows that loss of *BAP1* is mainly due to both larger deletions and point mutations (Nasu M. et al., 2015). In a recent study, 57% of MPM patients have somatic *BAP1* mutations (Hmeljak J. et al., 2018).

NF2 gene encodes merlin, a member of the ezrin/radixin/moesin (ERM) family proteins (Stamenkovic I. et al., 2010). Merlin is a multifunctional protein, having important role in cell motility, cell adhesion, cell proliferation and survival (Pećina-Šlaus N., 2013). In fact, merlin interacts with proteins involved in cytoskeletal dynamics and in cell-cell adhesion (Pećina-Šlaus N., 2013; Sato T. et al., 2018). Hence, the loss of merlin causes defects of adherens junctions (Lallemand D. et al., 2003) and the loss of contact inhibition of proliferation (Okada T. et al., 2005). Moreover, merlin regulates the mTOR and Hippo pathways, inhibiting cell proliferation (Pećina-Šlaus N., 2013; Sato T. et al., 2018). In the nucleus, merlin inhibits many pathways, causing the inactivation of oncogenes such as YAP/TAZ, c-myc, RAS and others (Sato T. et al., 2018). *NF2* acts as a tumor suppressor

gene (Pećina-Šlaus N., 2013; Sato T. et al., 2018). In fact, inactivating mutations of the *NF2* gene caused neurofibromatosis 2, a dominant familial cancer syndrome involved in the development of meningiomas, schwannomas (Ruttledge M. H. et al., 1994; Stemmer-Rachamimov A. O. et al., 1997), hamartoma and ependymomas (Pećina-Šlaus N., 2013). Somatic mutations of the *NF2* gene are well documented in MPM (Bianchi A. B. et al., 1995; Sekido Y. et al., 1995). Recently, a genomic study confirms that mutations of *NF2* gene are common in MPM patients: 34% of the samples showed deletions and 40% loss (Hmeljak J. et al., 2018).

Inactivating mutations of *LATS2* gene, *TRAF7* gene, *SETD2* and *SETDB1* gene have been identified in MPM. Other human cancers also have these genes inactivated, highlighting their role in tumor development. In fact, 25 % of meningiomas have *TRAF7* mutated (Zotti T. et al., 2017) and the inactivation of *SETD2* mainly occurs in cc-RCC (Li J. et al., 2016).

Large tumor suppressor 1, encoded by *LATS2* gene, is a member of the Hippo pathway involved in cell survival, proliferation, and differentiation (Ma S. et al., 2019). *TRAF7* gene encodes a multifunctional protein involved in many cellular processes such as, stress responses, apoptosis, the innate and acquired immune responses, cell growth and cell survival (Zotti T. et al., 2017). *SETD2* encodes an enzyme responsible for trimethylation of lysine 36 of Histone H3 (H3K36), involved in epigenetic modifications (Edmunds J. W. Et al., 2008). Finally, *SETDB1* gene encodes a methyltransferase that reversibly catalyzes the methylation of histone 3 (H3) K9 in euchromatic regions of chromosomes, inhibiting gene transcription (Strepkos D. et al., 2021). A study on MPM primary cell cultures shows 11% of the samples with *LATS2* mutations, consisting of

deletions and point mutations (Tranchant R. et al., 2017). Moreover, 8% of the MPM samples have mutations in both *LATS2* and *NF2*, showing a dysregulation of the Hippo signaling pathway (Tranchant R. et al., 2017). Genetic analysis of cells from pleural effusion of MPM patients show the loss of *TRAF7* gene, *LATS2* gene and *SETD2* gene respectively in 66%, 59% and 48% of the samples (Sneddon S. et al., 2018). Finally, a genomic study of a cohort of MPM samples identified a novel molecular subtype characterized by the association of *TP53* and *SETDB1* genes co-mutation (Hmeljak J. et al., 2018).

In addition, many genomic studies have identified epigenetic and non-coding RNAs aberrations involved in the pathogenesis of MPM (Hmeljak J. et al., 2018; Cakiroglu E.et al., 2020). These mutations can be a useful tool both in the diagnosis and in the development of new therapeutic approaches for MPM treatment.

1.6 Current therapeutic strategies for malignant pleural mesothelioma

MPM has limited therapeutic options based on chemotherapy, surgery and radiotherapy. Chemotherapy is the standard therapeutic approach used for MPM patients with unresectable tumor. The association of cisplatin and pemetrexed is the first-line chemotherapy approved for the treatment of MPM (Kindler H. L. et al., 2018). Bevacizumab, a VEGF antibody, can be combined with cisplatin and pemetrexed in MPM patients without cardiovascular comorbidities (Kindler H. L. et al., 2018). Carboplatin replaces cisplatin in case of intolerance (Kindler H. L. et al., 2018). In 2020, based on a open-label, randomised, multicentre phase III clinical trial, CheckMate 743 (NCT02899299), the US FDA (Food and Drug Administration) approved the association of nivolumab (anti-PD-1) with ipilimumab (anti-CTLA-4) as a first-line treatment for chemotherapy-naive MPM patients with unresectable tumor (Bass P. et al., 2021). This study shows that MPM patients treated with nivolumab+ipilimumab have an overall survival of about 18 months while 14 months of overall survival are reported for MPM patients treated with cisplatin+pemetexed. An approved second-line treatment option is still absent.

Cisplatin (cis-diamminedichloroplatinum) is one of the most widely used chemotherapy drugs for the treatment of various types of cancer, including MPM. Cells internalize cisplatin via the copper transporter Ctr1 (Ishida S. et al., 2002). Inside the cells, the water molecules in the cytoplasm replace the chlorides atoms on cisplatin. This electrophilic molecule binds nitrogen donor atoms on purine residue and the DNA structure becomes irreversibly damaged, resulting in cell death by apoptosis.

Cisplatin was first synthesized by Peyrone in 1844 and its chemical structure (Fig.3) was described a few decades later (Dasari S. et al., 2014). In the middle of the last century, a study showed that cisplatin inhibited cell division in *Escherichia Coli* (Rosenberg B. et al., 1965), becoming a good candidate for the treatment of tumors due to its cytotoxic properties. After several studies, the FDA approved cisplatin for the treatment of cancers in 1978 (Kelland L., 2007).

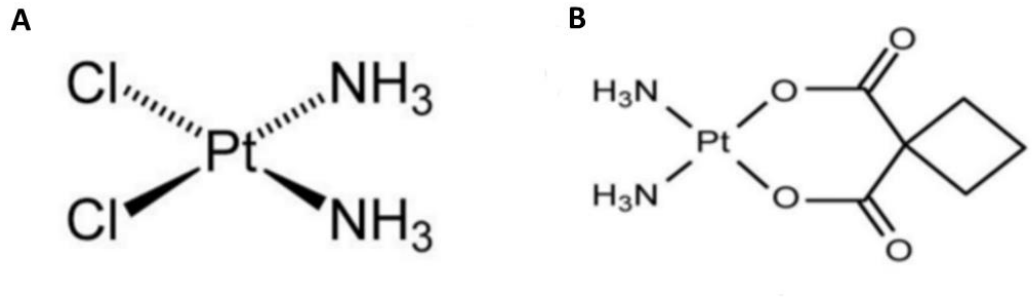

Figure 3. Molecular structure of cisplatin (A) and carboplatin (B) (Weiss R. B. et al., 1993).

Pemetrexed disodium ([ALIMTA®, "pemetrexed"], LY231514; Eli Lilly and Company; Indianapolis, IN) is a pyrrolo[2,3-d]pyrimidine-based antifolate (Fig.4), first discovered in 1992 (Taylor E. C. et al., 1992). This drugs is internalized by the cells through a reduced folate carrier. Subsequently it is polyglutamated by folylpolyglutamate synthase, inhibiting thymidylate synthase (TS), dihydrofolate reductase (DHFR) and aminoimidazole carboxamide ribonucleotide formyltransferase (AICARFT) (Grindey G. B. et al., 1992; Shih C. et al., 1996; Chen V. J. et al., 1996). Inhibition of TS disrupts DNA synthesis, due to a decrease of thymidine. Also, inhibition of DHFR and AICARFT, both involved in purine biosynthesis, interferes with DNA synthesis.

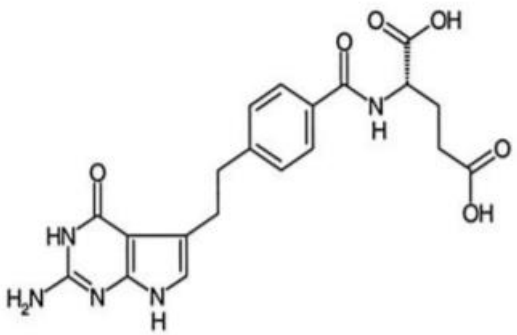

Figure 4. Molecular structure of pemetrexed (Hanauske A. R. et al., 2001).

Recently, some clinical trials have investigated new therapeutic approaches for the treatment of MPM, based on cisplatin and pemetrexed combined with molecules that target the tumor microenvironment. From 2016 to 2018, a phase III clinical trial, called LUME-Meso, evaluated the safety and efficacy of cisplatin and pemetrexed in association with nintedanib in MPM patients with epitelioid istotype (NCT01907100). This study showed a PFS of 6/8 months and 7 months in patients treated with nintedanib and those treated without, respectively (Scagliotti G. V. et al., 2019). Moreover, severe adverse events occurred more in patients treated with nintedanib than in patients treated with placebo (44% and 39%, respectively). Recently, a phase Ib clinical trial aimed to evaluate the safety of a molecule that blocks fibroblast growth factors (FGF_s) in association with cisplatin and pemetrexed in 36 MPM patients (NCT01868022). This study showed the efficacy and feasibility of this therapeutic approach, highlighting the possibility of further studies (van Brummelen E. M. J. et al., 2020).

Surgery and radiotherapy are always used in association with chemotherapy in a multimodality treatment regimen.

The surgical approach for MPM treatment is reserved for patients having early-stage tumor with epithelioid subtype and non-compromised cardiopulmonary

functions (Carbone M. et al., 2019). In this case, extrapleural pneumonectomy (EPP) and pleurectomy/decortication (P/D) aim to eliminate the tumor, having curative intent. EPP is the removal of the pleura, involving also the lung, pericardium and diaphragm. This surgical approach was replaced by P/D, involving only the pleura, or by extended PD (EPD), involving also pericardium and diaphragm, due to its very high mortality (Carbone M. et al., 2019). On the other hand, partial pleurectomy with pleurodesis is performed with palliative purpose (Carbone M. et al., 2019).

Radiation therapy is used before surgery or after surgery, depending on the type of tumor. In the first case, radiation therapy is a neoadjuvant treatment used to reduce the size of the tumor and facilitate the surgical approach. Radiation therapy after surgery, defined as adjuvant treatment, aims to avoid the formation of a tumor recurrence.

The radiotherapy approach is used for the treatment of MPM patients with a resectable tumor, mainly as hemithoracic adjuvant radiation therapy (Kindler H. L. et al., 2018). Moreover, radiotherapy can be used as a palliative treatment to reduce chest pain in MPM patients with symptoms (Kindler H. L. et al., 2018).

3-dimensional conformal radiation therapy (3D-CRT) and intensity-modulated radiation therapy (IMRT) are the two radiation therapy techniques used for the treatment of MPM (Kindler H. L. et al., 2018). 3D-CRT, based on the three-dimensional image of the tumor, releases a high dose of radiation towards the tumor tissue, reducing the radiation to healthy tissue. IMRT is a more recent radiotherapy technique, very similar to the previous one, used for the treatment of solid tumors with an unusual shape. Also in this case, the higher dose of

radiation affects the tumor tissue while healthy tissue receives a low intensity dose, decreasing side effects.

To date, the most effective therapeutic combination for MPM treatment has not yet been found as the data are controversial.

In 2007, a non-randomized clinical trial enrolled 21 MPM patients (95.2% with epithelioid phenotype and 4.8% with mixed phenotype) treated with trimodality therapy, consisting of induction chemotherapy (carboplatin/gemcitabine), EPP and adjuvant radiotherapy, in order to evaluate the feasibility and survival (Rea F. et al., 2007). Data showed 25.5 months of median survival and an overall 5-years survival rate of 19% (Rea F. et al., 2007).

In 2011, the Mesothelioma and Radical Surgery (MARS) feasibility study (ISRCTN95583524) aims to compare the clinical outcomes and survival of MPM patients treated with EPP and MPM patients treated without EPP in a multimodality treatment setting (Treasure T. et al., 2011). Data showed a median survival of 14.4 and 19.5 months for EPP patients and no-EPP patients, respectively. The EPP patients had serious adverse events, showing no benefit in surgical therapy (Treasure T. et al., 2011).

Some years later, a randomised phase II clinical trial (SAKK 17/04) aims to investigate the role of hemithoracic radiotherapy for the treatment of MPM in a multimodality therapy regimen (NCT00334594) (Stahel R. A. et al., 2015). In the first part of the clinical study, MPM patients were treated with neoadjuvant chemotherapy (cisplatin/pemetrexed) followed by extrapleural pneumonectomy, having total macroscopic resection of the tumor as primary endpoint. In this case, 64% of MPM patients achieved complete tumor resection. In the second part, patients with complete tumor resection were divided into two groups: some

patients received radiotherapy and others did not. In this case, locoregional relapse-free survival was the primary endpoint. 7.6 and 9.4 months were median locoregional relapse-free survival for MPM patients without radiotherapy and with radiotherapy, respectively. Data suggested no benefit for MPM patients treated with trimodality therapeutic approach.

A recently phase II clinical trial investigated a novel therapeutic approach for the treatment of MPM called surgery for mesothelioma after radiotherapy (SMART), having feasibility as the primary endpoint and 5-year cumulative incidence of distant recurrence as the secondary endpoint (NCT00797719). This study shows the feasibility of hemithoracic radiotherapy followed by extrapleural pneumonectomy for the treatment of MPM with long-term results (B. C. J. Cho et al., 2021).

1.7 The regulation of the mitotic cell cycle in somatic cells

Most of the cells of an adult individual are quiescent, being in phase G0. In fact, these cells are metabolically active without proliferating. Some cells, such as cardiomyocytes and neurons, are permanently in the G0 phase, while others, such as hematopoietic cells and epithelial cells, always cycle. When cells respond to mitogenic stimuli, they enter the cell cycle to generate two daughter cells with identical genomes (Fig.5). During the G1 (Gap1) phase, the first step of the cell cycle, cells synthesize proteins and enzymes necessary for the S phase, characterized by DNA synthesis. During the next G2 (Gap2) phase, cells check the integrity of the duplicated DNA and synthesizes molecules for mitosis, the last phase of the cell cycle. The M phase is characterized by the generation of two identical cells.

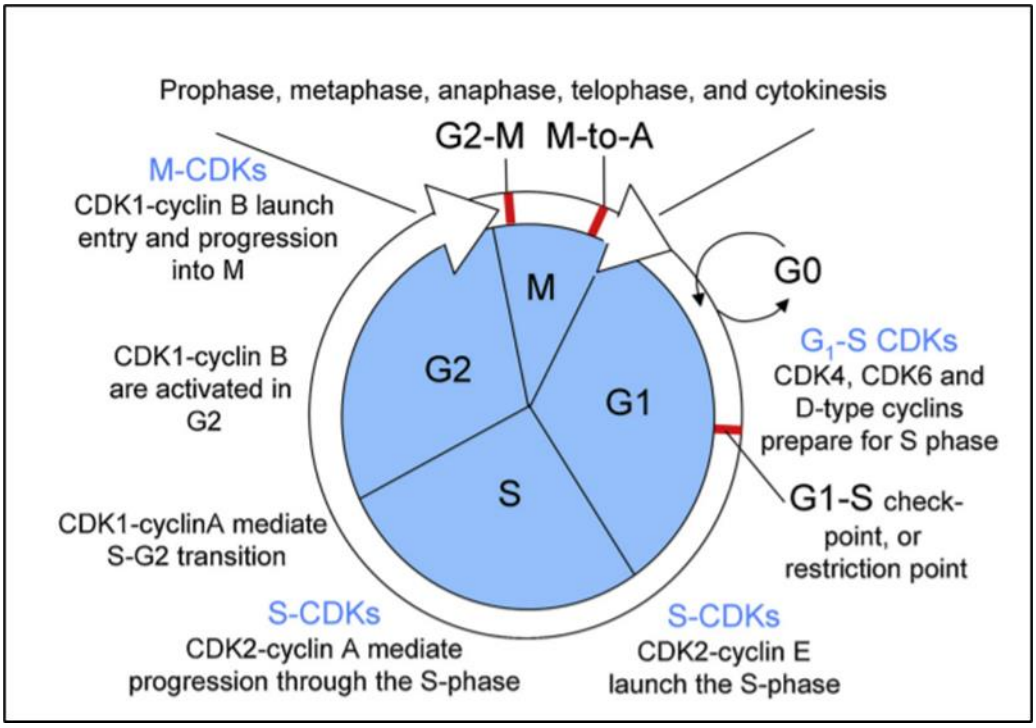

Figure 5. Cell cycle in somatic cells (Roskoski Jr R., 2018).

The cell cycle progression is regulated by cyclins and cyclin-dependent protein kinases (CDKs). About 29 proteins form the large family of cyclins, with 16 subfamilies and 3 main groups: group I, also called the cyclin B group, is composed of cyclins A, B, D, E, F, G and J; cyclin Y belongs to group II and finally the cyclins C, H, K, L and T form group III, also known as the cyclin C group (Ma Z. et al., 2013). In each phase of the cell cycle, cells express cyclins which are then degraded by process involving ubiquitin ligases (E3s) and proteasomes before moving on to the next phase (Nakayama K. I. et al., 2006). The 21 human CDKs are serine/threonine kinases, classified into three groups: regulators of the cell cycle (CDK1, CDK2, CDK4 and CDK6), regulators of gene transcription (CDK7, CDK8, CDK9, CDK 12, CDK13 and CDK19) and regulators of other cellular activities, including proteins with unknown function (CDK5, CDK10, CDK11, CDK14, CDK15, CDK16, CDK17, CDK18 and CDK20) (García-Reyes B. et al., 2018; Wood D. J. et al., 2018: Cassandri M. et al., 2020). Unlike cyclins, these enzymes do not vary during the phases of the cell cycle. In fact, cells express CDKs in their inactivated state throughout the cell cycle. The CDKs structure is characterized by two lobes with the catalytic site in-between (Malumbres M., 2014). The amino-terminal lobe is composed by β-sheets and α-helices characterized the carboxy-terminal lobe. When the CDKs are in their inactive state, the T-loop closes the catalytic site. The binding with cyclins causes a conformational change of the CDKs structure, making the catalytic site exposed to binding with ATP. In this case, cyclin/CDK complexes phosphorylate residues of serine and threonine on their substrate proteins.

Cells control the progression of the cell cycle through mechanisms that prevent the passage to the next phase, called checkpoints. During the first checkpoint,

which occurs between phases G1 and S, cells decide whether to start the cell cycle or remain quiescent. The next checkpoint, between phase G2 and M, is activated in response to damaged DNA. In this case, cells stop the cell cycle in order to repair the DNA, avoiding the proliferation of cells with genomic abnormalities. The first checkpoint is regulated by the expression of D-type cyclins, which binds CDK4/6. The cyclin D-CDK4/6 complexes enter the nucleus to be activated by CDK-activating kinase (Goel S. et al., 2018). The D-type cyclins (D1, D2, D3) are expressed in a cell-specific manner (Roskoski Jr R., 2018). The cyclin D-CDK4/6 complexes phosphorylate the retinoblastoma (Rb) tumor suppressor protein, promoting the release of the transcription factor E2F1 (Narasimha A. M. et al., 2014). Also the cyclin E-CDK2 complexes phosphorylate Rb, resulting in a further increase in E2F1 expression ((Hiebert S. W. et al., 1992). This transcription factor induces the expression of proteins necessary for the subsequent S phase of the cell cycle, causing cell cycle progression (Trimarchi J. M. et al., 2002). Hypophosphorylated Rb prevents the expression of genes necessary for the S phase both through the binding of E2F1 and through the recruitment of chromatin modifiers to DNA, silencing E2F1-target gene expression (Talluri S. et al., 2010; Chicas A. et al., 2012).

CDKs are inhibited by two protein families: INK4 and CIP/KIP. The INK4 family consists of 4 CDK endogenous inhibitors: p16/INK4A, p15/INK4B, p18/INK4C and p19/INK2D (Cánepa E. T. et al., 2007). All these proteins bind to CDK4 and CDK6 avoiding the binding to the D-type cyclins (Roskoski Jr R., 2018). The proteins of the INK4 family act as tumor suppressors, inhibiting the cell cycle (Malumbres M. et al., 2001). The CIP/KIP family has 3 members: p21/CIP/WAF1, p27/KIP1 and p57/KIP2 (Roskoski Jr R., 2018). p21/CIP/WAF1 is induces by

DNA damaged. p27/KIP1 characterizes the G0 phase of the cell cycle. Finally, p57/KIP2 inhibits cyclin A-CDK2, cyclin E-CDK2 and cyclin D-CDK4, acting as a negative regulator of the cell cycle.

Cell cycle dysregulation is one of the hallmarks of the tumor. In fact, many tumors are characterized by mutations involving cyclins, CDKs or CDK endogenous inhibitors (Roskoski Jr R., 2016). Amplification of cyclins and CDKs genes characterizes various types of human cancers. 15 to 40% of tumors have the amplification of the *cyclin D1* gene (Musgrove E. A., 2011). Cyclin E is over-expressed in uterine and ovarian carcinomas (Kuhn E. et al., 2014). *Cyclin A* gene amplification characterizes endometrial, thyroid, hepatocellular and esophageal carcinomas (Roskoski Jr R., 2016). Diffuse large B-cell lymphomas and melanomas have overexpression of CDK1 (Roskoski Jr R., 2016). *CDK4* and *CDK6* genes are amplified in a wide variety of tumors (Roskoski Jr R., 2018). Finally, the loss of CDK endogenous inhibitors gene led to an uncontrolled cellular proliferation, promoting the acquisition of the tumor phenotype. In fact, *p16/INK4A* gene is deleted in many tumors such as MPM, acute lymphoblastic leukemias (Drexler H. G. et al., 1998), NSCLC, melanomas, Hodgkin lymphomas, osteosarcomas and retinoblastomas (Roskoski Jr R., 2016). The loss of this gene is correlated with poor survival (Roskoski Jr R., 2018). The lack of expression of p21/CIP/WAF1 characterizes different types of tumors (Roskoski Jr R., 2016) and it is associated with metastases (Roskoski Jr R., 2018).

1.8 CDK4/6 inhibitors as anticancer drugs

CDK4 and CDK6 are promising therapeutic targets for the treatment of various types of human cancer. Currently, many clinical studies investigate the association of 12 CDK4/6 inhibitors with chemotherapy, immunotherapy and targeted therapy for the treatment of malignant tumors (Malumbres M., 2019). So far, the CDK4/6 inhibitors, approved by the US FDA for the treatment of breast cancer, are: palbociclib (PD-0332991), abemaciclib (LY2835219) and ribociclib (LEE-011). In fact, in 2009, an *in vitro* study shows for the first time that palbociclib inhibits proliferation in human breast cancer cell lines (Finn R. S. et al., 2009). A few years later, many clinical studies show the efficacy of combining palbociclib with letrozole for the treatment of advanced breast cancer (Finn R. S. et al., 2016). Due to their different pharmacokinetics and clinical toxicities, these CDK4/6 inhibitors have a different therapeutic strategy (Klein M. E. et al., 2018). The molecular structure of these CDK4/6 inhibitors consists of a pyrido [2,3-d] pyrimidinone core, a pyridine-pyrimidine-benzimidazole core and a pyrrolo [2,3-d] pyrimidine core for palbociclib, abemaciclib and ribociclib respectively (Roskoski Jr R., 2019) (Fig.6). Palbociclib and ribociclib have a similar structure, while abemaciclib is quite different. Some *in vitro* studies show that these molecules have a different affinity towards the targets. In fact, palbociclib antagonizes both cyclin D1-CDK4 and cyclin D2-CDK6 (Fry D. W. et al., 2004). Instead, abemaciclib and ribociclib have a greater efficacy towards CDK4 than CDK6 (Gelbert L. M. et al., 2014; Tripathy D. et al., 2017). Recent studies have shown that abemaciclib binds other kinases, including CDK1, CDK2, CDK7 and CDK9, with less inhibitory potency (Hafner M. et al., 2019).

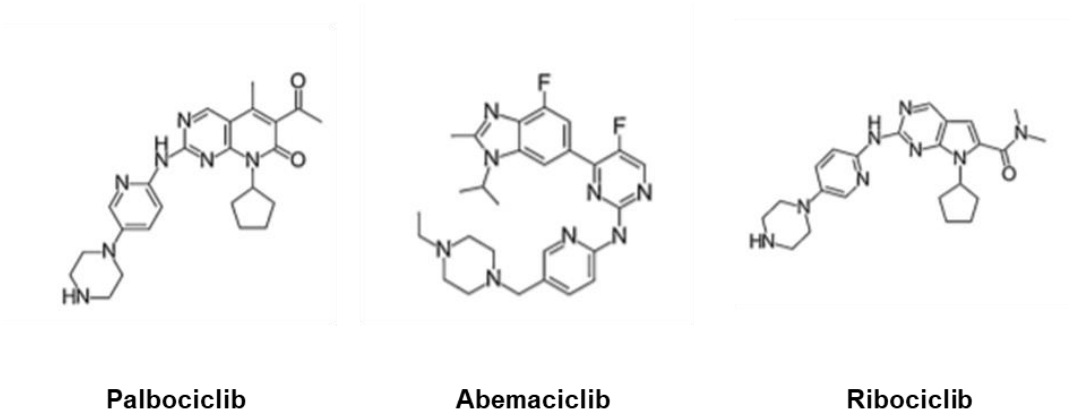

Figure 6. Molecular structure of FDA approved CDK4/6 inhibitors (Roskoski Jr R., 2019).

The CDK4/6 inhibitors target the cyclin D-CDK4/6 complexes, preventing the phosphorylation of Rb and causing cell cycle arrest. These drugs also act on other aspects of tumor biology, including senescence (Anders L. et al., 2011), metabolism (Wang H. et al., 2017), cancer metastasis (Liu T et al., 2017), and cancer immune surveillance (Zhang J. et al., 2018).

Cell cycle arrest, induced by CDK4/6 inhibitors, can cause quiescence or senescence, depending on the type of tumor. Quiescent cells enter the cell cycle in response to proliferative stimuli. While senescent cells are permanently out of the cell cycle. Quiescent cells are also able to become senescent and this biological mechanism is called geroconversion (Blagosklonny M. V., 2014). Cell senescence was first observed in a cell culture of human fibroblasts and was considered a block of cell proliferative capacity (Hayflick L. et al., 1961). Currently, senescence is interpreted as a cellular mechanism that prevents the proliferation of cells with genetic alterations, such as cancer cells (Hanahan D. et al., 2011). In fact, p16-INK4A-Rb and p53-p21/CIP/WAF1 signaling induce senescence in normal cells (Rodier F. et al., 2011), in response to stress stimuli

(Kuilman T. et al., 2010). Senescence induces various morphological changes, also observed in cells treated with CDK4/6 inhibitors, including increase in cell size, development of heterochromatin foci and increased activity of the β-galactosidase enzyme (Bonelli M. et al., 2019). Moreover, senescent cells express cytokines, chemokines, growth factors and many other proteins, called the senescence-associated secretory phenotype (the SASP). The SASP act on the tumor microenvironment promoting both the antitumor immune response (Xue W. et al., 2007) and tumorigenesis (Ruhland M. K. et al., 2016), highlighting the complex and ambiguous role of senescence. These data suggest that eradication of senescent cells could be a treatment option in the context of cancer (Sikora E. et al., 2019).

The CDK4/6-cyclin D-Rb-E2F pathway has an important role in both cell proliferation and metabolism. In fact, the CDK4-pRb-E2F1 pathway is involved in the secretion of insulin in mouse pancreatic cells (Annicotte J. S. et al., 2009). CDK4 plays a role in insulin signaling in adipocytes and hepatocytes (Lee Y. et al., 2014; Lagarrigue S. et al., 2016). Cyclin D1-CDK4 complex inhibits the expression of nuclear respiratory factor 1 (NRF-1), involved in the regulation of mitochondrial genes (Wang C. et al., 2006). An *in vitro* study showed that cyclin D1 binds to a voltage-dependent anion channel situated in the mitochondrial membrane of B-cell malignancies, inhibiting the mitochondrial activity (Tchakarska G. et al., 2011). Cyclin D3-CDK6 complex binds many enzymes involved in glycolisis in cancer cells (Wang Z. et al., 2017).

So far, the effects of CDK4/6 inhibitors on cellular metabolism have been predominantly studied *in vitro* in breast cancer cell lines. Many studies showed that palbociclib in association with endocrine therapy shows a greater inhibitory

effect on cell metabolism than the effect obtained with drugs used alone in breast cancer cell lines (Bonelli M. et al., 2019). It is worth of note that abemaciclib alone acts on cell metabolism causing a reduction of the metabolites of the tricarboxylic acid cycle in breast cancer cell lines (Torres-Guzman R. et al., 2017).

Many studies show that CDK4/6 inhibitors stimulate the innate antitumor response, enhancing the immunogenicity of cancer cells. A recent *in vitro* and *in vivo* study showed that both palbociclib and abemaciclib induce cancer cells to present antigens, stimulating an antitumor immune response (Goel S. et al., 2017). CDK4/6 inhibitors cause a reduction in the expression of type 1 DNA methyl-transferase (DNMT1), being a target of E2F. DNMT1, normally, downregulates endogenous retroviral elements. So, CDK4/6 inhibition leads to the production of type III interferons which in turn cause the production of the major histocompatibility complex class I molecules by the tumor cells. Another *in vivo* study performed on triple negative breast cancer models, shows that palbociclib or ribociclib in combination with a PI3Kα inhibitor induce an increase in the expression genes encoding for both cytokines and proteins of the major histocompatibility complex class I molecules (Teo Z. L. et al., 2017).

It is worth of note that CDK4/6 inhibitors also cause tumor immune escape. In fact, an increase in PD-L1 expression by tumor cells was observed in response to treatment with ribociclib or palbociclib in an *in vitro* and *in vivo* study of breast cancer models (Zhang J. et al., 2018). CDK4/6 inhibitors increase PD-L1 by avoiding the phosphorylation of the adaptor protein specle-type POZ (SPOP) (Zhang J. et al., 2018) and by promoting the activation of NF-kB (Bouillez A. et al., 2017). A combined inhibition of CDK4/6 with PD-L1/PD1 axis affect tumor

growth in an *in vivo* study in breast cancer (Zhang J. et al., 2018) and in melanoma (Kong Y. et al., 2019).

Cell death is also associated with CDK4/6 inhibitors: palbociclib induced apoptosis in T-cell acute lymphoblastic leukemia (Sawai C. M. et al., 2012) and autophagy in gastric cancer cells (Valenzuela C. A. et al., 2017). Autophagy is considered a form of cell death, characterized by the formation of autophagolysosomes in the cell cytoplasm (Shintani T. et al., 2004). The induction of autophagy by CDK4/6 inhibitors is not yet fully understood and needs further investigations (Goel S. et al., 2018).

Although CDK4/6 inhibitors represent an effective therapeutic approach for the treatment of advanced hormone-positive breast cancer, many resistance mechanisms to CDK4/6 inhibitors have emerged. (McCartney A. et al., 2019; Álvarez-Fernándex M. et al., 2020). Currently, many preclinical and clinical trials aim to identify biomarkers in order to predict resistance or sensitivity to CDK4/6 inhibitors. The primary resistance appears in the early phase of the therapy, resulting in no benefit from CDK4/6 inhibition. On the other hand, the acquired resistance can occur during the progression phase of the tumor. Many preclinical studies identify Rb deficiency as a driver of resistance to CDK4/6 inhibitors (Fry D. W. et al., 2004; Dean J. L. et al., 2012; Witkiewicz A. K. et al., 2014). By contrast, human breast cancer cell lines with high levels of Rb and cyclin D1 and concurrently low levels of p16 show sensitivity to palbociclib (Finn R. S. et al., 2009). However, the role of cyclin D1 and p16 as biomarkers is still controversial. In fact, a phase II clinical trial (NCT01037790) shows that palbocilib have no clinical benefit in Rb-positive breast cancer patients with amplification of cyclin D1 or low levels of p16 (DeMichele A. et al., 2015). In an another phase II study,

called PALOMA-1/TRIO-18, amplification of cyclin D1 or loss of p16 have no impact on PFS in breast cancer patients treated with palbociclib (Finn R. S. et al., 2015). In addition, high levels of cyclin E1 expression have been associated with resistance to palbociclib (Herrera-Abreu M. T. et al., 2016). Mutations in the catalytic subunit of PI3K have been related to mechanisms of resistance to CDK4/6 inhibitors (Cristofanilli M. et al., 2016; O'Leary B. et al., 2018). So far, no biomarkers have been validated to predict the response to this class of drugs (Goel S. et al., 2018).

1.9 The glucose metabolism in cancer cells

Cancer cells have abnormal energy metabolism, which includes glucose, glutamine and fatty acid metabolism (Park J. H. et al., 2020). Reprogramming of cellular metabolism is considered an emerging hallmark of the tumor, because it is observed in various types of human cancer (Hanahan D. et al., 2011). The study of the biological mechanisms that support the reprogramming of tumor metabolism has clinical implications, including cancer diagnosis, prognosis and therapy (Vander Heiden M. G. et al., 2017).

In 1927, Warburg and colleagues observed for the first time that the tumor cells were able to reprogram the metabolism of glucose (Warburg O. et al., 1927), a metabolic alteration called the Warburg effect. Cancer cells take high amounts of glucose and turn it into lactate even in the presence of oxygen, an abnormal process also called aerobic glycolysis. In fact, glycolysis is a metabolic adaptation of healthy cells to the hypoxic condition. The high consumption of glucose by cancer cells is a useful feature for diagnosis. In fact, radioactive glucose is the basis of PET-CT used to stage tumors.

Tumor metabolic reprogramming is caused by mutations of many oncogenes involving E2F1, c-myc and HIF1 and of several oncogenic pathways including the phosphatidylinositol-3-kinase (PI3K)/AKT/mammalian target of rapamyc (mTOR). The E2F family is composed by 8 transcription factors (E2F1-8), classified according to molecular structure, transcriptional features and targets (Black E. P. et al., 2005). E2F1, the first E2F transcription factor identified, is inactivated by binding to Rb in the absence of proliferative stimuli. E2F1 is one of the most important transcription factors, playing crucial role in many cellular

functions, including the regulation of energy metabolism (Denechaud P.D. et al., 2017).

In the context of the tumor metabolic reprogramming, E2F1 promotes the Warburg effect, enhancing the expression of many genes involved in glycolysis (Tarangelo A. et al., 2015). In fact, the metabolic switch against glucose oxidation in mitochondria is supported by E2F1, which favors the expression of the enzyme 6-phosphofructo-2-kinase/fructose-2,6-bisphosphate, a strong activator of glycolysis (Fernandez de Mattos S. et al., 2002). Moreover, E2F1 inhibits glucose oxidation, promoting the expression of pyruvate dehydrogenase kinase (PDK). In fact, in pancreatic cancer cells aerobic glycolysis is supported by the increased expression of PDK1 and PDK3 (Wang L. Y. et al., 2016).

The myc family is composed of the *c-myc* oncogene, an isoform found in most human tissues, *mycn* and *mycl*, physiologically expressed during development (Meyer N. et al., 2008). The c-myc transcription factor, one of the many targets of E2F1, is involved in many key mechanisms of cell biology, such as cell growth, cell proliferation, differentiation, cell cycle progression and metabolism (Meyer N. et al., 2008). c-myc acts as a transcription factor when it binds MAX, forming a heterodimer that binds a DNA sequence of target genes (Tarrado-Castellarnau M. et al., 2016). On the other hand, c-myc inhibits the transcriptional activity of MIZ1 and SP1, showing transcription repressive capacity (Herkert B. et al., 2010). Different types of human tumors are characterized by aberrant mutations of *c-myc* expression, including mechanisms of gene amplification and chromosomal translocation (Tarrado-Castellarnau M. et al., 2016). In the context of the tumor, c-myc favors tumorigenesis, supporting the progression of the cell cycle and tumor metabolic reprogramming. In fact, c-myc promotes the Warburg effect by

inducing the expression of genes involved in glucose uptake and glycolysis (Osthus R. C. et al., 2000).

The hypoxia inducible factors HIF1, expressed in most healthy tissues, HIF2 and HIF3, expressed in specific tissue, are transcription factors induced by hypoxia (Gordan J. D. et al., 2007). HIF transcription factors have two subunits: HIFα, a subunit sensitive to changes in oxygen and HIFβ, a subunit constitutively expressed (Gordan J. D. et al., 2007). In normoxic conditions, HIFα subunits are ubiquitinated by the tumor suppressor protein von Hippel-Lindau (VHL) to be degraded by the proteasome complex (Dang C. V. et al., 2008). On the contrary, the low oxygen concentration avoids the interaction of HIFα subunits with VHL (Dang C. V. et al., 2008). In this case, HIFα subunit binds to HIFβ subunit to form a transcription factor that binds specific sequences in the promoter region of target genes, mainly favoring angiogenesis (Semenza G. L., 2009). HIFα levels increase in various types of human tumors and often indicate a poor prognosis, showing a crucial role in tumorigenesis (Semenza G. L., 2010). In fact, the expression of HIFα, induced by the hypoxic condition of most solid tumors, promotes angiogenesis, the dissemination of metastases and metabolic reprogramming (Semenza G. L., 2010). In the context of glucose metabolism of cancer cells, HIF1 promotes the expression of genes involved in glucose uptake and in glycolysis, favoring the Warburg effect (Gordan J. D. et al., 2007). PI3K/AKT/mTOR pathway is characterized by hyperactivating mutations in most human cancers (Thorpe L. M. et al., 2015).

$PI3K_s$ are lipid kinases activated by various types of receptor tyrosine kinases (Lemmon M. A., 2010). Currently, 3 classes of $PI3K_s$ have been identified on the basis of molecular structure, regulatory mechanism and target (Vanhaesebroeck

B. et al., 2010). PI3Ks, belonging to class I, are composed of p85, a regulatory subunit, and p110, a catalytic subunit. Heterodimers composed of catalytic subunits (p110α, p110β and p110δ) and regulatory subunits (p85α, p85β, p55α, p55γ and p50α) belong to class IA. And finally, class IB is composed of p110γ, as a catalytic subunit, in association with p101 or p87, as regulatory subunits. PI3Ks convert PIP2 (phosphatidylinositol 4,5-bisphosphate) to PIP3 (phosphatidylinositol 3,4,5-triphosphate), adding a phosphate group. PIP3 promotes the interaction between PDK1 (phosphoinositide-dependent-kinase 1) and AKT, causing AKT phosphorylation (Fedele C. G. et al., 2010).

AKT, a serine-threonine kinase, is found in 3 tissue-specific isoforms: AKT1, AKT2 and AKT3. In fact, AKT2 has an important role in insulin-dependent tissues and AKT3 in the brain (Dummler B. et al., 2007; Manning B. D. et al., 2017). AKT regulates several aspects of cell biology including, proliferation, survival, growth and energy metabolism (Manning B. D. et al., 2017). In the contest of tumor metabolic reprogramming, AKT promotes Warburg effect, increasing glucose transporters (Rathmell J. C. et al., 2003; Elstrom R. L. et al., 2004) and activating glycolytic enzymes, including hexokinase 2 (Gottlob K. et al., 2001) and 6-phosphofructo-2-kinase/fructose-2,6-biphosphatase (Deprez J. et al., 1997).

The forkhead box O (FOXO) family, the glycogen synthase kinase 3 (GSK3) and mTOR are some downstream effectors of AKT signaling. FOXO, a family of transcription factors, is involved in apoptosis, DNA repair, differentiation and cell survival (Wątroba M. et al., 2012; Shats I et al., 2013). Phosphorylation of FOXO family members by AKT causes degradation of these transcription factors by the proteasome (Brunet A. et al., 1999). In the tumor context, the hyperactivation of AKT signaling determines the degradation of the transcription factors FOXO,

favoring cell survival (Wang Y. et al., 2014). GSK3 is another AKT substrate with the function of blocking glycogen synthesis (Cross D. A. et al., 1995). Also in this case, the phosphorylation of this kinase by AKT inhibits its function (Fumarola C. et al., 2014).

mTOR, a highly conserved serine/threonine kinase, is part of two distinct multiprotein complexes called mTORC1 and mTORC2 (Saxton R. A. et al., 2017). mTOR, DEPTOR, mLST8, Raptor and PRAS40 form mTORC1. This multi-protein complex promotes cell growth, cell survival and inhibits autophagy Fumarola C. et al., 2014). In the context of cell metabolism, mTORC1 supports lipid metabolism, inducing the espression of the transcription factors sterol regulatory element-binding protein 1/2 (SREBP1/2), which in turn regulates genes involved in lipid synthesis (Laplante M. et al., 2009). Moreover, this multiprotein complex promotes the expression of genes involved in oxidative phosphorylation in mitochondria (Cunningham J. T. et al., 2007).

mTORC1 is indirectly activated by AKT, which inhibits a negative regulator of this multiprotein complex, called the tuberous sclerosis complex 1/2 (TSC1/2), by phosphorylation (Menon S. et al., 2014; Valvezan A. J. et al., 2019).

The functions of mTORC2, composed of mTOR, Protor, Sin1, Rictor, mLST8 and DEPTOR, are not yet fully understood (Tarrado-Castellarnau M. et al., 2016). mTORC2 is known to induce AKT phosphorylation which in turn activates mTORC1 (Sarbassov D. D. et al., 2005).

The kinases of PI3K/AKT/mTOR signaling are attractive targets for the treatment of various types of cancers. In fact, several classes of drugs have been developed that inhibit this oncogenic pathway, including AKT inhibitors, mTOR catalytic site inhibitors, mTORC1 inhibitors, dual PI3K-mTOR inhibitors and PI3K inhibitors

(Fumarola C. et al., 2014). NVP-BEZ235, a reversible competitive inhibitor of the ATP-binding site of both PI3K and mTOR (Maira S.M. et al., 2008), belongs to the class of dual PI3K-mTOR inhibitors. This imidazoquinolynic compound is investigated in many clinical trials since 2006, especially for the treatment of breast cancer (Fumarola C. et al., 2014). The class of PI3K inhibitors is formed by several compounds, including NVP-BYL719, a specific inhibitor of the p110α subunit of PI3K (Furet P. et al., 2013).

1.10 Role of CDK9 in cancer

CDK9 belongs to the CDKs family, acting mainly as a transcription regulator. This protein, discovered in 1994 (Graña X. et al., 1994), is encoded by *CDK9* gene. It exists in two isoforms, transcribed by two different promoters (Shore S. M. et al., 2003): $CDK9_{42}$ and $CDK9_{55}$ (Bacon C. W. et al., 2019). $CDK9_{42}$ isoform is mainly located in the nucleoplasm and $CDK9_{55}$ isoform in the nucleolus (Liu H. et al., 2005). In its active state, CDK9 binds Cyclin T1 forming a heterodimeric complex called Positive-Transcription Elongation Factor-b (P-TEFb) (Mandal R. et al., 2021). Cyclin T2a and cyclin T2b are considered minor partners of CDK9 (Ramakrishnan R. et al., 2011). RNA Polymerase II (RNAP II) regulates the expression of genes through steps, such as pre-initiation, initiation, elongation, RNA processing and termination (Mandal R. et al., 2021). P-TEFb plays a crucial role during the elongation phase, involved in regulating the expression of most human genes (Chen F. X. et al., 2018). In fact, P-TEFb phosphorylates specific residues at the C-terminus domain of RNAP II, promoting the elongation phase of mRNA strands (Zhou Q. et al., 2012; Bowman E. A. et al., 2014).

P-TEFb plays a key role in cell cycle progression and cellular differentiation. In fact, it promotes c-myc, involved in cell proliferation, and myeloid cell leukemia-1 (MCL-1), an anti-apoptotic protein of the B-cell lymphoma-2 (Bcl-2) family (Mandal R et al., 2021). P-TEFb is also essential for the differentiation of various cell types, including neurons (De Falco G. et al., 2005), lymphocytes (Bellan C. et al., 2004) and adipocytes (Iankova I. et al., 2006).

The biological activity of P-TEFb is strictly regulated (Zhou Q. et al., 2012). In fact, most of the amount of P-TEFb reversibly binds other proteins, forming a

ribonucleoprotein complex with inhibitory function (Michels A. A. et al., 2004). Moreover, post-translational modifications, such as ubiquitination, acetylation and phosphorylation, targeting CDK9/Cyclin T1 acts on the P-TEFb activity (Anshabo A. T. et al., 2021).

Since its discovery, many studies have shown that CDK9 is involved in cardiovascular diseases, viral infections and different types of cancer (Franco L. C. et al., 2018), becoming an attractive therapeutic target. In fact, many CDK9 inhibitors have been developed, some of which are being investigated in clinical trials, for the treatment of various types of human cancer (Anshabo A. T. et al., 2021; Mandal R. et al., 2021).

In the context of cancer, CDK9 promotes carcinogenesis both in hematological malignancies and in solid tumors (Anshabo A. T. et al., 2021). In fact, the role of P-TEFb in different forms of leukemia is well known. These tumors are characterized by rearrangements and translocations at the chromosome level that lead to the formation of fusion genes. These genes often code for chimeric proteins, which act by recruiting P-TEFb and thus promote the transcription of other genes, supporting leukemogenesis (Lin C. et al., 2010).

P-TEFb supports the expression of a large plethora of mutated genes that characterize breast cancer (Anshabo A. T. et al., 2021). In fact, triple-negative breast cancer with high CDK9 level shows poor overall survival (Brisard D. et al., 2018). P-TEFb is also involved in prostate cancer due to its interaction with androgen receptor, promoting the expression of target genes (Lee D. K. et al., 2001). Moreover, androgen receptor is phosphorylated by P-TEFb, which modifies its transcriptional activity, its binding to DNA and its localization in the nucleus, supporting carcinogenesis in prostate cancer (Gordon V. et al., 2010;

Chen S. et al., 2012). Recently, a study on endometrial cancer biopsies revealed elevated levels of CDK9 expression, highlighting the role of this kinase as a potential prognostic biomarker and a therapeutic target (He S. et al., 2020).

2. Aims of the study

This study aims to investigate new therapeutic approaches for the treatment of MPM, as a target therapy is currently missing. The high frequency *CDKN2A/ARF* gene loss makes CDK4/6 inhibitors a potential treatment option for MPM. In 2016, Zhang et al. have demonstrated that CDK4/6 inhibitors enhance the AKT/mTOR pathway due to inhibition of Rb phosphorylation, which causes AKT activation (Zhang et al., 2016). In fact, in physiological conditions, hyper-phosphorylated Rb avoids the interaction between AKT and mTORC2, so that AKT/mTOR pathway is downregulated. This finding suggests the rationale for the combination of CDK4/6 inhibitors and PI3K inhibitors, as a potential therapeutic strategy for MPM treatment. As previously demonstrated by our research group, the combined inhibition of CDK4/6-cyclin D-Rb-E2F and PI3K/AKT/mTOR pathways affected proliferation in MPM cell lines, showing an anti-tumor efficacy (Bonelli M. A. et al., Neoplasia, 2017).

Based on these encouraging results, one of this study's goal was to evaluate the effect of the CDK4/6 inhibitor palbociclib in association with PI3K inhibitors (NVP-BEZ235 or NVP-BYL719) on glucose metabolism in human MPM cell lines. It is well known that CDK4/6-cyclin D-Rb-E2F and PI3K/AKT/mTOR pathways plays also a crucial role in the control of metabolic process: AKT regulates glucose metabolism through HIF1-α and c-myc has a role in glucose metabolism through the regulation of the glucose transporter GLUT1 and many genes involved in the glycolytic process. Palbociclib/PI3K inhibitors combined treatment might affect glucose metabolism due to inhibition of both PI3K/mTOR pathway and c-myc expression.

Another goal of this research was to find a treatment schedule based on the association of abemaciclib with the first-line chemotherapy approved for the treatment of MPM in order to investigate the antiproliferative effects on MPM cell lines.

Finally, this study also investigated the antitumor efficacy of a new molecule, called VS2-370, in MPM cell lines. VS2-370, developed by an Italian company for the treatment of various types of cancer, is a highly selectively inhibitors of both CDK4/6 and CDK9. Currently, this new drug is in an advanced preclinical phase of development.

3. Materials and Methods

3.1 Cell cultures

Human MPM cell lines MSTO-211H (biphasic istotype), H2052 (sarcomatoid istotype), H28 (epithelioid istotype) and H2452 (epithelioid istotype) were purchased from American Type Culture Collection ATCC (Manassas, VA, USA). ZS-LP was a primary cell line obtained from a MPM patient, after informed consent, diagnosed at Hospital of Parma (Bonelli M. A. et al., Neoplasia, 2017). All cell lines were cultured in RPMI-1640 growth medium supplemented with 10% of fetal bovine serum (FBS), 2 mM glutamine (GLN) and 1% of antibiotics (penicillin 100 UI/ml and streptomycin 100 µg/ml). H2052 were cultured in RPMI-1640 supplemented with 10% of FBS, 2 mM GLN, 1% of antibiotics, 10 mM Hepes, 12 mM glucose and 1 mM NaPyr. All cell lines, seeded in different densities, grew in Petri dishes of different sizes in a humified atmosphere with 5% CO_2 at 37°C. Hypoxic conditions were created by a cell culture incubator with controlled O_2 levels at 37°C (Binder GmbH).

3.2 Drug treatments

Palbociclib (PD-0332991), abemaciclib (LY2835219) and ribociclib (LEE-011) were provided by Selleckchem (Houston, Texas, USA). Palbociclib was dissolved in sterile water while abemaciclib and ribociclib were dissolved in DMSO.

NVP-BYL719 and NVP-BEZ235, provided both by Selleckchem (Houston, Texas, USA), were dissolved in DMSO. Cisplatin and pemetrexed were provided from the inpatient pharmacy of University Hospital of Parma and were dissolved in sterile water. VS2-370 was provided from Virostatics (Italy) and was dissolved in DMSO. DMSO was used at a concentration below 0.1% *(v/v)*.Control cells were treated with an equal amount of solvent.

3.3 Trypsinization and cell counting

Trypsinization was the process of cell dissociation using trypsin, a proteolytic enzyme that broke down proteins in order to dissociate adherent cells from the vessel in which they are being cultured. The culture medium was removed and an adequate volume of Trypsin EDTA 1X in PBS w/o calcium w/o magnesium w/o Phenol Red (Biowest) were added at 37°C, in order to facilitate the detachment of cells from the plate. Then, cells were transferred to sterile tubes and spiked with a volume of cultured medium equal to that of trypsin. The suspension was centrifuged at 500 x g for 4 minutes. Subsequently, the supernatant was removed and cells were re-suspended in culture medium. Cell counting was performed by light microscopy using a Bürker haemocytometer. Finally, cells were seeded at the density desired in plates with culture medium.

3.4 MTT assay

The MTT (3-(4,5-dimethylthiazol-2-yl)-2,5-diphenyltetrazolium bromide) was a colorimetric assay for measuring cell vitality. The assay was based on the reduction of the yellow tetrazole MTT into its insoluble formazan, giving a purple color. MTT-reduction was dependent on NAD(P)H-dependent oxidoreductase enzymes expressed in the cell. Therefore, reduction of MTT was directly proportional to cellular metabolic activity due to elevated NAD(P)H flux. 3-5 x 10^3 cells were seeded into 96-well plates in quadruplicate and were exposed to various treatments. After 72 hours of drug treatment, medium was removed and 100 µl of MTT solution (1 mg/ml, Sigma-Aldrich) was added to each well. The plate was incubated at 37°C. After an hour, crystalline formation was dissolved with DMSO and the absorbance was measured at 565 nm, using a microplate-reader (TECAN).

3.5 Cristal violet assay

Cristal violet (triphenylmethan dye (4-[(4-dimethylaminophenyl)-phenyl-methyl]-N, N-dimethyl-aniline) assay was a colorimetric assay for measuring cell vitality. Crystal violet dye stained nuclei. Upon solubilization, the intensity of the color produced was directly proportional to cells number. 3-5 x 10^3 cells were seeded into 96-well plates in quadruplicate and were exposed to drug treatments. After 72 hours of drug treatments, medium was removed and the cells were washed with cold PBS twice. Subsequently, cells were fixed with ice-cold methanol for 10 minutes and then stained with 0.5% crystal violet. The unbound dye was removed by washing carefully with water. Bound crystal violet was solubilized with 0.2% TritonX-100 in PBS. Light excitation, which increased linearly with cells number, was analyzed at 570 nm, using a microplate-reader (TECAN).

3.6 Analysis of cell death

Cell death was assessed by Hoechst 333342/propidium iodide staining, in order to differentiate apoptotic from necrotic cells, using the fluorescence microscope. Hoechst 33342 (bisbenzimide H33342 trihydrochloride) was a specific fluorescent DNA stain that crossed the cell membrane highlighting apoptotic cells in blue (Portugal J. et al., 1988). Propidium iodide (PI) was a DNA intercalating fluorescent agent of necrotic cells that appeared red under the fluorescence microscope (Tas J. et al., 1981).

Hoechst 33342 was dissolved in distilled water (50 μg/ml) while PI was dissolved in PBS, at the same concentration, with the addition of sodium citrate (0.1%) and NP40 (0.5%). 10^5 cells were seeded into medium plates in complete growth medium. 24 hours later, medium was replaced with drug-containing RPMI-1640 and the cells were cultured for additional 72 hours. Subsequently, the cells were detached and counted with trypan blue to distinguish dead cells from live cells.

Cell counting was performed by light microscopy using a Bürker haemocytometer. Finally, the cells were resuspended in culture medium added with Hoechst 33342 (3 μg/ml) and PI (2.5 μg/ml) and the cells were counted using the fluorescence microscope.

3.7 Colony formation assay

Colony formation assay (clonogenic assay) was an in vitro test that evaluated cell survival through colony formation (Franken N. A. P. et al., 2006). This test was based on the proliferation of a single cell forming a group of at least 50 cells, called a colony. 2 x 10^3 cells were seeded into small plates in complete growth medium. 24 hours later, medium was replaced with drug-containing RPMI-1640. After 72 hours, the medium was removed and replaced by medium with drugs or medium without drugs, depending on the type of cells treated. Medium replacement could continue for one to two weeks. The drug-free medium evaluated the resumption of cell proliferation after drugs treatment. Finally, colonies were stained with crystal violet assay.

3.8 Cellular glucose uptake

Cellular glucose uptake quantified the glucose transport by cells in different experimental conditions. 10^5 cells were seeded into 12-well plates in complete growth medium. 24 hours later, medium was replaced with drug-containing or free-RPMI-1640 and the cells were cultured for additional 24 hours. Kreb's Ringer HEPES (KRH) buffer (136 nM NaCl, 4.7 mM KCL, 1.25 mM $CaCl_2$, 1.25 mM $MgSO_4$, 10 mM HERPES; pH 7.4), containing 1 µCi/ml Deoxy-D-Glucose 2-[1,2-3H(N)] (2DG, 1 mCi/mmol, Perkin-Elmer, Waltham, MA, USA) was used for glucose uptake measurements. 2-D-deoxyglucose, analogue of glucose, was internalized by the cells and phosphorylated to 2-deoxyglucose-6-phosphate by the hexokinase. The compound produced was not further metabolized by the cells. The radioactivity was directly proportional to the quantity of labeled glucose internalized by the cells.

The cells were quickly rinsed with KRH and incubated with KRH containing labeled glucose (uptake buffer) at 37°C for 5 minutes. The incubation was stopped by removal of the uptake buffer. The cells were quickly rinsed three times in cold Earle's solution containing 0.1 mM phloretin (Sigma-Aldrich). Ice-cold trichloroacetic acid (TCA 5% w/v) was added for 15 minutes at 4° C, in order to precipitate proteins and extract small intracellular solutes. Subsequently, the radioactivity was measured by liquid-scintillation counting in 4 independent determinations. Then, proteins were dissolved in 0.5 N NaOH and their concentration was measured by a dye-fixation method (Bio-Rad Laboratories, Hercules, CA, USA), using bovine serum albumin as standard.

3.9 Glucose (HK) assay

The consumption of glucose by cells was detected by Glucose (HK) Assay Kit (Sigma-Aldrich). Hexokinase catalyzed the glucose phosphorylation due to adenosine triphosphate (ATP), causing the formation of glucose-6-phosphate (G6P) and adenosine diphosphate (ADP). Subsequently, glucose-6-phosphate dehydrogenase (G6PDH) catalyzed the oxidation reaction of G6P, forming 6-phospho-gluconate and NADH. In fact, an equimolar amount of NAD was reduced to NADH. In this case, the concentration of NADH, proportional to glucose concentration, was analyzed at 340 nm, using a microplate-reader (TECAN).

Culture media were collected 24 hours after drugs treatment and centrifuged to remove debris. 6 µl of sample (containing 0.05-5 mg of glucose/ml) were added to 300 µl of glucose assay reagent (containing ATP, NAD, hexokinase and glucose-6-phosphate dehydrogenase) for 15 minutes at room temperature. Subsequently, the absorbance of samples was measured and compared to the absorbance of RPMI-1640, containing 2 mg/ml of glucose.

3.10 Agilent Seahorse XFp phenotype test kit

Glycolysis and mitochondrial respiration, the two most important energy pathways of the cell, were measured by Agilent Seahorse XFp technology, both under baseline and stressed conditions. Results were reported considering two main parameters:

- Extracellular Acidification Rate (ECAR): the rate of increase in proton concentration (decrease of pH) in the assay medium. ECAR was a rate of the measure of the glycolysis of the cell.
- Oxygen Consuption Rate (OCR): the rate of decrease of oxygen concentration in the assay medium. OCR was a mesasure of the rate of mitichondrial respiration of the cell.

Glycolytic function and mitochondrial respiration were determined using the XFp extracellular flux analyzer (Seahorse Bioscience, North Billerica, MA).

Glycolytic function was investigated using Glycolysis Stress Test Kit. The cells were seeded in a Seahorse culture plate at an optimazed concentration of 12.000 cells per well. ECAR and OCR were detected after having added cells with a glucose-free medium. Glycolysis, glycolytic capacity, glycolytic reserve and non-glycolytic acidification were assessed after the addition respectively of 100 mM glucose, 10 µM oligomycin and 500 mM 2-deoxy-D-glucose.

Mitochondrial respiration was investigated using Mito Stress Test Kit. The cells were seeded in a Seahorse culture plate at an optimazed concentration of 12.000 cells per well. ECAR and OCR were measured in the presence of physiological concentrations of 10 mM glucose, 1 mM pyruvate and 2 mM glutamine. Mitochondrial ATP dependent respiration, uncoupled respiration and non-mitochondrial respiration were assessed after the addition respectively of 1 µM

oligomycin, 1.5 μM carbonylcyanide-p-trifluoromethoxyphenylhydrazone (FCCP) and the combination of 0.5 μM each of antimycin A and rotenone.

At the end of analysis, the Agilent Seahorse XFp produced a test report and it automatically calculated the baseline ECAR and OCR of the samples.

3.11 Western blotting analysis

Preparation of extracts

Cells were treated with drugs for a certain period of time and then the proteins were extracted for electrophoretic analysis. The cell monolayer was washed twice with 2 ml of saline solution in phosphate buffer (PBS) at 4°C. Subsequently, cells were treated with lysis buffer (150 mM NaCl, 5 mM $MgCl_2$, 50 mM Tris-HCL pH7.4, 0.1% sodiumdodecylsulphate (SDS), 1% Triton-X-100, 100 mg/ml 4-amidinophenylmethanesulfonyl fluoride (APMSF), 0.5 µg/ml leupeptin, 0.7 µg/ml pepstatin, 0.5 mM EDTA, 1 mM sodium ortovanadate, 50 mM NAF, 5 mM sodium pyrophosphate 10 mM sodium β-glycerophosphate, 0.5% sodium deoxycholate) and the lysate was collected using “cell scraper”. The extracts obtained were frozen at -80°C for at least 30 minutes, sonicated and centrifuged at 12000 x rpm for 10 minutes at 4°C in order to separate coarse components from the supernatant containing the proteins. Subsequently, the supernatant was transferred in eppendorf to quantify proteins.

Determination of protein content

Cell lysate proteins were determined using the BIO-RAD DC Protein Assay Kit (Richmond CA, USA). 125 µl of REAGENT A (alkaline solution of copper’s tartrate) was added to 2 µl of sample, vortexed and 1 ml of REAGENT B (Folin’s reagent) was added in each sample. Subsequently, all samples were incubated in the dark for 15 minutes at room temperature. The proteins induced a reaction that caused a purple color whose intensity was proportional to the protein concentration of each sample. Subsequently, the absorbance of samples was measured at 750 nM, using a microplate-reader (TECAN). The calibration curve

was constructed with a standard protein, such as bovine serum albumin (BSA). The protein concentration of each sample, including the samples of the calibration curve, was calculated by the absorbance.

Polyacrylamide gel electrophoresis in SDS (SDS-page)

The same amount of protein was taken from each sample with the addiction of the lysis buffer and sample buffer (62.5 mM Tris-HCL pH 6.8, 2% SDS, 2-5% β-mercaptoethanol, 0.002% blue bromine phenol, 20% glycerol). Subsequently, all samples were boiled at 100°C for 2-3 minutes and loaded into gel on SDS polyacrylamide slab gels (8x6x0.15 cm, using BIORAD equipment. On each lane, the same amount of protein was loaded. Subsequently, proteins were separated on a gel (acrylamide/polyacrylamide 30:0.8), according to the procedure described by Laemmli (Laemmli U. K., 1970), with a constant current of 60 mA at 4°C for about 1 hour. The molecular weight of each band was obtained by comparing the relative mobility of the same and that of standard proteins, colored and of known molecular weight, which were separated simultaneously with the samples.

Electrophoresis transfer

Following electrophoresis, the separated proteins were transferred (or blotted) onto a second matrix, PVDF (polyvinylidene difluoride) membrane, activated previously in methanol. The gel was placed in direct contact with a PVDF membrane and they were “sandwiched” between two electrodes. The transfer was performed by Lightning Blot Protein Transfer System (Perkin Elmer). When the electric field was applied, the proteins moved out of the polyacrylamide gel

onto the surface of the membrane, where the proteins became tightly attached. The resulting membrane was a copy of the protein pattern found in the polyacrylamide gel.

Protein detection

The membrane was incubated with blocking solution (5% non-fat-powdered milk or 5% BSA in TTBS buffered saline composed by 20 mM Tris, 137 mM NaCl, 1 mM HCl and 0.1% Tween 20) for 1 hour at 37°C, in order to block the non-specific binding site by proteins. Subsequently, the membrane was incubated with primary antibody overnight at 4°C on a shaker platform. After this time, 3 washes of 5 minutes each were performed with TTBS. Then, the membrane was incubated 1 hour with HRP-anti-mouse or HRP-anti-rabbit antibodies (secondary antibodies labelled with peroxidase) at 1:5000 dilutions. After this time, 3 washes of 5 minutes each were performed with TTBS. Immunoreactive bands were visualized using an enhanced chemiluminescence system: the transferred proteins, complexed with the secondary antibody, reacted with a chemiluminescent substrate, such as luminol (LuminataTM Crescendo Western HRP Substarte, Millipore Corporation, Billerica MA, USA), in order to produce immunoreactive bands which were visualized on photographic plates (C-DiGitTM Blot Scanner, Li-COR Biosciences, INC., Lincoln, NE, USA). The intensity of the signal correlated with the abundance of the antigen on the blotting membrane. The densitometric analysis of the bands, performed using Quantity One (BIO-RAD) software, allowed the quantification of the light signal that was a function of protein concentration.

3.12 β-Galactosidase staining

Cellular senescence was demonstrated using the Senescence β-Galactosidase Staining Kit (Cell Signaling Technology Inc.). Cells were cultured in small dishes (3×10^4 cells) and after 24 hours the medium was replaced with medium added to drugs. After 72 hours, the medium was removed and the cells were washed gently with PBS twice. Then, a fixative solution was added for about 15 minutes at room temperature. The cells were again washed with PBS twice. Finally, the solution containing the β-Galactosidase was added and the cells were incubated at 37 ° C overnight in the absence of CO_2. After a certain variable number of hours, depending on the type of cells, the senescent cells appeared blue. The cells were washed with PBS twice to remove the solution containing the enzyme and to stop the reaction. Finally, β-galactosidase positive cells were counted using the microscope.

3.13 CYTO-ID^{R} Autophagy detection Kit 2.0

Autophagy was demonstrated using the CYTO-ID^{R} Autophagy Detection Kit 2.0 (Enzo Life Sciences (ELS) AG). Cells were cultured on slides (10^{5} cells) and after 24 hours the medium was replaced with the medium containing the drugs. The positive control was done by adding medium with combined treatment of rapamycin (500 nM) and chloroquine (5 μM). After 72 hours, the medium was removed and the cells were washed gently with Assay Buffer 1X containing 5% FBS twice. Then, 100 μl of Microscopy Dual Detection Reagent was added for 30 minutes at 37°C. The cells were washed gentlly with Assay Buffer 1X containing 5% FBS once. Then, the cells were fixed with 4% formaldehyde for 20 minutes at room temperature. The cells were again washed with Assay Buffer 1X containing 5% FBS three times. Finally, the Hoechst 33342 Nuclear Stain (1μM) was added for 15 minutes at room temperature. At the end of the incubation time, the cells were observed using the confocal microscope.

3.14 Bliss analysis

The combined effects of drugs were investigated using the Bliss independence criterion for in vitro co-exposure (Goldoni M. et al., 2007).

The Bliss criterion is expressed by the following equation:

$$E(x,y) = E(x) + E(y) - E(x) \times E(y)$$

E(x) is the effect of the concentration for the first compound (between 0 and 1), E(y) is the effect of the concentration for the second compound and E(x,y) is the combined effect. If the combination effect is higher than the expected value from Bliss equation, the interaction is synergistic. If this effect is lower, the interaction is antagonistic. Otherwise, the effect is additive when drugs have no interaction.

3.15 Statistical analysis

Statistical analysis was carried out using GraphPad Prism version 8.0 software (GraphPad Software Inc. San Diego, CA, USA). Results were expressed as mean value ± standard deviation (SD) for the indicated number of independent measurements. Differences between the mean values recorded for different experimental conditions were evaluated by one-way Anova and Bonferroni's post- test. A p value <0.05 was considered as significant.

4. Results

Human MPM cell lines MSTO-211H (biphasic histotype), H2452, H28 (both of epithelioid histotype) and H2052 (sarcomatoid histotype) were characterized by *CDKN2A/ARF* loss and functional Rb pathway (Bonelli M. A. et al., Neoplasia, 2017). ZS-LP is a primary cell line obtained from a MPM patient, after informed consent, diagnosed at Hospital of Parma (Bonelli M. A. et al., Neoplasia, 2017). This primary cell line showed the same molecular characteristics described above (Bonelli M. A. et al., Neoplasia, 2017).

4.1 Effects of combined inhibition of CDK4/6 and PI3K/AKT/mTOR on metabolism in MPM cell lines

4.1.1 Background

The starting point of this research derived from previous data demonstrating that MPM cell lines, harboring *CDKN2A/ARF* deletion, were sensitive to palbociclib (Bonelli M. A. et al., Neoplasia, 2017). Moreover, MSTO-211H, H28 and ZS-LP cells treated with palbociclib for 24 hours, followed by the combined treatment of PI3K inhibitors (BEZ235 or BYL719) and palbociclib for further 48 hours, showed a synergistic/additive inhibition of cell proliferation in comparison with single drug treatments (Bonelli M. A. et al., Neoplasia, 2017).

The same treatment described above was also tested on H2052 cells, both in normoxia (Fig.1A-B) and hypoxia conditions (Fig.1C-D). In fact, the tumor microenvironment of various types of cancer, including MPM, is often characterized by poorly oxygenated areas. Also in this cell model, the combined treatment of palbociclib with BEZ235 or BYL719 caused an additive inhibition of

cell proliferation in both conditions. It is worth of note that this treatment schedule affected cell growth also in hypoxic conditions. Taken together these data suggested that palboliciclib in association with PI3K inhibitors (BEZ235 or BYL719) could be considered a new therapeutic approach for the treatment of MPM.

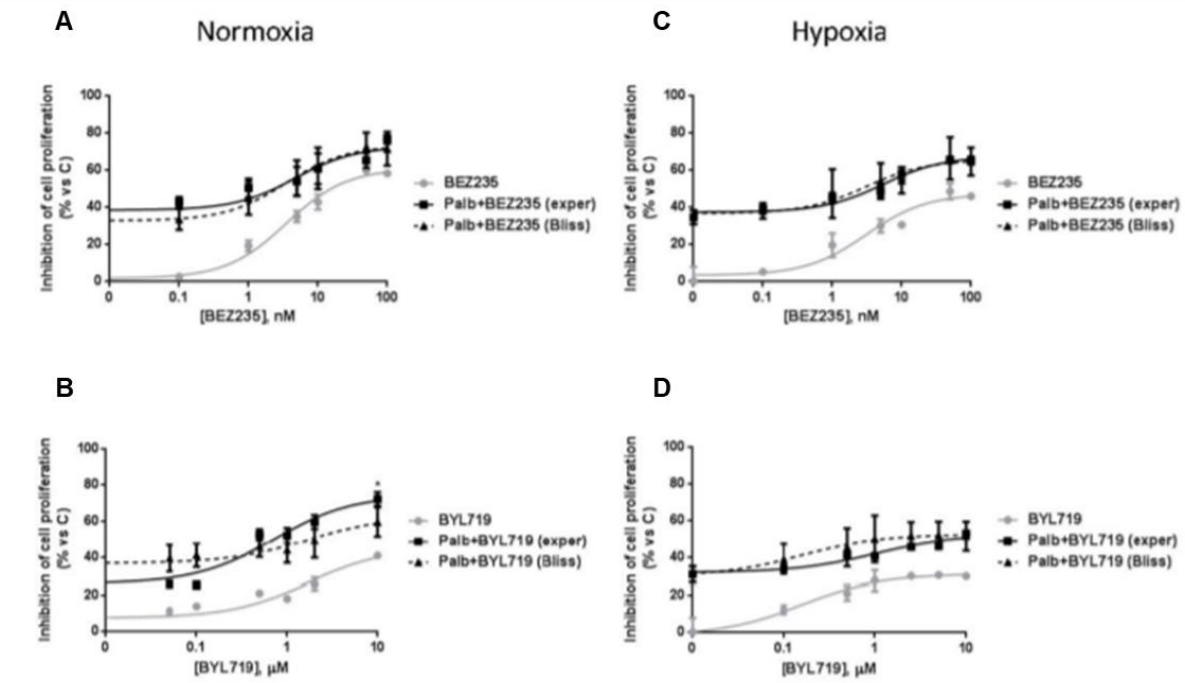

Figure 1. Effect of the combined treatment of palbociclib with PI3K/mTOR inhibitors on cell proliferation in H2052 cells. H2052 cells were treated with palbociclib 1 µM in association with BEZ235 (from 0.1 to 100 nM) or BYL719 (from 0.1 to 10 µM) for 72 hours in normoxia (A-B) and hypoxia (C-D). Cell proliferation was evaluated by MTT assay. The type of interaction (antagonistic, additive or synergistic) was determined through Bliss analysis. Data were expressed as percent inhibition versus control cells and were representative of two independent experiments. * $p < 0.05$ vs. Bliss.

4.1.2 Analysis of the metabolic phenotype in MPM cell lines

Since CDK4/6-cyclin D-Rb-E2F and PI3K/AKT/mTOR pathways are involved in the regulation of cell metabolism, in the context of the tumor they support metabolic reprogramming, becoming attractive therapeutic targets.

First, the metabolic characteristics were analyzed on a panel of human MPM cell lines: MSTO-211H, H2452, H28 and H2054 cells cultured in complete medium for 24 hours (Fig.2A). MSTO-211H cells showed the highest glycolytic and oxidative metabolism (energetic phenotype), measured respectively by extra cellular acidification (ECAR) and oxygen consumption rate (OCR) with the Agilent SeaHorse XFp analyzer, whereas H2052 cells had the lower glycolytic and oxidative metabolism (quiescent phenotype). H2452 and H28 cells showed an intermediate metabolic phenotype. Subsequently, all these MPM cell lines were subjected to glucose deprivation for 24 hours (Fig.2B). Glucose starvation moderately influenced the growth of H28 and H2452 cells. Cell viability of MSTO-211H cells was strongly impaired by the absence of glucose in the cultured medium, while H2052 cells adapted much better to this stress condition, as their growth was not inhibited. In fact, as shown in figure 2C, H2052 cells reacted better to the energy demand by maintaining high levels of both glycolysis and mitochondrial respiration. On the other hand, MSTO-211H cells were very susceptible, showing a lower metabolic potential. Finally, cell proliferation was observed in all MPM cell lines in hypoxia for 24 and 48 hours (Fig.2D). H2052 cells grew in hypoxic conditions at both 24 and 48 hours, due to their adaptability to metabolic stress conditions. Instead, MSTO-211H cells exhibited growth inhibition in hypoxia, confirming their low metabolic potential.

MSTO-211H and H2052 cells showed the highest and lowest energy phenotype, respectively. Based on these results, these two MPM cell lines were chosen to investigate the effects of palbociclib in association with PI3K inhibitors (BEZ235 or BYL719) on cell metabolism.

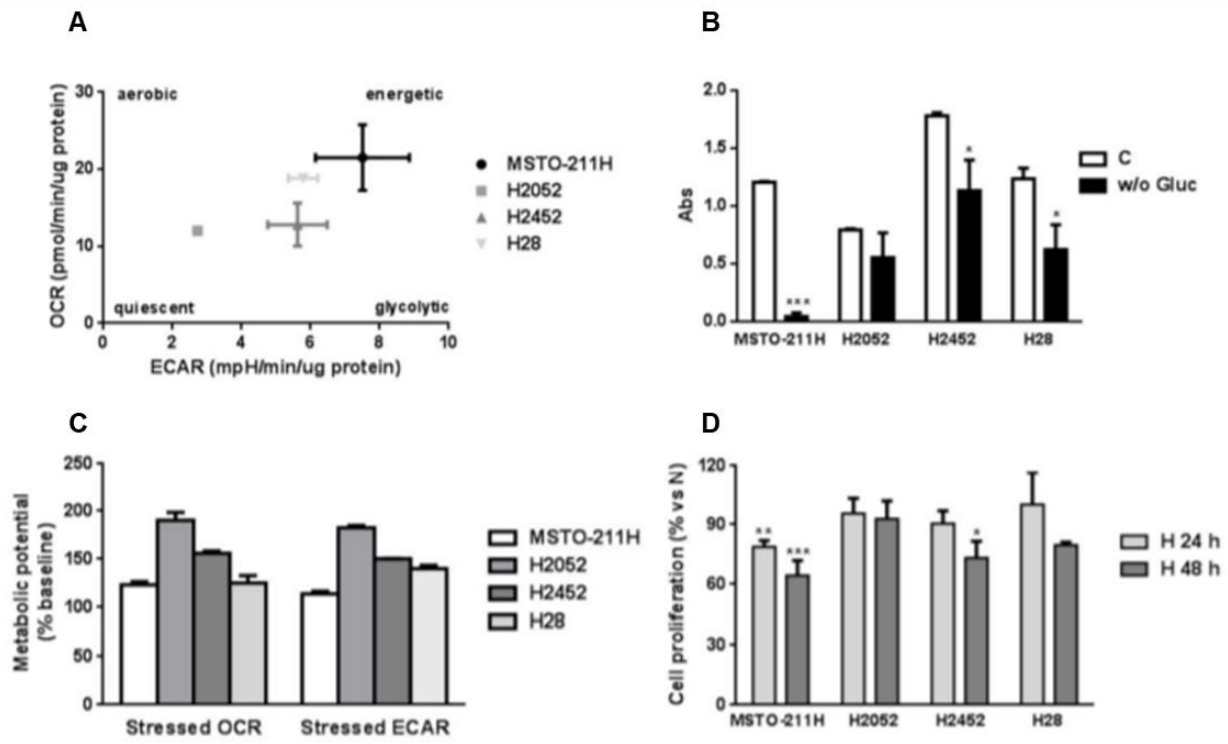

Figure 2. Metabolic profile of MPM cell lines. The Agilent SeaHorse Cell Energy Phenotype assay was used to analyze the metabolic features (A) and the metabolic potential (C) of MSTO-211H, H2052, H2452 and H28 cell lines. Data were representative of two independent experiments. (B) MPM cell lines were cultured under glucose starvation (w/o gluc) for 24 hours. Cell viability was measured by CV assay and data were representative of three independent experiments. *p<0.05, ***p<0.001 vs. control. (D) MPM cell lines were cultured in hypoxia for 24 hours and 48 hours. Cell viability was measured by CV assay and data were representative of three independent experiments. Data were expressed as percent versus control cells in normoxia (N) *p<0.05, **p<0.01, ***p<0.001 vs. N.

4.1.3 Analysis of the effects of the association of palbociclib with PI3K inhibitors (BEZ235 or BYL719) on glucose metabolism in MPM cell lines

The glycolytic activity of MSTO-211H and H2052 cells was analyzed with the Agilent SeaHorse XFp analyzer, in order to better characterize the effects of palbociclib and BEZ235 individually or in association.

The glycolytic function was measured by evaluating the extracellular acidification rate (ECAR). Cells were incubated with palbociclib 1 μM and BEZ235 40 nM, alone or in association, for 24 hours. Palbociclib or BEZ235 caused a reduction in basal ECAR levels in both cell models. It should be noted that ECAR levels showed a drastic decrease when MSTO-211H and H2052 cells were treated with the association of palbociclib with BEZ235 (Fig.3A-D). Afterwards, the cells were analyzed using the Agilent SeaHorse Glycolysis Stress Test, based on the sequential addition of glycolysis modulators to get glycolytic metabolic parameters (Fig.3B-E). The initial measurement was considered as a basal cell glycolytic activity in the absence of glucose (non-glycolytic acidification). The first injection of glucose activated glycolysis and ECAR increased due to the production and release of lactate. In cells used as controls, with a drug-free medium, this measurement was the normal rate of glycolysis. When glucose was injected in MSTO-211H and H2052 cells, treated with palbociclib and BEZ235 individually or in association, the induction of ECAR was significantly reduced, confirming the inhibition of their glycolytic capability. In the next step of the analysis, the ATP synthase inhibitor oligomycin was injected, thus producing a rapidly hyperpolarization of the mitochondrial membrane and blocking the generation of ATP by oxidative phosphorylation. The cells responded to this dramatic decrease of ATP production by activating glycolysis at their maximum

capability, and this was measured by a secondary increase of ECAR level. As shown in figure 3B-E, MSTO-211H and H2052 cells treated with palbociclib combined with BEZ235 showed a greater decrease of their glycolytic capacity than the cells treated with the drugs used alone. In fact, palbociclib and BEZ235 combination prevented oligomycin effects, maintaining ECAR at a similar rate to the baseline. At the end, glycolysis was completely inhibited by the injection of the glucose analog 2-DG, and the ECAR returned to its non-glycolytic level.

Moreover, as shown in figure 3C-F, the glycolytic capacity (the maximum ECAR rate reached after oligomycin injection) and the glycolytic reserve (the capability of cells to respond to an energetic demand) strongly decreased when MSTO-211H and H2052 cells were treated with the combined treatment. It is worth of note that MSTO-211H cells showed a greater reduction in the glycolytic reserve levels compared to H2052 cells treated with palbociclib in association with BEZ235, highlighting the ability of H2052 cells to better adapt to metabolic stress conditions.

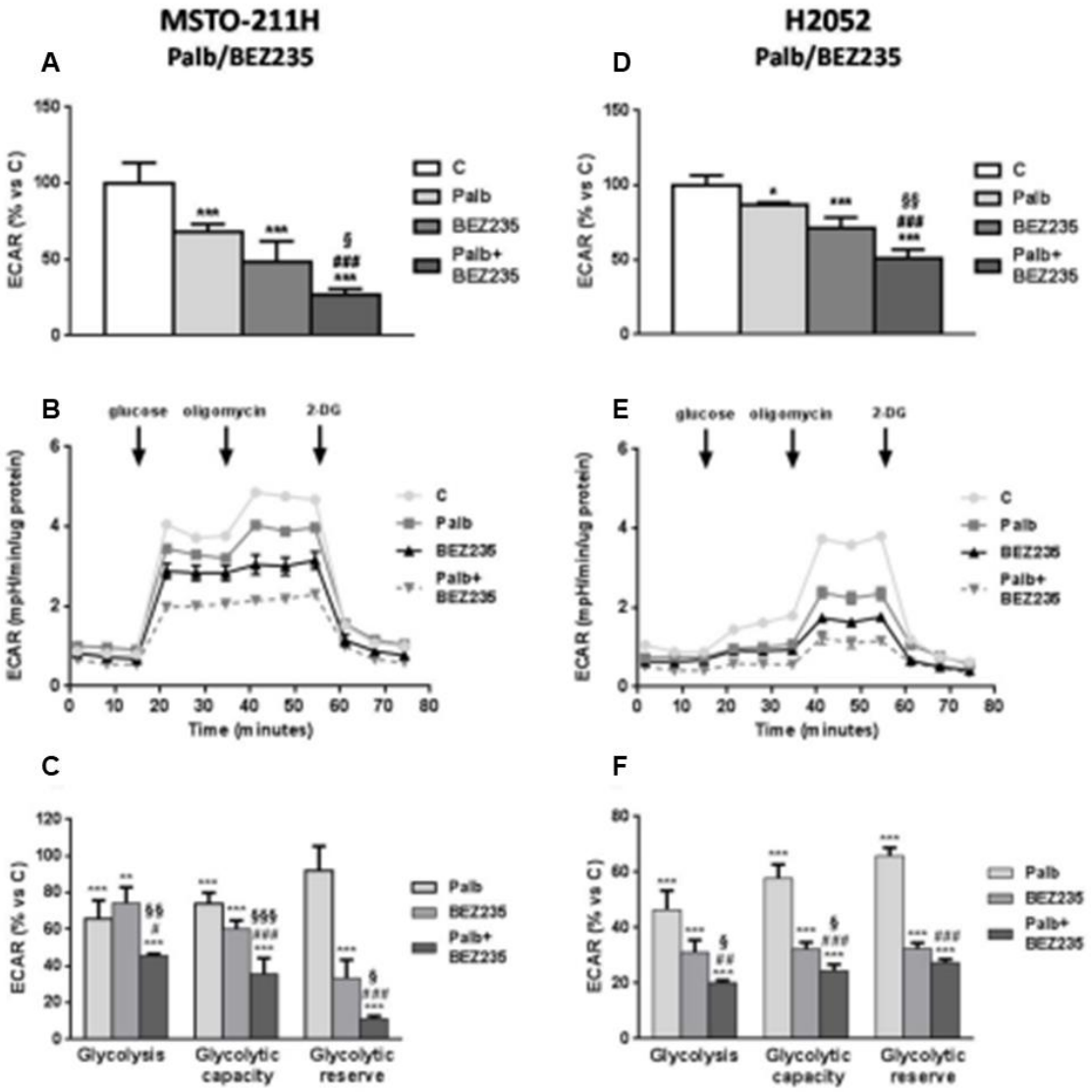

Figure 3. Effect of the combined treatment of palbociclib and BEZ235 on glycolysis in MSTO-211H and H2052 cells. Cells were treated with palbociclib (1μM) in association with BEZ235 (40nM) or with palbociclib or BEZ235 for 24 hours. (A-D) The glycolytic activity was evaluated by the extracellular acidification rate (ECAR) using Agilent SeaHorse XFp analyzer. Data were shown as mpH/min normalized to proteins and they were representative of four independent experiments. (B-E) Glycolytic profile was measured by ECAR using Agilent SeaHorse XFp analyzer Glycolysis Stress Test Kit. Data were representative of two independent experiments. (C-F) Glycolysis, glycolytic capacity (ECAR rate reached at the maximal cellular glycolytic capability after oligomycin addition) and glycolytic reserve (difference between the maximum ECAR reached after oligomycin injection and baseline ECAR) were calculated as percent versus control cells. Data were expressed as the media of at least three independent experiments. *p<0.05, **p<0.01, ***p<0.001 vs. C; #p<0.05, ##p<0.01, ###p<0.001 vs. palbociclib; §p<0.05, §§<0.01, §§§p<0.001 vs BEZ235.

Subsequently, the same analysis described above was performed on MSTO-211H and H2052 cells to investigate the effects of palbociclib and BYL719 individually or in association on the glycolytic activity (Fig.4). Cells were incubated with palbociclib 1 μM and BYL719 1 μM for MSTO-211H cells or BYL719 2.5 μM for H2052 cells, alone or in association, for 24 hours.

As shown in figure 4A-D, palbociclib combined with BYL719 caused a decrease in basal ECAR levels in both MSTO-211H and H2052 cells. It should be noted that basal ECAR levels were reduced by BYL719 in H2052 cells whereas this reduction was not detected in MSTO-211H cells. Subsequently, the cells, analyzed using the Agilent SeaHorse Glycolysis Stress Test, showed a reduced glycolytic activity due to combined treatment (Fig.4B-E). Moreover, MSTO-211H and H2052 cells had a strong downregulation of their glycolytic capacity and glycolytic reserve, when both cell models were treated with palbociclib in association with BYL719 (Fig.4C-F).

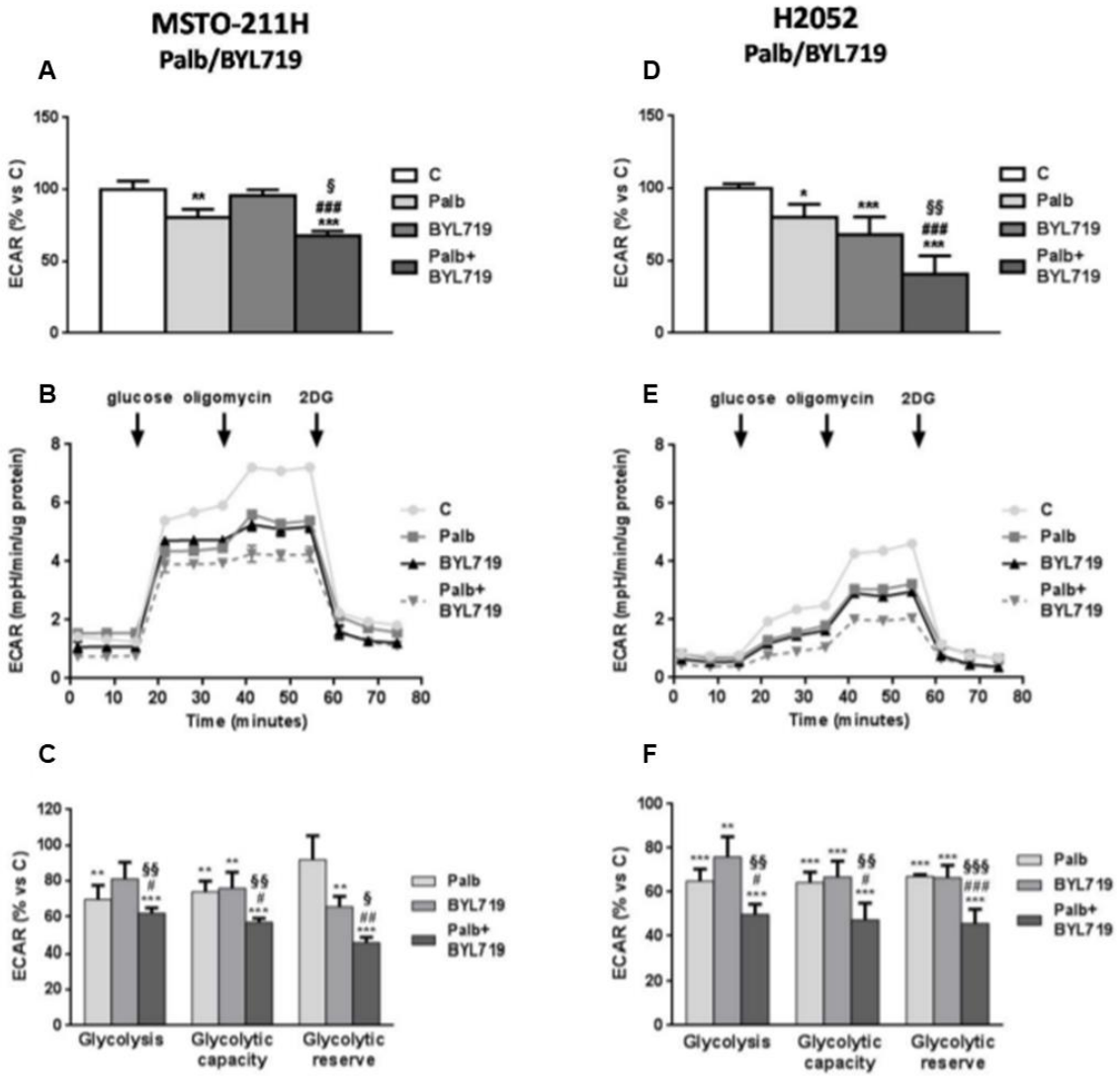

Figure 4. Effect of the combined treatment of palbociclib and BYL719 on glycolysis in MSTO-211H and H2052 cells. (A-D) The glycolytic activity was evaluated by the extracellular acidification rate (ECAR) using Agilent SeaHorse XFp analyzer. Data were shown as mpH/min normalized to proteins and they were representative of four independent experiments. (B-E) Glycolytic profile was measured by ECAR using Agilent SeaHorse XFp analyzer Glycolysis Stress Test Kit. Data were representative of two independent experiments. (C-F) Glycolysis, glycolytic capacity (ECAR rate reached at the maximal cellular glycolytic capability after oligomycin addition) and glycolytic reserve (difference between the maximum ECAR reached after oligomycin injection and baseline ECAR) were calculated as percent versus control cells. Data were expressed as the media of at least three independent experiments. **p<0.01, ***p<0.001 vs. C; #p<0.05, ##p<0.01, ###p<0.001 vs. palbociclib; §p<0.05, §§<0.01, §§§p<0.001 vs BYL719.

The effects of palbociclib in associations of PI3K inhibitors on glucose metabolism were further investigated by evaluating other parameters. First, the effects of palbociclib alone or combined with BEZ235 or BYL719 on cell glucose consumption rate were measured under both normoxic and hypoxic conditions by Glucose (HK) Assay Kit (Fig.5A-B). MSTO-211H and H2052 cells were treated with palbociclib 1 μM, BEZ235 40 nM or BYL719 (1 μM for MSTO-211H cells or 2.5 μM for H2052 cells), individually or in association (palbociclib + BEZ235 or palbociclib + BYL719) in both normoxic and hypoxic conditions (0.5 % O_2) for 24 hours. In normoxic conditions, both palbociclib and BEZ235, used individually, induced about 20% decrease in glucose consumption in both MPM cell models. On the contrary, BYL719 alone affected glucose consumption only in H2052 cells. The association of palbociclib with BEZ235 or BYL719 caused a decrease in glucose consumption of about 30% in MSTO-211H cells and about 40% in H2052 cells. In hypoxic conditions, the combination of palbociclib with PI3K inhibitors prevented hypoxia-mediated stimulation of glucose consumption more than individual treatments in both MPM cell models. In fact, the consumption of glucose decreased by 30% due to the combined treatment and by 15-20% due to the drugs used individually. The reduced glucose consumption observed after palbociclib/PI3K inhibitors combined treatment was ascribed to a reduced glucose uptake (Fig.5C-D). In this case, MSTO-211H and H2052 cells were treated with palbociclib 1 μM or BEZ235 40 nM, individually or in association, in both normoxic and hypoxic conditions (0.5 % O_2) for 24 hours. The association of palbociclib with BEZ235 induced a greater glucose uptake inhibition than single drug treatment in both MSTO-211H and H2052 cells, in both normoxic and hypoxic conditions. In addition, both MPM cell models adapted to the hypoxic

condition by increasing glucose uptake; this adaptation was more efficaciously inhibited by the combined treatment as compared with single treatments.

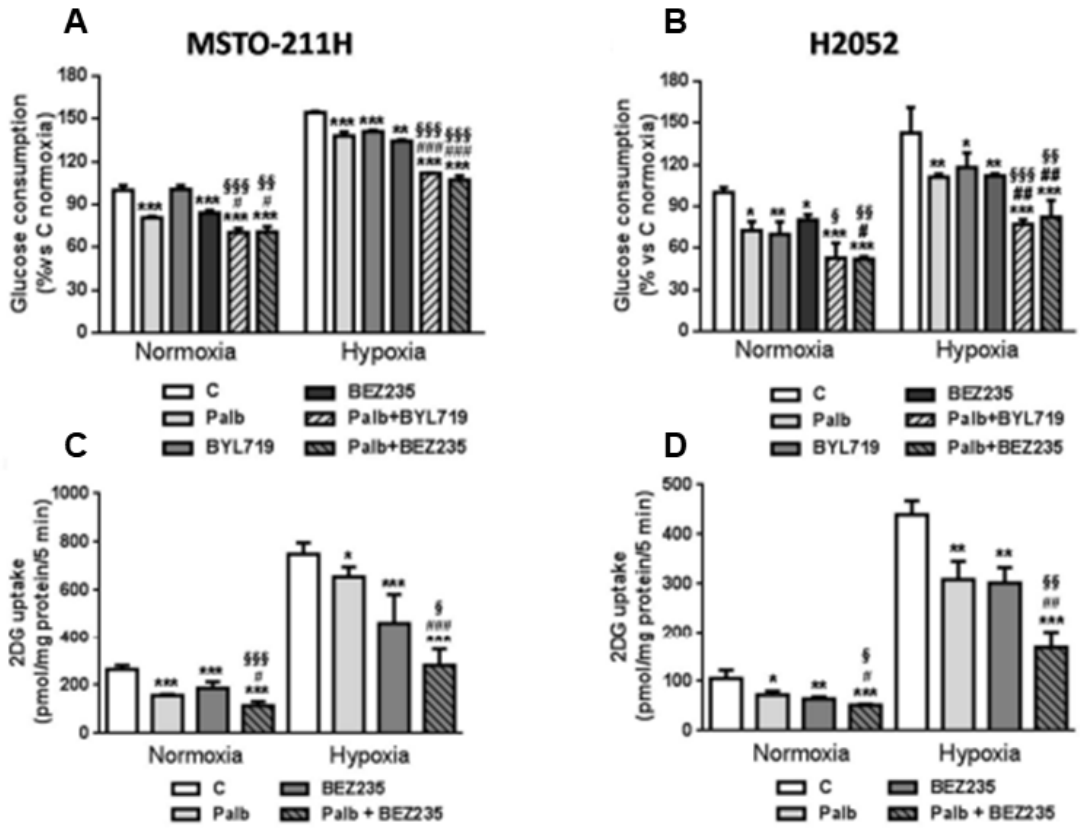

Figure 5. Effect of the combined treatment of palbociclib and PI3K inhibitor BEZ235 or BYL719 on glucose consumption and cellular glucose uptake in MSTO-211H and H28 cells. (A,B) MSTO-211H cells were treated with palbociclib (1 μM), BEZ235 (40 nM), BYL719 (1 μM) and H2052 cells were treated with palbociclib (1 μM), BEZ235 (40 nM), BYL719 (2.5 μM) or palbociclib in association with BEZ235 or BYL719 for 24 h in normoxia and hypoxia conditions. At the end of the treatments, glucose consuption was evaluated with Glucose (HK) assay kit. *p<0.05, **p<0.01, ***p<0.001 vs. C normoxia; #p<0.05, ##p<0.01, ###p<0.001 vs. palbociclib; §p<0.05, §§<0.01, §§§p<0.001 vs BEZ235 or BYL719. (C,D) MSTO-211H and H2052 cells were treated with palbociclib (1 μM) and BEZ235 (40 nM), individually or in association, for 24 h in normoxia and hypoxia conditions. At the end of the treatments, glucose uptake was evaluated. *p<0.05, **p<0.01, ***p<0.001 vs. C; #p<0.05, ##p<0.01, ###p<0.001 vs. palbociclib; §p<0.05, §§<0.01, §§§p<0.001 vs BEZ235.

Subsequently, the effects of the association of palbociclib with PI3K inhibitors were investigated by Western blotting in order to analyze the expression of proteins involved in both cell cycle regulation and cell energy metabolism. MSTO-211H and H2052 cells were treated with palbociclib 1 μM, BEZ235 40 nM or BYL719 (1 μM for MSTO-211H cells or 2.5 μM for H2052 cells), individually or in association (palbociclib + BEZ235 or palbociclib + BYL719) in both normoxic and hypoxic conditions (0.5 % O_2) for 24 hours (Fig.6A-B). The association of palbociclib with BEZ235 or BYL719 induced a decreased expression of the phosphorylated Rb protein and its target c-myc in MSTO-211H cells, more evident in hypoxic condition. On the other hand, H2052 cells treated with single drugs showed a strong decreased of Rb phosphorylation under both normoxic and hypoxic conditions. The inhibition of both Rb and mTOR, due to the combined treatment of palbociclib with BEZ235 or BYL719, induced a decrease in c-myc expression in H2052 cells. Palbociclib induced an increase in the expression of phosphorylated AKT, due to the lack of activation of the Rb protein (Zhang J. et al., 2016), in both MPM cell lines and in both culture conditions. PI3K/mTOR inhibitors reduced phosphorylated AKT in both MSTO-211H and H2052 cells and the association of BEZ235 or BYL719 with palbociclib was more effective in H2052 cells under hypoxic condition. The modulation of mTORC1 was shown by the decrease in 4E-BP1 due to PI3K/mTOR inhibitors used individually and in combination with palbociclib. MSTO-211H cells showed greater 4E-BP1 reduction in hypoxic condition than H2052 cells.

GLUT-1 and HIF-1α were both up-regulated in MSTO-211H cells by hypoxic condition. The association of palbociclib with PI3K inhibitors induced a more evident decrease of GLUT-1 compared to single treatments. On the other hand,

HIF-1α protein levels were reduced only by the treatment with PI3K inhibitors. H2052 cells showed GLUT-1 in both normoxic and hypoxic conditions and hypoxia did not increase its level. Palbociclib strongly reduced the level of expression of GLUT-1, compared to the combined treatments.

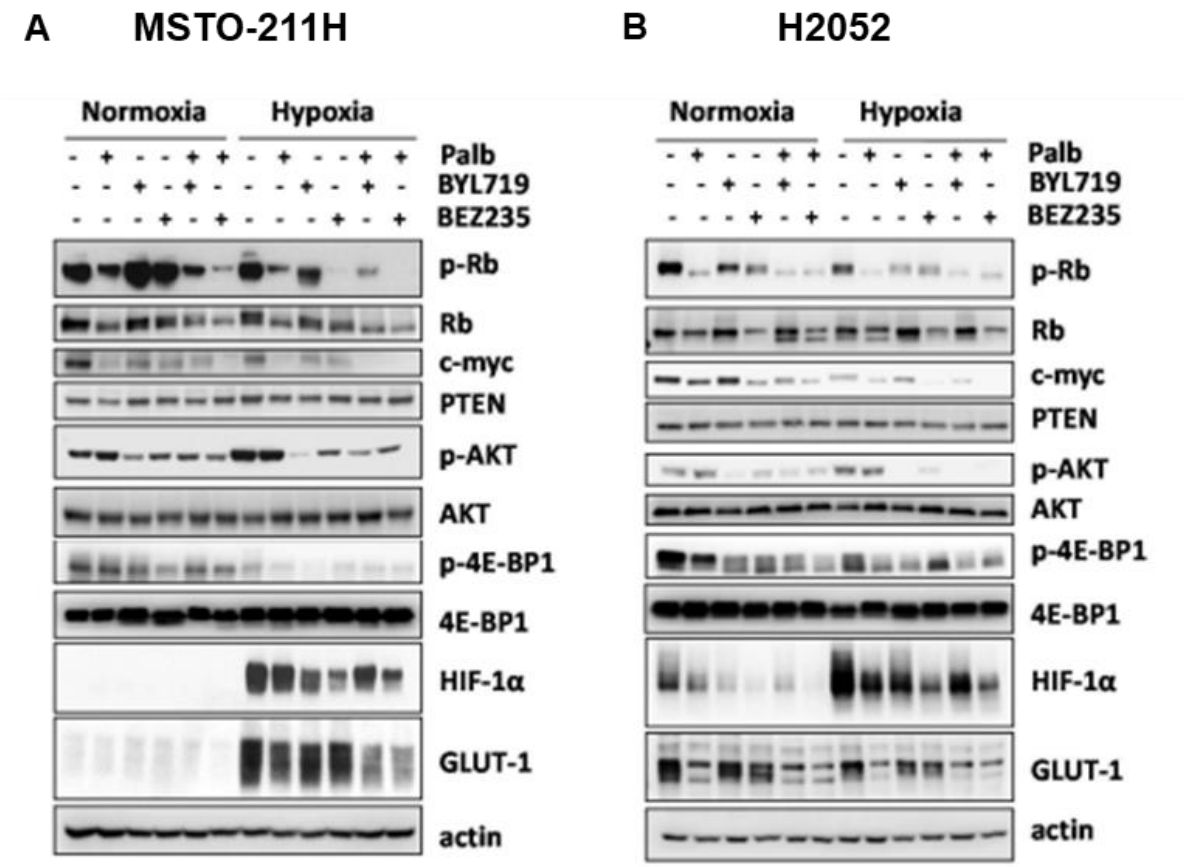

Figure 6. Western blotting analysis of the effects of the combined treatment of palbociclib and PI3K inhibitors on proteins involved in the regulation of cell cycle and glucose metabolism in MSTO-211H and H28 cells. MSTO-211H cells were treated with palbociclib (1 μM), BEZ235 (40 nM), BYL719 (1 μM) and H2052 cells were treated with palbociclib (1 μM), BEZ235 (40 nM), BYL719 (2.5 μM) or palbociclib in association with BEZ235 or BYL719 for 24 h in normoxia and hypoxia conditions. Data were representative of two independent experiments.

4.1.4 Effects of combined inhibition of CDK4/6 and PI3K/AKT/mTOR on mitochondrial respiration in MPM cell lines

To better characterize the effects of palbociclib in association with BEZ235 or BYL719 on metabolism in MSTO-211H and H2052 cells, the Agilent SeaHorse XFp analyzer was used to investigate the mitochondrial function. MSTO-211H and H2052 cells were incubated with palbociclib 1 μM and BEZ235 40 nM individually or with palbociclib in association with BEZ235 for 24 hours.

The cells were analyzed using the Agilent SeaHorse Cell Mito Stress Test, based on a sequential addition of respiration modulators to get mitochondrial metabolic parameters. The mitochondrial activity was measured as oxygen consumption rate (OCR), related to the rate of decrease of oxygen concentration in the assay medium. MSTO-211H and H2052 cells treated with palbociclib or BEZ235 alone showed impaired mitochondrial activity, measured as OCR, whereas the association of palbociclib with BEZ235 caused a more pronounced decrease of this parameter. In fact, as shown in figure 7 A-B, the injection of oligomycin, an enzyme that blocks the production of ATP in the mitochondria, caused a decrease of OCR both in control cells and in treated cells. Subsequently, the addition of the uncoupling agent FCCP rapidly reversed the hyperpolarized state of mitochondria caused by oligomycin and, consequently, the oxygen consumption reaches its maximum, causing an increase in OCR. After FCCP injection, MSTO-211H and H2052 treated cells showed a lower oxygen consumption maximum level than control cells. In fact, the association of palbociclib with BEZ235 maintained OCR at almost baseline levels. Finally, the addition of antimycin A and rotenone, two electron transport chain inhibitors, blocked completely mitochondrial respiration and, as a consequence, OCR decreased at its lowest

level. In this case, the OCR measured a process outside the mitochondria (non-mitochondrial respiration).

Subsequently, the effect of the combined treatment on mitochondrial respiration was evaluated with other parameters in MSTO-211H and H2052 cells (Fig.7C-D). The spare respiratory capacity occured when cells responded to an energy demand, indicating its theoretical maximum. This parameter was obtained by the difference of OCR after FCCP injection and OCR at the baseline. Also in this case, MSTO-211H and H2052 cells treated with the drugs individually and in combination showed a reduced spare respiratory capacity. It is worth of note that MSTO-211H had a greater inhibition of spare respiratory capacity due to the combined treatment than H2052 cells. Taken together these data confirmed again that the drugs prevent the cells from adapting their metabolism when there was an energy demand. Finally, the ATP production was downregulated by the association of palbociclib with BEZ235 in both MPM cell models.

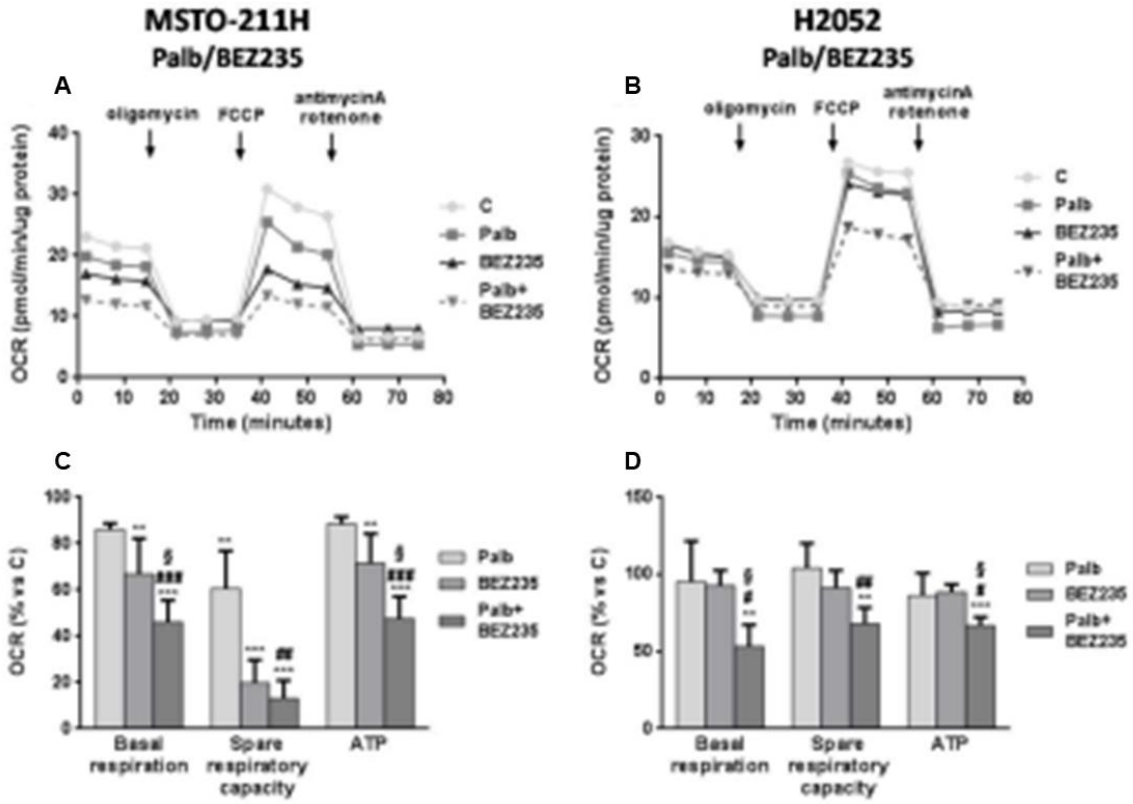

Figure 7. Effect of palbociclib and BEZ235 on mitochondrial activity in MSTO-211H and H2052 cells. (A-B) Oxygen consumption rate (OCR) was measured using Agilent Seahorse XFp analyzer Cell Mito Stress Test Kit. Data were shown as mpH/min normalized to proteins and they were representative of four independent experiments. (C-D) Basal respiration, spare respiratory capacity and ATP production were calculated as percent versus control cells. Data were expressed as the media of at least three independent measurements. *p<0.05, **p<0.01, ***p<0.001 vs. C; #p<0.05, ##p<0.01, ###p<0.001 vs. palbociclib; §p<0.05, §§p<0.01, §§§p<0.001 vs BEZ235.

Subsequently, the same analysis described above was performed on MSTO-211H and H2052 cells to investigate the effects of palbociclib and BYL719 individually or in association on mitochondrial respiration. Cells were incubated with palbociclib 1 μM and BYL719 1 μM for MSTO-211H cells or BYL719 2.5 μM for H2052 cells, alone or in association, for 24 hours. MSTO-211H and H2052 cells treated with the association of palbociclib with BYL719 showed a stronger downregulation of mitochondrial activity, measured as OCR, in comparison with single drug treatment (Fig.8A-B). Also in this case, MSTO-211H and H2052 cells showed an inhibition of spare respiratory capacity due to the combined treatment (Fig.8C-D). This inhibition was more pronounced in MSTO-211H cells than in H2052 cells, highlighting again the ability of H2052 cells to better adapt to stress conditions. The association of palbociclib with BYL719 inhibited ATP production very little in both MPM cell models.

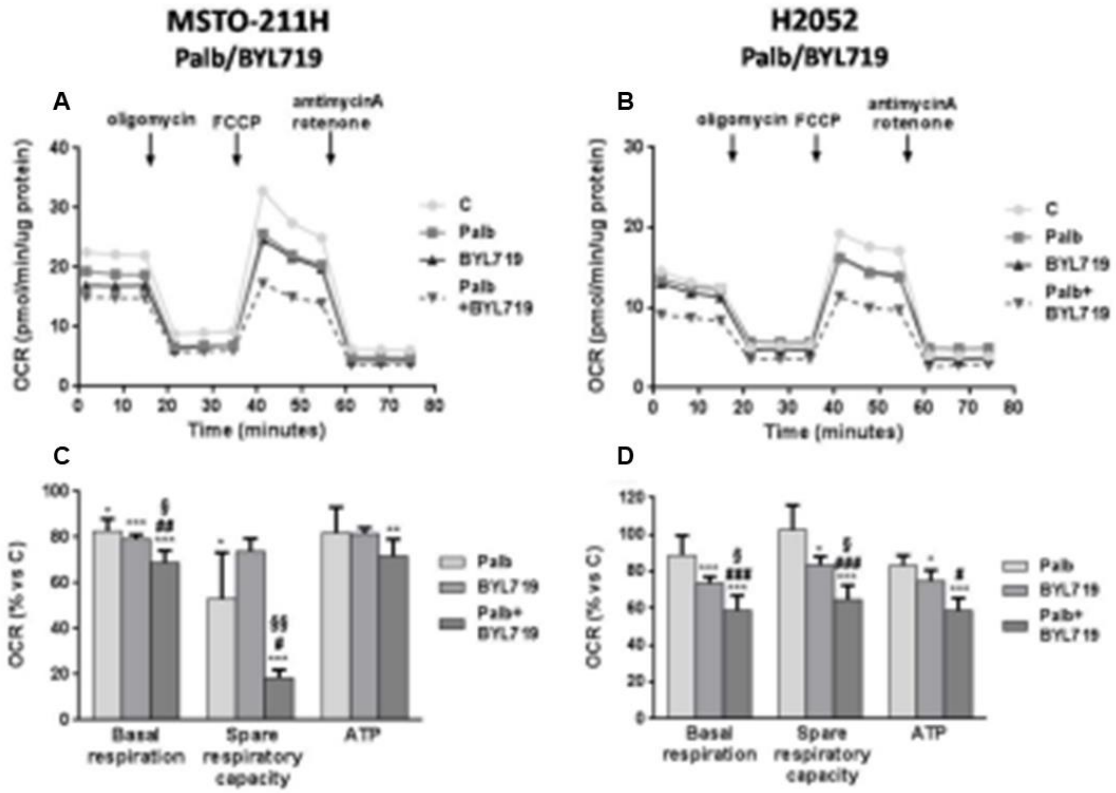

Figure 8. Effect of palbociclib and BYL719 on mitochondrial activity in MSTO-211H and H2052 cells. Oxygen consumption rate (OCR) was measured using Agilent Seahorse XFp analyzer Cell Mito Stress Test Kit. (A-B) Oxygen consumption rate (OCR) was measured using Agilent Seahorse XFp analyzer Cell Mito Stress Test Kit. Data were shown as mpH/min normalized to proteins and they were representative of four independent experiments. (C-D) Basal respiration, spare respiratory capacity and ATP production were calculated as percent versus control cells. Data were expressed as the media of at least three independent measurements. *p<0.05, **p<0.01, ***p<0.001 vs. C; #p<0.05, ##p<0.01, ###p<0.001 vs. palbociclib; §p<0.05, §§<0.01, §§§p<0.001 vs BYL719.

4.2 Effects of abemaciclib combined with cisplatin and pemetrexed in MPM cell lines

As previously demonstrated, palbociclib had an anticancer effect on human MPM cell lines, highlighting that CDK4/6 inhibitors could play a role in the treatment of MPM (Bonelli M. A. et al., Neoplasia, 2017). This part of the research aimed to investigate on MPM cell lines the anticancer effects of abemaciclib in association with the standard chemotherapy approved as first line treatment in MPM patients. First, IC_{50} values of abemaciclib, cisplatin and pemetrexed have been determined for MSTO-211H, H2452, H28 and ZS-LP cell lines (Table 1). All the MPM cell lines analyzed were sensitive to abemaciclib, with IC_{50} values ranging from 0.5 to 1 μM. By contrast, the MPM cell lines had a variable response to cisplatin and pemetrexed. In fact, MSTO-211H cells were the most sensitive to cisplatin while ZS-LP cells were the most resistant, with IC_{50} values of 0.4 μM and 4.0 μM respectively. H2452 cells were the most resistant to pemetrexed, with an IC_{50} value of 0.5 μM.

Cell line	**Abemaciclib**	**Cisplatin**	**Pemetrexed**
MSTO-211H	0.5 μM	0.4 μM	0.03 μM
H2452	1.5 μM	2.6 μM	0.5 μM
H28	1.2 μM	2.5 μM	0.06 μM
ZS-LP	1 μM	4.0 μM	0.04 μM

Table 1. Abemaciclib, cisplatin and pemetrexed sensitivity in MPM cell lines. After 24 h from seeding, MPM cell lines were treated with increased concentrations of abemaciclib, cisplatin and pemetrexed for 72 h. Cells proliferation was assessed by MTT assay and data, expressed as a percentage of inhibition versus control, were representative of three independent experiments. IC_{50} values were calculated using GraphPad Prism 8.00 software.

Then, MSTO-211H, H28 and ZS-LP cells were used to investigate the effects of abemaciclib in combination with cisplatin and pemetrexed on cell proliferation (Fig.9). Two different schedules of combination were tested: a simultaneous and a sequential treatment. In the first schedule, cells were treated with the association of cisplatin and pemetrexed or abemaciclib combined with cisplatin and pemetrexed. The second approach was based on a sequential treatment; in in this case, cells were treated with abemaciclib for 24 hours, then abemaciclib was removed and the cells were exposed to the association of cisplatin and pemetrexed or to the association of abemaciclib with cisplatin and pemetrexed, for further 48 hours. Simultaneous treatment with abemaciclib in combination with cisplatin and pemetrexed induced a greater inhibition of cell proliferation than the other treatments, in both MSTO-211H and H28 cells (Fig.9A-B). It is worth of note that the sequential treatment (replacement of abemaciclib after 24 hours with abemaciclib combined with cisplatin and pemetrexed) caused an inhibitory effect on ZS-LP cells similar to that observed in the simultaneous treatment (abemaciclib combined with cisplatin and pemetrexed) (Fig.9C). As demonstrated by the Bliss experimental model, the simultaneous association of abemaciclib with chemotherapy produced a synergistic inhibitory effect on cell proliferation in MSTO-211H cells (Fig.9D). Additive inhibitory effect was observed in H28 and ZS-LP cells, due to the abemaciclib combined with cisplatin and pemetrexed (Fig.9E-F). On the basis of these results, the simultaneous treatment of abemaciclib in association with cisplatin and pemetrexed was used for subsequent experiments.

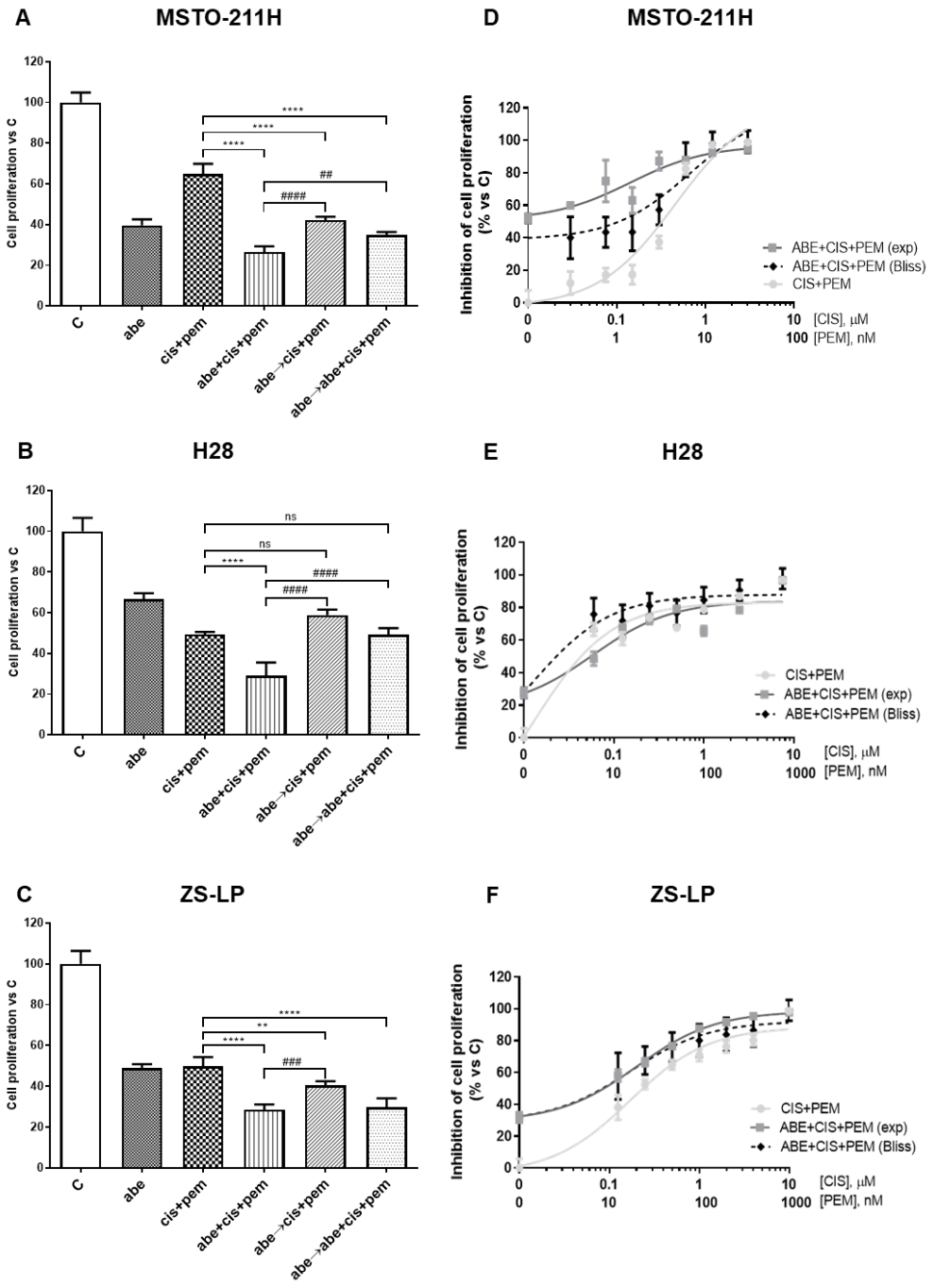

Figure 9. Effects of the combination of abemaciclib with cisplatin and pemetrexed on cell growth in MPM cell lines. (A-B-C) MSTO-211H cells were treated with abemaclib (0.5 μM), cisplatin (0.3 μM) and pemetrexed (0.02 μM). H28 and ZS-LP cells were treated with abemaclib (1 μM), cisplatin (1 μM) and pemetrexed (0.05 μM). Cells proliferation was assessed by MTT assay and data, expressed as a percentage of cell proliferation versus control, were representative of three independent experiments. Comparison among groups was made by using analysis of variance (one-way ANOVA), followed by Bonferroni's post-test. (D-E-F) The type of interaction (synergistic, additive, antagonistic) was evaluated through Bliss analysis. MSTO-211H cells were treated with abemaclib 0.5 μM, H28 and ZS-LP cells with abemaciclib 0.8 μM and with increased concentrations of cisplatin and pemetrexed. Data were expressed as a percentage of inhibition versus control. Cells proliferation was assessed by MTT assay and data were representative of three independent experiments. **p<0.01, ****p<0.0001 vs. cis+pem; ##p<0.01, ###p<0.001, ####p<0.0001 vs. abe+cis+pem.

Then, the effects of the association of abemaciclib with cisplatin and pemetrexed were investigated by Western blotting in both MSTO-211H and H28 cells, in order to evaluate the expression of proteins having a role in cell cycle regulation (Fig.10). Simultaneous treatment seemed to have different effects on the inhibition of cell proliferation in the MPM cell lines analyzed. Abemaciclib, alone or in association with cisplatin, pemetrexed or the combination of cisplatin and pemetrexed induced a decrease in the expression of pRb in both MPM cell lines. MSTO-211H cells showed a greater reduction in Rb expression than H28 cells, under the same treatment conditions described above. MSTO-211H cells treated with abemaciclib alone and in combination with cisplatin, pemetrexed or the association of cisplatin and pemetrexed showed a decrease in c-myc levels (Fig.10A). p-AKT (thr) expression was dramatically reduced by the simultaneous treatment of abemaciclib combined with chemotherapy drugs in MSTO-211H cells (Fig.10A). By contrast, H28 cells had a strong reduction in c-myc levels induced by the simultaneous treatment of abemaciclib in association with cisplatin and pemetrexed (Fig.10B). Moreover, the expression of p-AKT (thr) was drastically reduced by abemaciclib alone and in combination with cisplatin, pemetrexed or the association of cisplatin and pemetrexed in H28 cells (Fig.10B).

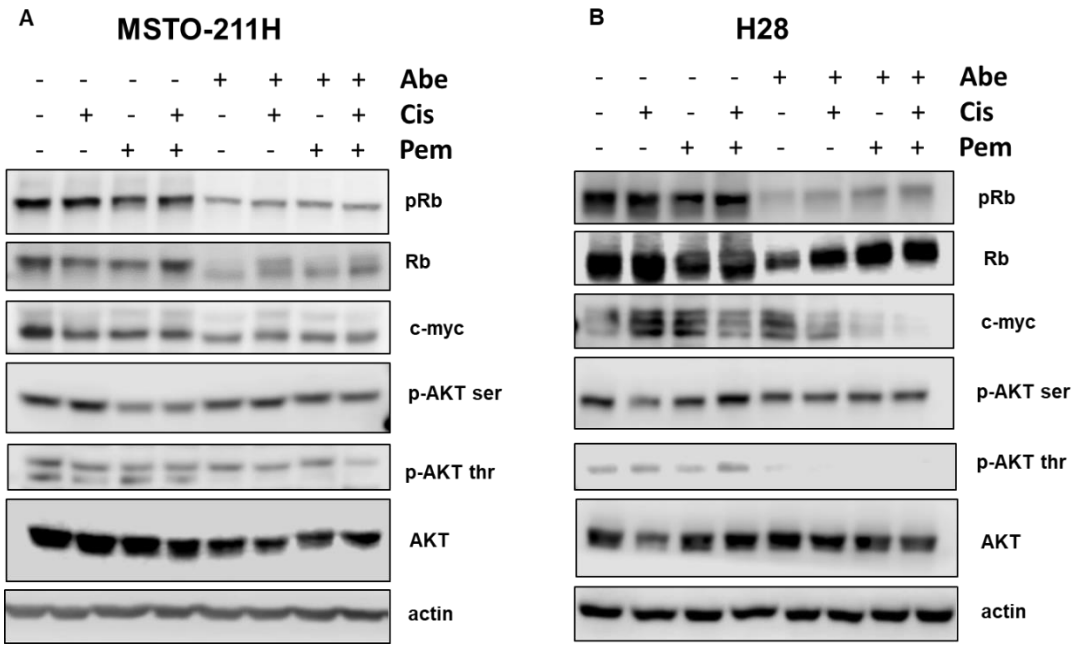

Figure 10. Western blotting analysis of the antiproliferative effects of the combined treatment of abemaciclib with cisplatin and pemetrexed on proteins involved in the regulation of cell cycle. (A) MSTO-211H cells were treated with abemaclib (0.5 μM), cisplatin (0.3 μM) and pemetrexed (0.02 μM) for 24 h. (B) H28 cells were treated with abemaclib (1 μM), cisplatin (1 μM) and pemetrexed (0.05 μM) for 24 h. At the end of the treatments, the expression levels of proteins involved in signal trasduction was analyzed by Western blotting. Data were representative of two independent experiments.

Since it is well known that CDK4/6 inhibitors might cause senescence, the next step was to investigate the effects of the association of abemaciclib with cisplatin and pemetrexed on the induction of senescence in both MPM cell lines. Abemaciclib alone and in combination with cisplatin, pemetrexed or the association of cisplatin and pemetrexed caused an accumulation of senescent-like cells, with flat and enlarged morphology, in MSTO-211H cells (Fig.11B). As shown in figure 11A, abemaciclib alone induced about 40% of senescent cells. Abemaciclib combined with cisplatin or pemetrexed caused about 60% of senescent cells while the simultaneous treatment of abemaciclib in association with chemotherapy drugs induced almost 80 % of senescent cells. Unlike MSTO-211H cells, no senescence was observed in H28 cells (data not shown).

Finally, to test for the reversibility of the effects of the simultaneous treatment of abemaciclib combined with cisplatin and pemetrexed, MSTO-211H cells were treated with the drugs for 72 hours; then, the medium was replaced with drug-free medium and the cells were cultured for additional 72 hours (fig.11C). After the recovery period, MSTO-211H cells treated with cisplatin and pemetrexed, alone or in combination, showed a resumption of cell proliferation. By contrast, abemaciclib in association with cisplatin showed a greater inhibition of the resumption of cell proliferation in MSTO-211H cells compared to abemaciclib combined with pemetrexed. The simultaneous treatment of abemaciclib in association with cisplatin and pemetrexed caused the highest inhibition of the resumption of cell proliferation in MSTO-211H cells, indicating that this treatment caused an irreversible inhibition of cell proliferation.

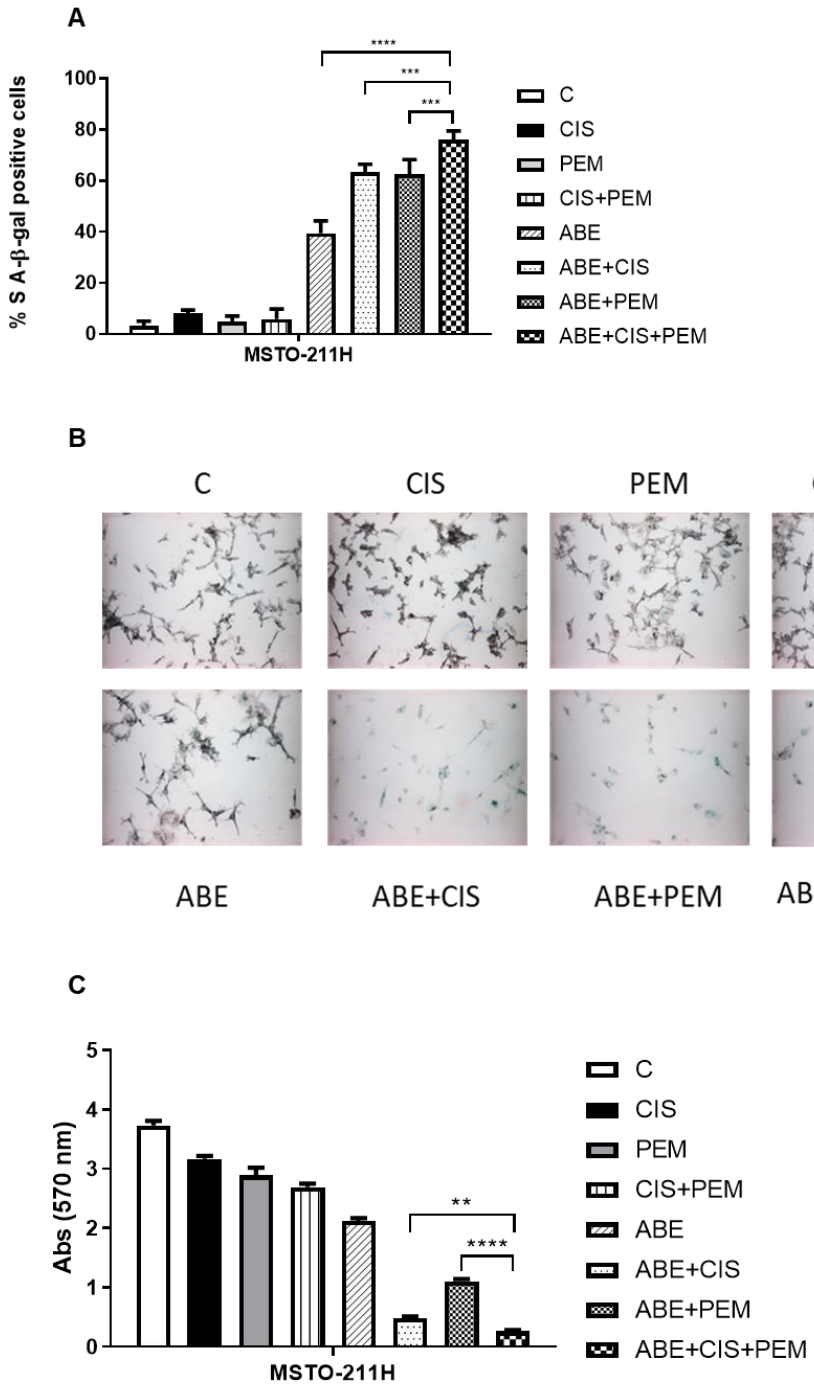

Figure 11. Effects of abemaciclib in association with cisplatin and pemetrexed on senescence induction in MSTO-211H cells. MSTO-211H cells were treated with abemaciclib (1 μM), cisplatin (0.3 μM) and pemetrexed (0.02 μM) after 72 h. (A) Histograms represented the percentage of senescent cells positive for SA-β-Gal expression. Comparison among groups was made by using analysis of variance (one-way ANOVA), followed by Bonferroni's post-test. (B) Representative images of MSTO-211H cells, treated as described above, stained with SA-β-Gal Kit. (C) Effects of removal of abemaciclib, cisplatin and pemetrexed on cell proliferation in MSTO-211H cells. Cells were treated with abemaciclib (0.5 μM), cisplatin (0.3 μM) and pemetrexed (0.02 μM) for 72 h; then, cells were cultured for additional 72 h in a drug-free medium (recovery time). Cell proliferation was evaluated by crystal violet staining. Comparison among groups was made by using analysis of variance (one-way ANOVA), followed by Bonferroni's post-test. **p<0.01 ***p<0.001, ****p<0.0001 vs. abe+cis+pem.

As shown in figure 12 (A-B), abemaciclib in association with cisplatin and pemetrexed had a different effect on cell death in MSTO-211H and H28 cells. In fact, abemaciclib alone and in combination with cisplatin or pemetrexed caused about 10% of cell death in MSTO-211H cells. The simultaneous treatment of abemaciclib combined with cisplatin and pemetrexed induced about 15% of cell death in MSTO-211H cells. By contrast, the association of abemaciclib with cisplatin or pemetrexed caused about 20 % of cell death in H28 cells. In addition, the percentage of cell death reached about 30% in H28 cells treated with the simultaneous treatment of abemaciclib combined with cisplatin and pemetrexed. Then, the expression level of proteins involved in cell cycle arrest, senescence induction and autophagy was evaluated on both MSTO-211H and H28 cells (Fig.12C-D). In MSTO-211H cells, Abemaciclib alone and in combination with cisplatin, pemetrexed or the association of cisplatin and pemetrexed caused a strong decrease in MDM2 phosphorylation, consequently inducing the accumulation of p53 and p21. Finally, an accumulation of cyclin D1 was observed in MSTO-211 cells treated with abemaciclib alone and in combination with cisplatin, pemetrexed or the association of cisplatin and pemetrexed. By contrast, H28 cells treated with abemaciclib alone and in combination with cisplatin, pemetrexed or the association of cisplatin and pemetrexed showed a reduction of the expression of p53, p21 and p27. Activation of lipidate microtubule-associated protein light chain 3 (LC3B), considered a marker of autophagy, was observed in H28 cells treated with abemaciclib alone and in combination with cisplatin, pemetrexed or the association of cisplatin and pemetrexed. In fact, abemaciclib induced an increase in cell size and the formation of cytoplasmic vacuoles in H28 cells, confirming an autophagic phenotype (Fig.12Ea-b).

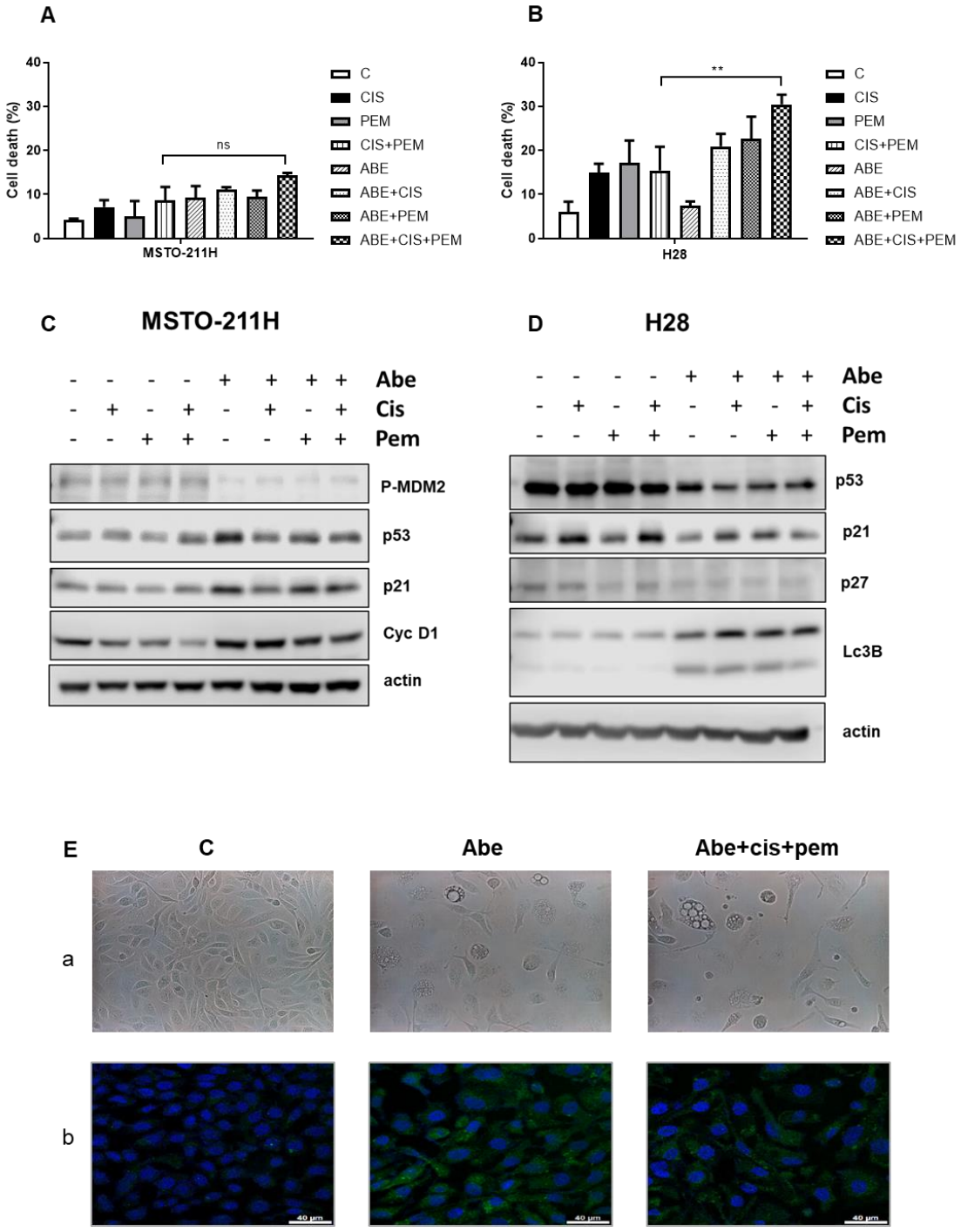

Figure 12. Effects of abemaciclib in association with cisplatin and pemetrexed on cell death in MSTO-211H and H28 cells. MSTO-211H cells were treated with abemaciclib (1 μM), cisplatin (0.3 μM) and pemetrexed (0.02 μM) for 72 h. H28 cells were treated with abemaciclib (1 μM), cisplatin (0.5 μM) and pemetrexed (0.05 μM) for 72 h. (A-B) Histograms represented the percentage of dead cells staining with Hoechst 33342 and Propidium Iodide. Comparison among groups was made by using analysis of variance (one-way ANOVA), followed by Bonferroni's post-test. (C-D) Western blotting analysis on proteins involved in cell cycle regulation and senescence induction. Data were representative of two independent experiments. (E) Representative images of H28 cells, treated as described above, stained with CYTO-ID^R Autophagy detection Kit 2.0 (b). **p<0.01 vs. abe+cis+pem.

4.3 Effects of dual inhibition of CDK4/6 and CDK9 in MPM cell lines

VS2-370 is a new molecule developed to simultaneously inhibit CDK4/6 and CDK9. This is the first *in vitro* study that aimed to investigate the antitumor effects of VS2-370 in MPM cell lines.

As shown in table 2, all the MPM cell lines analyzed showed a greater sensitivity to VS2-370 than the other CDK4/6 inhibitors.

Cell line	**VS2-370**	**Abemaciclib**	**Palbociclib**
MSTO-211H	0.05 μM	0.5 μM	0.3 μM
H2452	0.13 μM	1.5 μM	0.7 μM
H28	0.11 μM	1.2 μM	0.3 μM
H2052	0.18 μM	0.5 μM	1.2 μM

Table 2. CDK4/6 inhibitors and VS2-370 sensitivity in MPM cell lines. After 24 h from seeding, MPM cell lines were treated with increased concentrations of VS2-370, abemaciclib and palbociclib for 72 h. Cells proliferation was assessed by MTT assay and data, expressed as a percentage of inhibition versus control, were representative of three independent experiments. IC_{50} values were calculated using GraphPad Prism 8.00 software.

Then, the antiproliferative effects of VS2-370 were investigated by Western blotting in both MSTO-211H and H28 cell lines (Fig.13). In fact, the expression levels of different proteins involved in the regulation of the cell cycle were evaluated on both MPM cell lines, treated with increased concentrations of VS2-370. The expression of pRb and c-myc decreased in a dose-dependent manner in MSTO-211H cells. The highest concentration of VS2-370 downregulated Rb protein expression in MSTO-211H cells. Furthermore, the two higher doses of

VS2-370 caused a drastic reduction of the expression of pMAPK and, similarly MAPK expression was reduced in a dose-dependent manner. A reduction in pMAPK expression was also observed with the two highest concentrations of VS2-370 in H28 cells. Treatment with VS2-370 down-regulated p-AKT (ser) in a dose–dependent manner in both MPM cell lines, whereas a reduction in p-AKT (thr) expression was observed only in MSTO-211H cells. The impairment in the AKT/mTOR pathway was demonstrated in both MPM cell lines by the reduced activation of p-4EBP1, a downstream effector of mTOR.

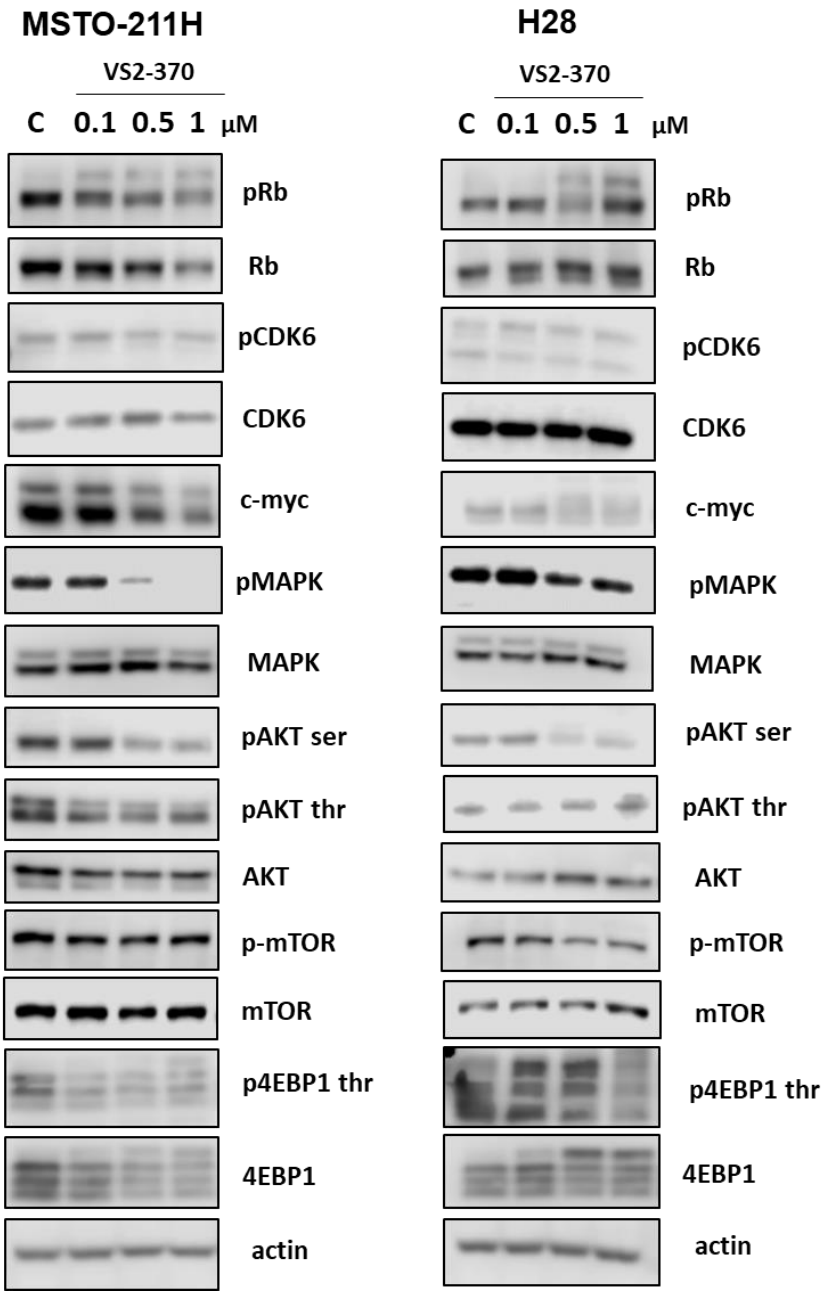

Figure 13. Western blotting analysis of the effects of VS2-370 on proteins involved in the regulation of cell cycle and in signal transduction pathways. MSTO-211H and H28 cells were treated with increasing concentration of VS2-370 (0.1, 0.5 and 1 μM) for 24 h. Data were representative of two independent experiments.

Subsequently, the effects of VS2-370 on cell death were investigated in both MSTO-211H and H28 cells, treated with increased concentrations of the drug for 72 hours (Fig.14). Signs of death were detected in both MPM cell lines, in a dose-dependent manner. As shown in figure 3A, MSTO-211H cells were more sensitive towards VS2-370 than H28 cells. In fact, the percentage of cell death in MSTO-211H cells reached about 50% at the intermediate concentration of the drug and reached 100% at the highest concentration. Instead, H28 cells showed a death rate of just over 50% at the highest concentration of VS2-370. These data suggested that VS2-370 induced cytotoxic effects in MPM cell lines. By contrast, CDK4/6 inhibitors palbociclib and abemaciclib showed cytostatic effects on MSTO-211H cells. In fact, as previously demonstrated, palbociclib induced a rate of cell death below 10% in MSTO-211H cells (Bonelli M. A. et al., Neoplasia, 2017) and a similar rate of cell death was also observed in both MSTO-211H and H28 cells treated with abemaciclib. Then, the expression level of different proteins involved in cell death signaling was evaluated on both MPM cell lines (Fig.14C-D). The expression of MCL1, a target of CDK9, decreased at the highest concentration of VS2-370 in MSTO-211H (Fig.14C), whereas in H28 cells MCL1 expression was reduced in a dose-dependent manner (Fig.14D). An increased expression of p53 and p21 was observed in a dose-dependent manner in MSTO-211H cells (Fig.14C). All drug concentrations induced an increase in p21 expression in H28 cells (Fig.14D). Caspase 3 activation was observed at the two highest doses of VS2-370 in both MPM cell lines (Fig.14C-D), indicating apoptotic cell death.

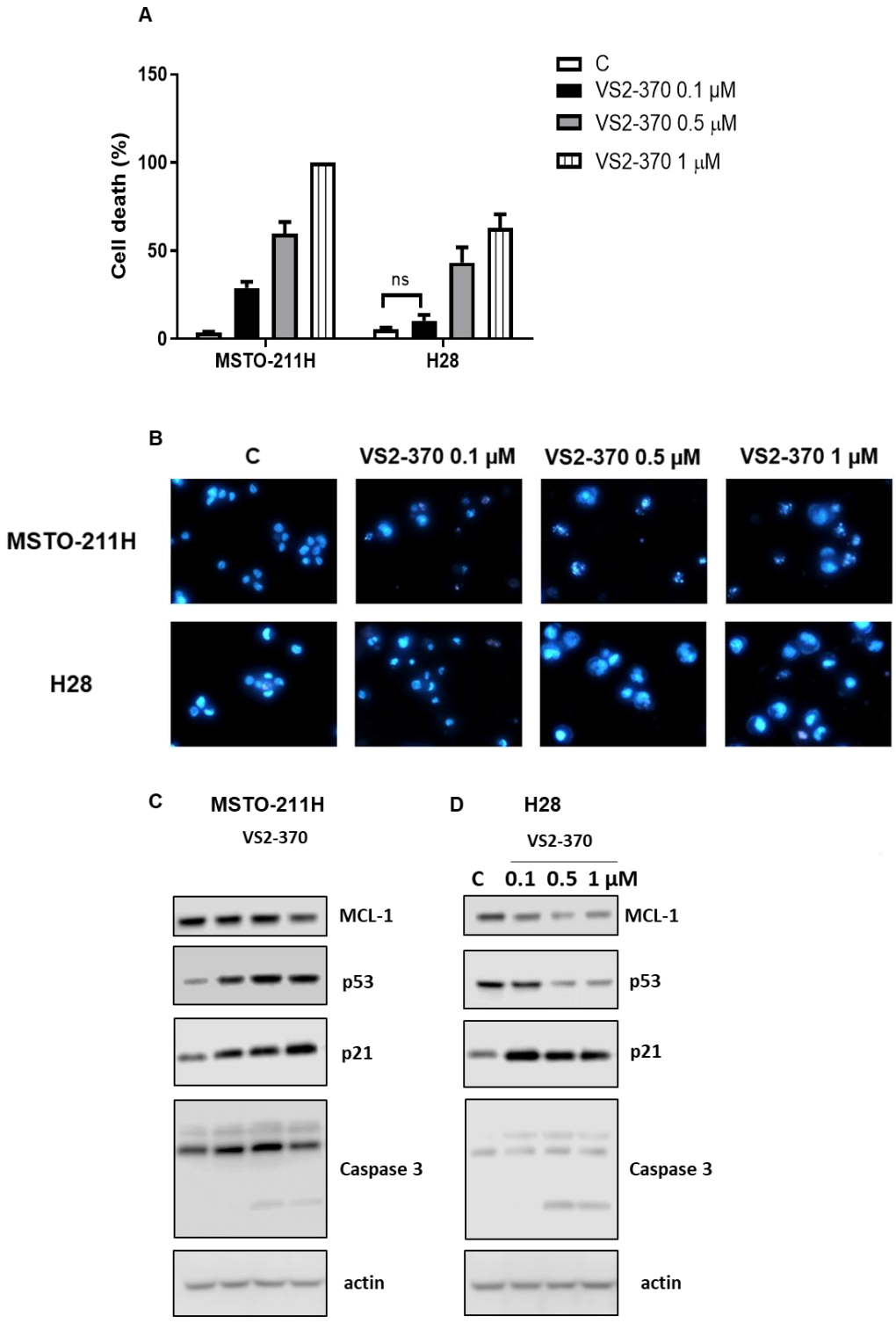

Figure 14. Effects of VS2-370 on cell death in MSTO-211H and H28 cells. Cells were treated with increasing concentration of VS2-370 (0.1, 0.5 and 1 µM) for 72 h. (A) Histograms represented the percentage of dead cells staining with Hoechst 33342 and Propidium Iodide. Comparison among groups was made by using analysis of variance (one-way ANOVA), followed by Bonferroni's post-test. (B) Representative images of MSTO-211H and H28, treated as described above, stained with Hoechst 33342 and Propidium Iodide. (C) Western blotting analysis of the effects of VS2-370 on proteins involved in cell death pathways. Data were representative of two independent experiments.

5. Discussion

MPM is a malignant tumor of the pleura, predominantly asbestos related and supported by a chronic inflammatory process. This rare and aggressive malignancy is characterized by poor prognosis, due to limited therapeutic options. In 2003, the association of cisplatin and pemetrexed was approved as first-line therapy for the treatment of MPM (Vogelzang N. J. et al., 2003). Very recently, nivolumab combined with ipilimumab has been approved by US FDA as first line treatment in untreated patients with unresectable MPM (Baas P. et al., 2021). Currently, there is no approved second-line treatment option, although many pre-clinical and clinical studies have investigated new anticancer strategies for MPM. MPM is currently considered a heterogeneous tumor with a variety of genomic and molecular alterations including the loss of tumor suppressor genes such as, *CDKN2A/ARF*, *BAP1* and *NF2*, single nucleotide polymorphisms (SNP_s) in genes involved in DNA repair mechanisms (Panou V. et al., 2020) and epigenetic and non-coding RNA_s mutations (Hmeljak J. et al., 2018; Cakiroglu E.et al., 2020). Investigating the genomic background of MPM aims to search for a molecular target to find a therapeutic approach in the context of precision medicine.

Based on these considerations, this *in vitro* study aims to investigate new anticancer strategies for the treatment of MPM.

The lack of the *CDKN2A/ARF* gene in most forms of MPM may justify the use of CDK4/6 inhibitors, in order to inhibit the Rb/E2F/myc axis. The combination with PI3K inhibitors results from the fact that the downregulation of Rb causes activation of PI3K/AKT/mTOR pathway (Zhang et al., 2016). As previously demonstrated by our research group, palbociclib combined with PI3K inhibitors BEZ235 or BYL719 synergistically inhibited proliferation in MPM cell lines (Bonelli

M. A. et al., Neoplasia, 2017). In the context of cancer, both Rb/E2F/myc and PI3K/AKT/mTOR pathways have a crucial role also in reprogramming of the cellular metabolism. The Warburg effect is considered a characteristic of malignant tumors, including MPM. In fact, MPM is characterized by the activation of PI3K/AKT/mTOR axis, caused by high levels of ROS in the tumor microenvironment (Urso L. et al., 2020). ROS can directly promote the inactivation of phosphatase and tensin homolog (PTEN), which acts as a negative regulator of PI3K/AKT/mTOR pathway (Urso L. et al., 2020). In fact, a recent study shows that PTEN is lost in most sarcomatoid histotype MPM (Marques M. et al., 2020). Moreover, MPM patients frequently show mutation of PI3K, associated with a poor prognosis (Lo Iacono M. et al., 2015; Hylebos M. et al., 2016). Tumors characterized by the loss of the *NF2* gene show hyperactivation of mTOR (Cooper J. et al., 2017). *NF2* gene is mutated in H2052 cell line, highlighting the possibility that hyperactivation of PI3K/AKT/mTOR pathway may promote the Warburg effect (Sekido Y. et al., 1995).

Based on this background, we investigated the effects of both inhibition of Rb/E2F/myc and PI3K/AKT/mTOR pathways on energy metabolism to find a new therapeutic strategy for the treatment of MPM.

This study showed that MSTO-211H, H2052, H2452 and H28 cells had a different metabolic profile. It is worth of note that H2052 cells were characterized by a greater metabolic plasticity than other MPM cell lines, despite having the lowest energy phenotype. In fact, these cells adapted to metabolic stress conditions, including the absence of glucose and hypoxia, by reprogramming their energy metabolism. Palbociclib combined with BEZ235 or BYL719 had a greater impact on glucose metabolism than the same drugs used alone. In fact, MSTO-211H

and H2052 cells were characterized by a significant reduction of the parameters of glycolysis, glycolytic capacity and glycolytic reserve, obtained from ECAR measurements. These data suggested that MPM cell lines treated with palbociclib in association with PI3K inhibitors failed to increase energy metabolism under metabolic stress conditions, avoiding metabolic adaptation. The effects of palbociclib combined with PI3K inhibitors on glucose metabolism in MSTO-211H and H2052 cells were confirmed by a significant decrease of both glucose consumption and glucose uptake, even in hypoxia. It is worth of note that MSTO-211H cells, despite having the highest energy phenotype, were unable to proliferate in the absence of glucose, highlighting their inability to adapt to conditions of strong metabolic stress.

In the context of molecular mechanisms, palbociclib affected glycolysis by downregulation of Rb/E2F/myc pathway in both MSTO-211H and H2052 cell lines. It is worth of note that palbociclib decreased the expression of HIF-1α in both normoxia and hypoxia. The downregulation of HIF-1α by palbociclib was also detected in colon cancer cells (Zhang J. et al., 2017). The expression of HIF-1α was also strongly inhibited by PI3K inhibitors in both MSTO-211H and H2052 cell lines. In fact, the PI3K/AKT/mTOR pathway had a crucial role also in the regulation of HIF-1α (Bakker W. J. et al., 2007). Both c-myc and HIF-1α regulate the transcription of several genes involved in the glycolytic process, such as pyruvate dehydrogenase 1 and hexokinase 2 (Kim J. V. et al., 2007), and in glucose uptake, such as glucose transporter protein 1 (GLUT-1) (Gordan J. D. et al., 2007). Our results demonstrated that the inhibition of both these transcription factors, observed after the treatment with palbociclib combined with PI3K inhibitors, significantly reduced the glycolytic activity of MPM cells, affecting

glucose uptake and glucose consumption. A previous study showed that inhibition of mTORC1/C2 and HIF-1α caused a decrease in 18F-FDG uptake in MPM cells, highlighting a new target for the treatment of this malignancy (Kaira K. et al., 2012).

The association of palbociclib with PI3K inhibitors had also an inhibitory effect on mitochondrial oxidative metabolism. In fact, the parameters of basal respiration, spare respiratory capacity and ATP production, obtained from OCR measurements, decreased due to the combined treatment in both MPM cell lines. This inhibitory effect could be explained by the inhibition of both Rb/E2F/myc and PI3K/AKT/mTOR pathways. In fact, c-myc was involved in the expression of many mitochondrial genes including cytochrome c, having a key role in the mitochondrial respiration (Morrish F. et al., 2014). mTORC1 also regulates mitochondrial genes that code for Transcription Factor A Mitochondrial (TFAM) and for proteins having a role in the electron transport chain (Morita M. et al., 2015).

Taken together these data suggested that the combined inhibition of Rb/E2F/myc and PI3K/AKT/mTOR pathways impaired both glucose and mitochondrial metabolism in MPM cell lines, showing the antitumor efficacy of this therapeutic strategy. The association of palbociclib with PI3K inhibitors could represents a new therapeutic approach for the treatment of MPM.

Chemotherapy, based on the combination of cisplatin with pemetrexed, still remains the standard first line treatment approach for MPM patients. Recently, both *in vitro* and *in vivo* studies have demonstrated the antitumor efficacy of CDK4/6 inhibitors for the treatment of MPM (Bonelli M. A. et al., Neoplasia, 2017;

Aliagas E. et al., 2021). Based on these considerations, this part of the study aimed to investigate the antitumor efficacy of a treatment schedule based on the association of abemaciclib with cisplatin and pemetrexed in MPM cell lines. Cytotoxic chemotherapeutic drugs usually act on cells in the S phase of the cell cycle. On the other hand, the CDK4/6 inhibitors exhibit their anticancer effect by causing cell cycle arrest. Based on these considerations, the combination of these two types of drugs for the treatment of tumors would seem to have no rationale. Despite this expected antagonistic effect, in recent years preclinical (Cretella D. et al., 2019; Salvador-Barbero B. et al., 2020) and clinical (Clark A. S. et al., 2019) studies have shown that the combination of CDK4/6 inhibitors and chemotherapy drugs was a safe and feasible therapeutic approach for the treatment of different types of cancer.

Abemaciclib is the only CDK4/6 inhibitor used as a monotherapy for the treatment of breast cancer (Dickler M. N. et al., 2017). In fact, abemaciclib differs from the other two CDK4/6 inhibitors for some characteristics: a different molecular structure, the highest affinity towards its targets (Hafner M. et al., 2019) and a low myelotoxicity (Vidula N. et al., 2016). In addition, abemaciclib is administered with a continuous therapeutic approach while palbociclib and ribociclib need a period of interruption (Patnaik A. et al., 2016). Currently, many clinical trials are evaluating the effects of abemaciclib in different types of cancers, including MPM (Chong Q. Y. et al., 2020). An ongoing phase II clinical trial aims to investigate the antitumor effects of various types of drugs, including abemaciclib, on MPM patients (NCT03654833).

In this study, abemaciclib was effective in three commercial MPM cell lines and in a primary cell line derived from the pleural fluid of a MPM patient. The sensitivity

of MPM cell lines to cisplatin and pemetrexed was also evaluated. In this case, MSTO-211H cells were the most sensitive to both cisplatin and pemetrexed. By contrast, ZS-LP cells and H2452 cells were the most resistant to cisplatin and pemetrexed respectively. Subsequently, the type of association of abemaciclib with cisplatin and pemetrexed (simultaneous or sequential treatment) was investigated in MSTO-211H, H28 and ZS-LP cells. Simultaneous treatment, based on the association of abemaciclib with cisplatin and pemetrexed, showed the greatest inhibition of cell growth in both MSTO-211H and H28 cells. In fact, synergistic/additive inhibitory effects on cell proliferation were observed in MSTO-211H, H28 and ZS-LP cell lines treated with abemaciclib combined with cisplatin and pemetrexed.

In the context of cell cycle progression, abemaciclib alone or in combination with cisplatin, pemetrexed or the association of cisplatin and pemetrexed induced a downregulation of pRb and c-myc in both MSTO-211H and H28 cells, confirming its inhibitory effect on the Rb/E2F/myc pathway. H28 cellls treated with abemaciclib alone and in combination with cisplatin, pemetrexed or the association of cisplatin and pemetrexed showed a stronger downregulation of p-AKT (thr) expression than MSTO-211H cells.

Since it is well established that CDK4/6 inhibitors predominantly have a cytostatic effect, we evaluated whether the association with chemotherapy might induce cell death. This study showed that the rate of cell death caused by the simultaneous treatment of abemaciclib combined with cisplatin and pemetrexed is lower in MSTO-211H cells than in H28 cells. As previously demonstrated by an *in vitro* study, the CDK4/6 inhibitor palbociclib also induces less than 10% cell death in MSTO-211H cells (Bonelli M. A. et al., Neoplasia, 2017). These findings

suggested that both abemaciclib and palbociclib promoted senescence in MSTO-211H cells, showing a cytostatic effect. By contrast, the percentage of cell death reached about 30 % in H28 cells treated with the simultaneous treatment of abemaciclib combined with cisplatin and pemetrexed. Exposure to abemaciclib caused senescence in MSTO-211H cells but not in H28 cells, showing a different impact according to the histological subtype or the molecular features of the cell lines. In MSTO-211H cells, the simultaneous treatment of abemaciclib combined with cisplatin and pemetrexed caused the higher percentage of senescent cells than abemaciclib alone and abemaciclib in association with cisplatin or pemetrexed. By contrast, in a previous *in vitro* study, palbociclib induced senescence in MSTO-211H, H28, and ZS-LP cells (Bonelli M. A. et al., Neoplasia, 2017). These findings suggested that abemaciclib and palbociclib had a different effect on the induction of senescence in MPM cell lines. In fact, abemaciclib caused the upregulation of the p53/p21 pathway, inducing senescence in MSTO-211H cells. The p53 transcription factor is involved in the regulation of many target genes playing a crucial role in cell cycle arrest, DNA repair mechanisms, senescence and apoptosis (Fischer M., 2017). p21, one of the many targets of p53, induces senescence by inhibiting many caspases involved in apoptosis (Mijit M. et al., 2020). In addition, abemaciclib alone and in combination with cisplatin, pemetrexed or the association of cisplatin and pemetrexed induced an accumulation of cyclin D1 in MSTO-211H cells. The increased expression of cyclin D1 indicated the arrest of the cell cycle in the G0 phase and could be considered a marker of induction of cellular senescence (Leontieva O. V. et al., 2013). In this study, abemaciclib, alone and in combination with cisplatin, pemetrexed or the association of cisplatin and pemetrexed induced large

cytoplasmic vacuoles in H28 cells. The activation of LC3B in H28 cells suggested that cell death could be autophagic, showing a cytotoxic effect of abemaciclib in this MPM cell line. Taken together these data suggested a different effect of abemaciclib according to the MPM histological subtype. Recently, *in vitro* and *in vivo* studies showed that abemaciclib induced a cytotoxic effect, associated with a multivacuolar phenotype, in Rb negative breast cancer cell lines, showing an off-target effect (Knudsen E. S. et al., 2017). Subsequently, another *in vitro* study showed that abemaciclib could act on V-ATPase, a proton pump that causes acidification of the intralysosomal compartment, resulting in a new possible molecular mechanism of cell death due to lysosome defects (Hino H. et al., 2020). Finally, we demonstrated that the inhibition of cell proliferation observed in MPM cells treated with the combined treatment was irreversible and was maintained even after drugs withdrawal. Differently, cells treated with chemotherapy alone reacquired proliferative capability after drugs removal.

Our findings demonstrated that CDK4/6 inhibitors might represent an attractive therapeutic approach for the treatment of MPM, however, since these drugs have mainly a cytostatic effect, the association with other drugs (target agents as PI3K/mTOR inhibitors or chemotherapy) seems critical to enhance their efficacy. In the last part of this research, we evaluated the efficacy of a dual target drug against both CDK4/6 and CDK9. CDK9 is considered a transcription regulator. In fact, P-TEFb, formed by the binding of CDK9 with Cyclin T1, interacts with RNA Polymerase II (RNAP II), regulating the expression of many genes (Zhou Q. et al., 2012; Bowman E. A. et al., 2014). VS2-370 has been recently developed by an Italian company and it is a small molecule that simultaneously inhibits CDK4/6

and CDK9. All the MPM cell lines analyzed were more sensitive to VS2-370 than to palbociclb and abemaciclib treatment, with about a tenfold decrease in IC_{50} values. The inhibition of cell proliferation was due to a strong downregulation of both the MAPK pathway (that was unaffected by CDK4/6 inhibitors treatment) and PI3K/AKT/mTOR pathway, in association with a decreased expression of proteins involved in the cell cycle regulation such as p-CDK6, pRb, and c-myc. The considerable inhibition on cell proliferation observed after VS2-370 treatment was associate with the induction of cell death, related to the downregulation of MCL-1 and the activation of caspase 3, in both MPM cell lines at the highest concentrations of VS2-370.

It is worth of note that the anti-apoptotic protein MCL-1, a member of the Bcl-2 family, is a target of CDK9 (Mandal R et al., 2021). An *in vivo* study showed that CDK9 inhibition caused a decrease of MCL-1 expression, highlighting antitumor activity in acute myeloid leukemia (Scholz A. et al., 2016). P-TEFb is also involved in the development of diffuse large B-cell lymphoma, whose most aggressive forms are characterized by overexpression of c-MYC (Rahl P. B. et al., 2010). In fact, many *in vitro* studies have shown that CDK9 inhibitors induced a decrease of MCL-1 and c-myc expression and promoted apoptosis in diffuse large B-cell lymphoma (Rowland T. et al., 2016; Hashiguchi T. et al., 2019). An ongoing study aimed to evaluate the safety and feasibility of a highly selective CDK9 inhibitor, called AZD4573, in patients with hematological malignancies (NCT03263637). Recently, some *in vitro* and *in vivo* studies have shown antitumor efficacy of CDK9 inhibitors for the treatment of colorectal cancer (Rahaman M. H. et al., 2019) and hepatocarcinoma (Borowczak J. et al., 2020).

The treatment of breast cancer with CDK4/6 inhibitors has highlighted the onset of resistance to this class of compounds and the need to find an alternative therapeutic approach. Recently, an *in vitro* study showed that MSTO-211H cells could develop resistance to palbociclib and that the combination of palbociclib with PI3K inhibitors was able to overcome this resistance, showing cytotoxic effects (Digiacomo G. et al., 2018).

Taken together, these data showed that VS2-370 exhibited antiproliferative effects in MPM cell lines. Moreover, as this molecule simultaneously inhibits CDK4/6 and CDK9, it might represent a possible therapeutic approach to overcome resistance to CDK4/6 inhibitors, due to its cytotoxic effects.

6.References

- Aliagas E., Alay A., Martínez-Iniesta M., Hernández-Madrigal M., Cordero D., Gausachs M., Pros E. et al. "*Efficay of CDK4/6 inhibitors in preclinical models of malignant pleural mesothelioma*". British Journal of Cancer 125:1365-1376, 2021.
- Álvarez-Fernández M. and Malumbres M. "*Mechanisms of sensitivity and resistance to CDK4/6 inhibition*". Cancer Cell, 37:514-529, 2020.
- Anders L., Ke N., Hydbring P., Choi Y. J., Widlund H. R., Chick J. M. et al. "*A systemic screen for CDK4/6 substrates links FOXM1 phosphorylation to senescence suppression in cancer cells*". Cancer Cell. 20:620-634, 2011.
- Annicotte J. S., Blanchet E., Chavey C., Iankova I., Costes S., Assou S. et al. *"The CDK4-pRB-E2F1 pathway controls insulin secretion".* Nat. Cell Biol. 11, 1017–1023, 2009.
- Anshabo A. T., Milne R., Wang S. and Albrecht H. "*CDK9: a comprehensive review of its biology and its role as a potential target for anti-cancer agents*". Front. Oncol. 11:678559, 2021.
- Attanoos R. L., Churg A., Galateau-Salle F., Gibbs A. R. and Roggli V. L. *"Malignant mesothelioma and its non-asbestos causes"*. Arch Pathol Lab Med, vol. 142, 2018.
- Baas P., Scherpereel A., Nowak A. K., Fujimoto N., Peters S., Tsao A. S., Mansfield A. S., Popat S. et al. "*First-line nivolumab plus ipilimumab in unresectable malignant pleural mesothelioma (CheckMate 743): a multicentre, randomised, open-label, phase 3 trial*". Lancet, 397, 375-386, 2021.
- Bacon C. W. and Iván D'Orso. "*CDK9: a signaling hub for transcriptional control*". TRANSCRIPTION, 10(2):57-75, 2019.
- Bakker W. J., Harris I. S. and Mak T. W. "*FOXO3a is activated in response to hypoxic stress and inhibits HIF1-induced apoptosis via regulation of CITED2*". Molecular Cell 28(6): 941-953, 2007.
- Baumann F., Ambrosi J. P. and Carbone M. *"Asbestos is not just asbestos: un unrecognised health hazard"*. Lancet Oncol, 14:576-578, 2013.
- Beasley M. B., Galateau-Salle F. and Dacic S. *"Pleural mesothelioma classification update"*. Virchows Archiv, 478:59-72, 2021.

- Bellan C., De Falco G., Lazzi S., Micheli P., Vicidomini S., Schurfeld K. et al. "*Cdk9/Cyclin T1 expression during normal lymphoid differentiation and malignant transformation*". J Pathol 203(4):946-52, 2004.
- Bergsagel D. J., Finegold M. J., Butel J. S. et al. "*DNA sequences similar to those of simian virus 40 in ependymomas and choroid plexus tumors of childhood*". N Engl J Med, 326:988-93, 1992.
- Bianchi M. E., Crippa M., Manfredi A. A., Mezzapelle R., Rovere Querini P. and Venereau E. "*High-mobility group box 1 protein orchestrates responses to tissue damage via inflammation, innate and adaptive immunity and tissue repair"*. Immunol Rev,280:74-82, 2017.
- Bianchi A. B., Mitsunaga S. I., Cheng J. Q., Klein W. M., Jhanwar S. C., Seizinger B., Kley N., Klein-Szanto A. J. and Testa J. R. "*High frequency of inactivating mutations in the neurofibromatosis type 2 gene (NF2) in primary malignant mesotheliomas*". Proc. Natl. Acad. Sci. USA 92, 10854–10858, 1995.
- Black E. P., Hallstrom T., Dressman H. K., West M. and Nevins J.R. "*Distinctions in the specificity of E2F function revealed by gene expression signatures*". Proc Natl Acad Sci U S A, 102(44):15948-53, 2005.
- Blagosklonny M. V. "*Geroconversion: irreversible step to cellular senescence*". Cell Cycle 13 (23):3628-3635, 2014.
- Bonelli M. A., Digiacomo G., Fumarola C., Alfieri R., Quaini F., Falco A., Madeddu D., La Monica S. et al. "*Combined inhibition of CDK4/6 and PI3K/AKT/mTOR pathways induces a synergistic anti-tumor effect in malignant pleural mesothelioma cells*". Neoplasia, 19(8):637-648, 2017.
- Bonelli M. A., Fumarola C., La Monica S. and Alfieri R. *"New therapeutic strategies for malignant pleural mesothelioma"*. Biochemical Pharmacology, 123:8-18, 2017.
- Bonelli M., La Monica S., Fumarola C. and Alfieri R. "*Multiple effects of CDK4/6 inhibition in cancer: from cell cycle arrest to immunomodulation"*. Biochemical Pharmacology 170, 113676, 2019.
- Bononi A., Giorgi C., Patergnani S., Larson D., Verbruggen K., Tanji M., Pellegrini L., Signorato V., Olivetto F., Pastorino F. et al. "*BAP1 regulates IP3R3-mediated Ca2+ flux to mitochondria suppressing cell transformation*". Nature, 546:549-553, 2017.

- Borowczak J., Szczerbowski K., Stec E., Grzanka D. and Szylberg L. "*CDK9: therapeutic perspective in HCC therapy*". Curr Cancer Drug Targets 20(5):318-324, 2020.
- Bouilliez A., Rajabi H., Jin C., Samur M., Tagde A., Alam M., Hiraki M. et al. "*MUC1-C integrates PD-L1 induction with repression of immune effectors in non-small cell lung cancer*". Oncogene, 36(28):4037-4046, 2017.
- Bowman E. A. and Kelly W. G. "*RNA polymerase II transcription elongation and Pol II CTD Ser2 phosphorylation: a tail of two kinases*". Nucleus 5:224-236, 2014.
- Brisard D., Eckerdt F., Marsh L. A., Blyth G. T., Jain S., Cristofanilli M. et al. "*Antineoplastic effects of selective CDK9 inhibition with atuveciclib on cancer stem-like cells in triple negative breast cancer*". Oncotarget, 9(99):37305-18, 2018.
- Broaddus V. C., Yang L., Scavo L. M., Ernst J. D., Boylan A. M. et al., *"Asbestos induces apoptosis of human and rabbit plural mesothelial cells via reactive oxygen species"*. J clin Invest, 98:2050-9,1996.
- Bruno C., Tumino R., Fazzo L., Cascone G., Cernigliaro A., De Santis M. et al. *"Incidence of pleural mesothelioma in a community exposed to fibres with fluoro-edenite composition in Biancavilla (Sicily, Italy)"*. Ann Ist Super Sanità, 50(2):111-8, 2014.
- Cakiroglu E. and Senturk S. "*Genomics and functional genomics of malignant pleural mesothelioma*". Int. J. Mol. Sci. 21,6342, 2020.
- Carbone M., Adsumilli P. S., Alexander R., Baas P., Bardelli F., Bononi A., Bueno R., Felly-Bosco E., Galateau-Salle F. et al. *"Mesothelioma: scientific clues for prevention, diagnosis and therapy".* CA Cancer J Clin, 69:402-429, 2019.
- Carbone M., Ferris L. K., Baumann F., Napolitano A., Lum C. A. et al. "*BAP1 cancer syndrome: malignant mesothelioma, uveal and cutaneous melanoma and MBAITs*". J Transl Med. 10:179, 2012.
- Carbone M., Gazdar A. and Butel J. S. *"SV40 and human mesothelioma"*. Transl Lung Cancer Res, 9 (Suppl 1): S47-S59, 2020.
- Carbone M., Harbour J. W., Brugarolas J., Bononi A., Pagano I. et al. "*Biological mechanisms and clinical significance of BAP1 mutations in human cancer*". Cancer Discov, 10(8): 1103-20, 2020.

- Carbone M., Pass H. I., Rizzo P. et al. "*Simian virus 40-like DNA sequences in human pleural mesothelioma*". Oncogene, 9:1781-90,1994.
- Carbone M., Rizzo P., Grimley P. M. et al. *"Simian virus-40 large-T antigen binds p53 in human mesotheliomas*". Nat Med, 3:908-12, 1997.
- Carbone M., Rizzo P., Procopio A. et al. "*SV-40 like sequences in human bone tumors*". Oncogene, 13:527-35,1996.
- Cassandri M., Fioravanti R., Pomella S., Valente S., Rotili D., Del Baldo G., De Angelis B., Rota R. and Mai A. "*CDK9 as a valuable target in cancer: from natural compounds inhibitors to current treatment in pediatric soft tissue sarcomas*". Front. Pharmacol. 11, 1230, 2020.
- Cerami E., Gao J., Dogrusoz U., Gross B. E., Aksoy B. A., Jacobsen A., Byrne C. J., Heuer M. L. et al. "*The cBio cancer genomics portal: an open platform for exploring multidimensional cancer genomics data"*. Cancer Discov. 2:401-404, 2012.
- Chen V. J., Bewley J. R., Gossett L. et al. *"Activity of LY231514 against several enzymes in the folate-dependent pathways"*. Proc Am Assoc Cancer Res, 37:381, 1996.
- Chen S., Gulla S., Cai C. and Balk S. P. "*Androgen receptor serine 81 phosphorylation mediates chromatin binding and transcriptional activation*". J Biol Chem 287(11):8571-83, 2012.
- Chen F. X., Smith E. R. and Shilatifard A. "*Born to run: control of transcription elongation by RNA polymerase II*". Nat. Rev. Mol. Cell Biol. 19:464-478, 2018.
- Choe N., Tanaka S., Xia W., Hemenway D. R., Roggli V. L. and Kagan E. *"Pleural macrophage recruitment and activation in asbestos-induced pleural injury"*. Environ Health Perspect, 105(Suppl 5):1257-60,1997.
- Cho B. C. J., Donahoe L., Bradbury P. A., Leighl N., Keshavjee S. et al. *"Surgery for malignant pleural mesothelioma after radiotherapy (SMART): final results from single-centre, phase 2 trial"*. Lancet Oncol, 22:190-197, 2021.
- Chong Q. Y., Hok Z. H., Bui N. L. C. Xiang X., Wong A. L. A. et al. "*A unique CDK4/6 inhibitor: current and future therapeutic strategies of abemaciclib*". Pharmacological Research 156, 104686, 2020.
- Cicala C., Pompetti F. and Carbone M. "*SV-40 induces mesotheliomas in hamsters*". Am J Pathol, 142:1524-33, 1993.

- Clark A. S., McAndrew N. P., Troxel A., Feldman M., Lal P., Rosen M., Burrel J. et al. *"Combination paclitaxel and palbociclib: results of a phase I trial in advanced breast cancer".* Clin. Cancer Res. 25, 2072-2079, 2019.
- Comba P., D'Angelo M., Fazzo L., Magnani C., Marinaccio A., Mirabelli D. and Terracini B. *"Mesothelioma in Italy: the Casale Monferrato model to a national epidemiological surveillance system".* Ann Ist Super Sanità, vol. 54, n° 2:139-148,2018.
- Comba P. and Fazzo L. (Eds) *"Mortalità per mesotelioma pleurico in Italia, 2003-2014"* Roma: Istituto Superiore di Sanità (Rapporti ISTISAN 17/37), 2017.
- Comba P., Gianfagna A. and Paoletti L. *"The pleural mesothelioma cases in Biancavilla are related to the new fluoro-edenite fibrous amphibole"*. Arch Environ Occup. Healt, 58:229-32, 2003.
- Cooper J., Xu Q., Zhou L., Pavlovic M., Ojeda V., Moulick K., de Stanchina E. et al. "*Combined inhibition of NEED8-activating enzyme and mTOR suppresses NF-2 loss-driven tumorigenesis*". Mol. Cancer Ther, 16, 1693-1704, 2017.
- Cornelissen R., Lievense L.A., Maat A. P., Hendriks R.W., Hoogsteden H. C. et al. "*Ratio of intratumoral macrophage phenotype is a prognostic factor in epithelioid malignant pleural mesothelioma*". PLos ONE 5;9(9):e106742, 2014.
- Cretella D., Fumarola C., Bonelli M., Alfieri R., La Monica S., Digiacomo G., Cavazzoni A., Galetti M., generali D. and Petronini P.G. "*Pre-treatment with the CDK4/6 inhibitor palbociclib improves the efficacy of paclitaxel in TNBC cells*". Scientific Reports, 10;9(1):13014, 2019.
- Cristofanilli M. Turner N. C., Bondarenko I., Ro J., Seock-Ah I., Masuda N. et al. "*Fulvestrant plus palbociclib versus fulvestrant plus placebo for treatment of hormone-receptor-positive, HER2R-negative metastatic breast cancer that progressed on previous endocrine therapy (PALOMA 3): final analysis of the multicentre, double blind, phase 3 randomised controlled tria*l". Lancet Oncol., 17:425-39, 2016.
- D'Agostin F., De Michieli P., Chermaz C. and Negro C. *"Pleural and peritoneal mesotheliomasin the Friuli Venezia Giulia register: data analysis from 1995 to 2015 in Northeastern Italy"*. J Thorac Dis, 9(4):1032-45, 2017.
- Dang C. V., Kim J. W., Gao P. and Yustein J. "*The interplay between MYC and HIF in cancer*". Nat Rev Cancer, 8:51-56, 2008.

- Dasari S. and Tchounwou P. B. *"Cisplatin in cancer therapy: molecular mechanisms of action"*. Eur J Pharmacol 0:364-378, 2014.
- Dean J. L., McClendon A. K., Hickey T. E., Butler L. M., Tilley W. D., Witkiewicz A. K. et al. "*Therapeutic response to CDK4/6 inhibition to breast cancer defined by ex vivo analyses of human tumors*". Cell Cycle, 11:2756-61, 2012.
- De Falco G., Bellan C., D'Amuri A., Angeloni G., Leucci E., Giordano A. et al. "*Cdk9 regulates neural differentiation and its expression correlates with the differentiation grade of neuroblastoma and PNET tumors*". Cancer Biol Ther 4(3):277-81, 2005.
- Delgermaa V., Takahashi K., Park E., Le G., Hara T. and Sorahan T. "*Global mesothelioma deaths reported to the World Health Organisation between 1994 and 2008". Bull World Health Organ.* 89:716–724, 2011.
- De Luca A., Baldi A., Esposito V. et al. *"The retinoblastoma gene family pRb/p105, p107, pRb2/p130 and simian virus-40 large-T antigen in human mesotheliomas".* Nat Med, 3:913-6, 1997.
- DeMichele A., Clare A. S., Tan K. S., Heitjan D. F., Gramlich K., Gallagher M. et al. "*CDK4/6 inhibitor palbociclib (PD0D332991) in Rb+ advanced breast cancer: phase II activity, safety and predictive biomarker assessment*". Clin Cancer Res., 21:995-1001, 2015.
- Denechaud P. D., Fajas L. and Giralt A. "*E2F1, a novel regulator of metabolism*". Front. Endocrinol. 8:311, 2017.
- Dickler M. N., Tolaney S. M., Rugo H. S., Cortes J., Dieras V. et al., "*1 MONARCH, a phase II study of abemaciclib, a CDK4 and CDK6 inhibitor, as a single agent, in patients with refractory HR (+)/HER2(-) metastatic brest cancer*." Clin. Cancer Res. 23, 5218-5224, 2017.
- Digiacomo G., Fumarola C., Cretella D., Alfieri R., La Monica S., Petronini P. G., Bonelli M. and Cavazzoni A. "*Overcoming palbociclib resistance by combined treatment with PI3K/AKT/mTOR inhibitors in mesothelioma cells*". J Mol Clin Med 1(3):151-156, 2018.
- Dostert C., Petrilli V., Van Bruggen R., Steele C., Mossman B. T. and Tschopp J. "*Innate immune activation throughNalp3 inflammosome sensing of asbestos and silica*". Science, 320(5876): 674-7, 2008.

- Edmunds J. W., Mahadevan L. C. and Clayton A. L. "*Dynamic histone H3 methylation during gene induction: HYPB/Setd2 mediates all H3K36 trimethylation*". EMBO J. 27, 406-420, 2008.
- Engels E. A., Sarkar C., Daniel R. W. et al. "Absense of simian virus 40 in human brain tumors from northern India". Int J Cancer, 101:348-52, 2002.
- Farley M. N., Schmidt L. S., Mester J. L., Pena-Llopis S., Pavia-Jimenez A., Christie A. et al. "*A novel germline mutation in BP1 predisposes to familial clear-cell renal cell carcinoma*". Mol Cancer Res, 11:1061-71, 2013.
- Fazzo L., Minelli G., De Santis M., Bruno C., Zona A., Conti S. and Comba P. *"Epidemiological surveillance of mesothelioma mortality in Italy".* Cancer Epidemiolog, 55:184-191, 2018.
- Fernandez de Mattos S., Lam E. V. and Tauler A. "*An E2F-binding site mediates the activation of the proliferative isoform of 6-phosphofructo-2-kinase/fructose-2,6-bisphosphate by phosphatidylinositol 3-kinase*". Biochem J. 368(Pt 1):283-91, 2002.
- Ferrante D., Bertolotti M., Todesco A., Mirabelli D., Terracini B. and Magnani C. *"Cancer mortality and incidence in a cohort of wives of asbestos workers in Casale Monferrato, Italy".* Environ Health Perspesct, 115 (10): 1401-5, 2007.
- Finn R. S., Crown J. P., Lang I., Boer K., Bondarenko I. M., Kulyk S. O. et al. "*The cyclin-dependent kinase 4/6 inhibitor palbociclib in combination with letrozole versus letrozole alone as first-line treatment of oestrogen receptor-positive, HER2R-negative, advanced breast cancer (PALOMA-1/TRIO-18): a randomised phase 2 study*". Lancet Oncol. 16:25-35, 2015.
- Finn R. S., Dering J. Conklin D., Kalous O., Cohen D. J. Desai A. J., Ginther C. et al. "*PD 0332991, a selective cyclin D kinase 4/6 inhibitor, preferentially inhibits proliferation of luminal estrogen receptor-positive human breast cancer lines in vitro*". Breast Cancer Res. 11:R77, 2009.
- Finn R. S., Martin M., Rugo H. S., Jones S., Im S. A., Gelmon K., Harbeck N., Lipatov O. N. et al. "*Palbociclib and letrozole in advanced breast cancer*". N Engl J Med, 375:1925-1936, 2016.
- Fischer M. "*Census and evaluation of p53 target genes*". Oncogene 36, 3943-3956, 2017.
- Franco L. C., Morales F., Boffo S. and Giordano A. "*CDK9: a key player in cancer and other diseases*". J Cell Biochem. 119:1273-1284, 2018.

- Franken N. A. P., Rodermond H. M., Stap J., Haveman J. and van Bree C. "*Clonogenic assay of cells in vitro*". 1(5):2315-9, 2006.
- Fry D. W., Harvey P. J., Keller P. R., Elliott W. L., Meade M., Trachet E., Albassam M. et al. "*Specific inhibition of cyclin-dependent kinase 4/6 by PD 0332991 and associated antitumor activity in human tumor xenografts*". Mol Cancer Ther. 3:1427-1438, 2004.
- Galateau-Salle F., Churg A., Roggli V., Travis W. D., on behalf of the World Health Organization Committee for Tumors of the Pleura. *"The 2015 World Health Organization classification of the tumors of the pleura: advances since the 2004 classification".* Journal of Thoracic Oncology, vol. 11 n°2:142-154, 2015.
- García-Reyes B., Kretz A. L., Ruff J.P., Von Karstedt S., Hillenbrand A., Knippschild U., Henne-Bruns D. and Lemke J. "*The emerging role of cyclin-dependent kinases (CDKs) in pancreatic ductal adenocarcinoma*". Int. J. Mol. Sci. 19, 3219, 2018.
- Gelbert L. M., Cai S., Lin X., Sanchez-Martinez C., Del Prado M., Lallena M. J. et al. "*Preclinical characterization of the CDK4/6 inhibitor LY2835219: in-vivo cell cycle-dependent/independent anti-tumor activities alone/in combination with gemcitabine*". Invest New Drugs, 32:825-837, 2014.
- Goel S., DeCristo M. J., McAllister S. S. and Zhao J. J. "*CDK4/6 inhibition in cancer: beyond cell cycle arrest*". Trends Cell Biol, 28(11):911-925, 2018.
- Goel S., DeCristo M. J., Watt A. C., BrinJones H., Sceneay J., Li B. B., Khan N. et al. "*CDK4/6 inhibition triggers anti-tumor immunity*". Nature. 548 (7668), 2017.
- Goldoni M. and Johansson C. "*A mathematical approach to study combined effects of toxicants in vitro: evaluation of the Bliss independence criterion and the Loewe additivity model*". Toxicol in Vitro, 21(5):759-69, 2007.
- Gordan J. D., Thompson C. B. and Simon M. C. "*HIF and c-Myc sibling rivals for control of cancer cell metabolism and proliferation*". Cancer cell, 12:108-113, 2007.
- Graña X., De Luca A., Sang N., Fu Y., Claudio P. P., Rosenblatt J., Morgan D. O. and Giordano A. "*PITALRE, a nuclear CDC"-related protein kinase that phosphorylates the retinoblastoma protein in vitro*". Proc. Natl. Acad. Sci. U. S. A. 91,3834-3838,1994.

- Grindey G. B., Shih C., Barnett C. J. et al. *"LY231514, a novel pyrrolopyrimidine antifolate that inhibits thymidylate synthase (TS)"*. Proc Am Assoc Cancer Res, 33:411, 1992.
- Gordon V., Bhadel S., Wunderlich W., Zhang J., Ficarrro S. B., Mollah S. A. et al. "*CDK9 regulates AR promoter selectivity and cell growth through serine 81 phosphorylation*". Mol Endocrinol 24(12):2267-80, 2010.
- Hafner M., Mills C. E., Subramanian C., Chen M., Chung S. A., Boswell R. A., Everley C. et al. "*Multiomics profiling establishes the polypharmacology of FDA-approved CDK4/6 inhibitors and the potential for differential clinical activity*". Cell Chem. Biol. 26:1067-1080, 2019.
- Hanahan D. and Weinberg R. A. "*Hallmarks of cancer: the next generation*". Cell, 144:646-674, 2011.
- Hashiguchi T., Bruss N., Best S., Lam V., Danilova O., Paiva C. J. et al. "*Cyclin-dependent kinase-9 is a therapeutic target in MYC-espressing diffuse large B-cell lymphoma*". Mol Cancer Ther 18(9):1520-32, 2019.
- Hayflick L. and Moorhead P.S. "*The serial cultivation of human diploid cell strains*". Exp Cell Res, 25:585-621, 1961.
- He S., Fang X., Xia X., Hou T. and Zhang T. "*Targeting CDK9: A novel biomarker in the treatment of endometrial cancer*". Oncol Rep 44(5):1929-1938, 2020.
- Herkert B. and Eilers M. "*Transcriptional repression: the dark side of myc*". Genes Cancer, 1:580-586, 2010.
- Herrera-Abreu M. T., Palafox M., Asghar U., Rivas M. A., Cutts R. J., Garcia-Murillas I. et al. "*Early adaption and acquired resistance to CDK4/6 inhibition in estrogen receptor-positive breast cancer*". Cancer Re. 76:2301-13, 2016.
- Hino H., Iriyama N., Kokuba H., Kazama H., Morya S. et al. "*Abemaciclib induces atypical cell death in cancer cells characterized by formation of cytoplasmic vacuoles derived from lysosomes*". Cancer Science 111:2132-2145, 2020.
- Hmeljak J., Sanchez-Vega F., HoadleyK. A., Shih J., Stewart C., Heiman D., Tarpey P., Danilova L. et al. "*Integrative molecular characterization of malignant pleural mesothelioma*". Cancer Discov. 8(12):1548-1565, 2018.

- Hylebos M., Van Camp G., van Meerbeeck J. P. and Op de Beeck K. "*The genetic landscape of malignant pleural mesothelioma: results from massively parallel sequencing*". J. Thorac. Oncol. 11, 1615-1626, 2016.
- Iankova I., Petersen R. K., Annicotte J. S., Chavey C., Hansen J. B., Kratchmarova I. et al. "*Peroxisome proliferator-activated receptor gamma recruits the positive transcrption elongation factor B complex to activate transcription and promote adipogenesis*". Mol Endocrinol 20(7):1494-505, 2006.
- Ishida S., Lee J., Thiele D. J. and Herskowitz I. *"Uptake of the anticancer drug cisplatin mediated by the copper transporter Ctr1 in yeast and mammals"*. Proc. Natl. Acad. Sci. U.S.A., 99:14298-14302, 2002.
- Jiménez L. A., Zanella C., Fung H., Janssen Y. M., Vacek P., Charland C. et al. "*Role of extracellular signal-regulated protein kinases in apoptosis by asbestos and H_2O_2*". Am J Physiol, 273:L1029-L1035, 1997.
- Jube S., Rivera Z. S., Bianchi M. E., Powers A., Wang E., Pagano I., Pass H. I. et al. "*Cancer cells secretion of the DAMP protein HMGB1 supports progression in malignant mesothelioma"*. Cancer Res, 72:3290-3301, 2012.
- Kaira K., Serizawa M., Koh Y., Takahashi T., Hanaoka H., Oriuchi N. et al. "*Relationship between 18F-FDG uptake on positron emission tomography and molecular biology in malignant pleural mesothelioma*". Eur. J. Cancer 48, 1244-1254, 2012.
- Kelland L. *"The resurgence of platinum-based cancer chemotherapy"*. Nat. Rev. Cancer, 7:573-584, 2007.
- Kim J. W., Gao P., Liu Y. C., Semenza G. L. and Dang C. V. "*Hypoxia-inducible factor 1 and dysregulated c-Myc cooperatively induce vascular endothelial growth factor and metabolic switches hexokinase 2 and pyruvate dehydrogenase kinase 1*". Mol. Cell Biol. 27, 7381-7393, 2007.
- Kindler H. L., Ismaila N., Armato III S. G., Bueno R., Hesdorffer M., Jahan T., Jones C. M. et al. *"Treatment of malignant pleural mesothelioma: American Society of Clinical Oncology Clinical Practice Guideline"*. J Clin Oncol, 36:1343-1373, 2018.
- Klein M. E., Kovatcheva M., Davis L. E., Tap W. D. and Koff A. "*CDK4/6 inhibitors: the mechanism of action may not be as simple as once thought*". Cancer Cell. 34(1):9-20, 2018.

- Knudsen E. S., Hutcheson J., Vail P. and Witkiewicz A. K. "*Biological specificity of CDK4/6 inhibitors: dose-response relationship, in vivo signaling, and composite response signature*". Oncotarget 8, 43678-43691, 2017.
- Kong Y., Yu J., Yan J., Gou Q., Chi Z., Tang B., Zheng B. et al. "*Genetic aberrations in the CDK4 pathway are associated with innate resistance to PD-1 blockade in Chinese patients with non-cutaneous melanoma*". Clin. Cancer Res., 2019.
- Kryukov G.V., Wilson F. H., Ruth J. R., Paulk J., Tsherniak A., Marlow S. E., Vazquez F. et al. *"MTAP deletion confers enhanced dependency on the arginine methyltransferase PRMT5 in human cancer cells"*. Science, 351(6278):1214-1218, 2016.
- Kuilman T. Michaloglou C., Mooi W. J. and Peeper D. S. "*The essence of senescence*". Genes Dev, 24:2463-2479, 2010.
- Laemmli U. K. "Cleavage of structural proteins during the assembly of the head of bacteriophage T4". Nature, 15;227(5259):680-5, 1970.
- Lagarrigue S., Lopez-Mejia I. C., Denechaud P. D., Escote X., Castillo-Armengol J., Jimenez V. et al. "*CDK4 is an essential insulin effector in adipocytes*". J. Clin. Invest. 126, 335–348, 2016.
- Lallemand D., Curto M., Saotome I., Giovannini M. and McClatchey A. I. "*NF2 deficiency promotes tumorigenesis and metastasis by destabilizing adherens junctions*". Genes Dev, 17:1090-1100, 2003.
- Lee Y., Dominy J. E., Choi Y. J., Jurczak M., Tolliday N., Camporez J. P. et al. "*Cyclin D1-Cdk4 controls glucose metabolism independently of cell cycle progression*". Nature 510, 547–551, 2014.
- Lee D. K., Duan H. O. and Chang C. "*Androgen receptor interacts with the positive elongation factor P-TEFb and enhances the efficiency of transcriptional elongation*". J Biol Chem 276(13):9978-84, 2001.
- Lee H. S., Lee S. A., Hur S. K., Seo J. W. and Kwon J. "*Stabilization and targeting of INO80 to replication forks by BAP1during normal DNA synthesis"*. Nat Commun 5:5128, 2014.
- Lee H. S., Seo H. R., Lee S. A., Choi S., Kang D. and Kwon J. "*BAP1 promotes stalled fork restart and cell survival via INO80 in response to replication stress*". Biochem J, 476:3053-66, 2019.

- Leontieva O. V. and Blagosklonny M. V. "*CDK4/6-inhibiting drug substitutes for p21 and p16 in senescence: duration of cell cycle arrest and MTOR activity determine geroconversion*". Cell Cycle 12: 3063-3069, 2013.
- Li J., Duns D., Westers H., Sijmons R., van den Berg A. and Kok K. "*SETD2: an epigenetic modifier with tumor suppressor functionality*". Oncotarget, 7(31):50719-50734, 2016.
- Lin C., Smith E. R., Takahashi H., Lai K. C., Martin-Brown S., Florens L. et al. "*AFF4, a component of the ELL/P-TEFb elongation complex and a shared subunit of MLL chimeras, can link transcription elongation to leukemia*". Mol Cell 37(3):429-37, 2010.
- Liu H. and Herrmann C. H. "*Differential localization and expression of the Cdk9 42k and 55k isoforms*". J Cell Physiol., 1:251-260, 2005.
- Liu T., Yu J., Deng M., Yin Y., Zhang H., Luo K., Qin B., Li Y., Wu C. et al. "*CDK4/6-dependent activation of DUB3 regulates cancer metastasis through SNAIL1*". Nat Commun 8, 13923, 2017.
- Lo Iacono M., Monica V., Righi L., Grosso F., Libener R., Vatrano S., Bironzo P., Novello S. et al. "*Targeted next-generation sequencing of cancer genes in advanced stage malignant pleural mesothelioma: a retrospective study*". J. Thorac. Oncol. 10,492-499, 2015.
- Lòpez-Rìos F. Illei P. B., Rush V. et al. "*Evidence against a role for SV40 infection in human mesotheliomas and high risk of false-positive PCR results owing to presence of SV40 sequences in common laboratory plasmids*". Lancet, 364:1157-66, 2004.
- Ma S., Meng Z., Chen R. and Guan K-L. "*The Hippo pathway: biology and pathophysiology*". Annu. Rev. Biochem., 88:577-604, 2019.
- Machida Y. J., Machida Y., Vashisht A. A., Wohlschlegel J. A. and Dutta A. "*The deubiquitinating enzyme BAP1 regulates cell growth via interaction with HCF-1*". J Biol Chem, 284:34179-88, 2009.
- Malumbres M. "*CDK4/6 inhibitors: what is the best cocktail?*". Clin. Cancer Res. 25, 6-8, 2019.
- Mandal R., Becker S. and Strebhardt K. "*Targeting CDK9 for anti-cancer therapeutics*". Cancers 13,2181, 2021.

- Marconi A., Cecchetti G. and Barbieri M. “Airborne mineral fibre concentrations in an urban area near an asbestos-cement plant”. International Agency for Research on Cancer (AIRC) Scientific Pubblications, 90: 336-46, 1989.
- Marques M., Tranchant R., Risa-Ebri B., Suarez-Solis M. L., Fernandez L. C., Carrillo-de-Santa-Pau E. et al. “*Combined MEK and PI3K/p110beta inhibition as a novel targeted therapy for malignant mesothelioma displaying sarcomatoid features*”. Cancer Res. 80, 843-856, 2020.
- Marsili D., Angelini A., Bruno C., Corfiati M., Marinaccio A., Silvestri S. et al. *“Asbestos ban in Italy: a major milestone, not the final cut”.* Int j Environ Res Public Health, 14(11), 2017.
- McCartney A., Migliaccio I., Bonechi M., Biagioni C., Romagnoli D., De Luca F. et al. “*Mechanisms of resistance to CDK4/6 inhibitors: potential implications and biomarkers for clinical practice*”. Front. Oncol. 9:666, 2019.
- Meyer N. and Penn L. Z. “*Reflecting on 25 years with MYC*”. Nat Rev Cancer 8:976-990, 2008.
- Michels A. A., Fraldi A., Li Q., Adamson T. E., Bonnet F., Nguyen V. T. et al. “*Binding of the 7SK snRNA turns the HEXIM1 protein into P-TEFb(CDK9/Cyclin T) inhibitor*”. EMBO J 23(13):2608-19, 2004.
- Mijit M., Caracciolo V., Melillo A., Amicarelli F. and Giordano A. “*Role of p53 in the regulation of cellular senescence*”. Biomolecules, 10, 420, 2020.
- Morita M., Gravel S. P., Hulea L., Larsson O., Pollak M., St-Pierre J. and Topisirovic I. “*mTOR coordinates protein synthesis, mitochondrial activity and proliferation*”. Cell Cycle 14, 473-480, 2015.
- Morrish F. and Hockenbery D. “*MYC and mitochondrial biogenesis*”. Cold Spring Harb. Perspect Med. 4, a014225, 2014.
- Napolitano A., Pellegrini L., Dey A., Larson D., Tanji M., Flores E. G. et al. “*Minimal asbestos exposure in germline BAP1 heterozygous mice is associated with deregulated inflammatory response and increased risk of mesothelioma*”. Oncogene, 35:1996-2002, 2016.
- Nasu M., Emi M., Pastorino S., Tanji M., Powers A., Luk H. et al. “*High incidence of somatic BAP1 alterations in sporadic malignant mesothelioma*”. J Thorac Oncol, 10:565-76, 2015.
- Nicholson A. G., Sauter J. L., Nowak A. K., Kindler H. L., Gill R. R., Remy-Jardin M., Armato III S. G., Cuesta-Fernandez L., et al. *“EURACAN/IASLC proposals*

for updating the histologic classification of pleural mesothelioma: towards a more multidisciplinary approach". Journal of Thoracic Oncology, vol. 15 n°1:29-49, 2020.

- Oddone E., Bollon J., Nava C. R., Bugani M., Consonni D., Marinaccio A., Magnani C. and Barone-Adesi F. *"Predictions of mortality from pleural mesothelioma in Italy after the ban of asbestos use"*. Int. J. Environ. Res. Public Health, 17, 607, 2020.
- Odisio E. G., Marom E. M., Shroff G. S., Wu C. C., Benveniste A. A.P., Truong M. T. and Benveniste M. F. "Malignant pleural mesothelioma: diagnosis, staging, pitfalls and follow-up". Semin Ultrasound CT MRI38:559-57 Elsevier Inc, 2017.
- Okada T., Lopez-Lago M. and Giancotti F. G. "*Merlin/NF-2 mediates contact inhibition of growth by suppressing recruitment of Rac to the plasma membrane*". J Cell Biol, 171:361-371, 2005.
- O'Leary B., Cutts R. J., Liu Y., Hrebien S., Huang X., Fenwick K. et al. "*The genetic landscape and clonal evolution of breast cancer resistance to palbociclib plus fulvestrant in the PALOMA-3 trial*". Cancer Discover. 8:1390-403, 2019.
- Osthus R. C., Shim H., Kim S., Li Q., Reddy R., Mukherjee M., Xu Y. et al. "*Deregulation of glucose transporter 1 and glycolytic gene expression by c-Myc*". The Journal of biological chemistry, 275:21797-21800, 2000.
- Panou V. and Røe O. D. *"Inherited genetic mutations and polymorphisms in malignant mesothelioma: a comprehensive review*". Int J Mol Sci 17;21(12):4327, 2020.
- Park Jae Hyung, Woo Yang Pyun and Hyun Woo Park. "*Cancer metabolism: phenotype, signaling and therapeutic targets*". Cells, 9, 2308, 2020.
- Pastorino S., Yoshikawa Y., Pass H. I. et al. "*A subset of mesotheliomas with improved survival occurring in carriers of BAP1 and other germline mutations*". J Clin Oncol, 36:3485-94, 2018.
- Patnaik A., Rosen L. S., Tolaney S. M., Tolcher A. W., Goldman J. W. et al. "*Efficacy and safety of abemaciclib, an inhibitor of CDK4 and CDK6, for patients with breast cancer, non-small cell lung cancer, and other solid tumors*". Cancer Discov. 6, 740-753, 2016.

- Pećina-Šlaus N. "*Merlin, the NF2 gene product*". Pathol. Oncol. Res., 19:365-373, 2013.
- Portugal J. and Waring M. J. "*Assignment of DNA binding sites for 4',6-diamidine-2-phenylindole and bisbenzimide (Hoechst 33258). A comparative footprinting study*". Biochim Biophys Acta, 949(2):158-68, 1988.
- Rahaman M. H., Lam F., Zhong L., Teo T., Adams J., Yu M., Milne R.W., Pepper C. et al. "*Targeting CDK9 for treatment of colorectal cancer*". Mol Oncol 13(10):2178-2193, 2019.
- Rahl P. B., Lin C. Y., Seila A. C., Flynn R. A., McCuine S., Burge C. B. et al. "*c-Myc regulates transcriptional pause release*". Cell 141(3):432-45, 2010.
- Ramakrishnan R., Yu W. and Rice A. P. "*Limited redundancy in genes regulated by Cyclin T2 and Cyclin T1*". BMC Res. Notes 4,260, 2011.
- Rea F., Marulli G., Bortolotti L., Breda C., Favaretto A. G. et al. *"Induction chemotherapy, extrapleural pneumonectomy (EPP) and adjuvant hemi-thoracic radiation in malignant pleural mesothelioma (MPM): feasibility and results"*. Lung Cancer, 57:89-95, 2007.
- Rodier F. and Campisi J. "*Four faces of cellular senescence*". J Cell Biol, 192:547-556, 2011.
- Romeo E., Ascoli V., Ancona L., Balestri A., Scalzo C. C., Cavariani F. et al. *"Occupational exposure to asbestosand incidence of malignant mesothelioma in the Lazio region, years 2001-2009: results of the activities of the regional register"*. Med Lav, 104(2):115-25, 2013.
- Rosenberg B., Vancamp L. and Krigas T. *"Inhibition of cell division in Escherichia Coli by electrolysis products from a platinum electrode"*. Nature, 205:698-699, 1965.
- Roskoski R. Jr. "*Cyclin-dependent protein serine/threonine kinase inhibitors as anticancer drugs*". Pharmacological Research. 139:471-488, 2019.
- Roushdy-Hammady I., Siegel J., Emri S., Testa J. R. and Carbone M. "*Genetic-susceptibility factor and malignant mesothelioma in the Cappadocian region of Turkey*". Lancet, 357:444-5, 2001.
- Rowland T., Paiva C., Rowley J., Chen A., Drew L., Hurlin P. et al. "*Selective targeting cyclin-dependent kinase-9 (Cdk9) downmodulates c-MYC and induces apoptosis in diffuse large B-cell Lymphoma (Dlbcl)*". Cells. Blood. 128 (22):289, 2016.

- Ruas M. and Peters G. "*The p16INK4a/CDKN2A tumor suppressor and its relatives*". Biochim Biophys Acta 1378, F115-F177, 1998.
- Ruhland M. K., Loza A. J., Capietto A. H., Luo X., Knolhoff B. L., Flanagan K. C., Belt B. A. et al. "*Stromal senescence establishes an immunosuppressive microenvironment that drives tumorigenesis*". Nat Commun, 7:11762, 2016.
- Ruttledge M. H., Sarrazin J., Rangaratnam S., Phelan C. M., Twist E., Merel P., Delattre O. et al. "*Evidence for the complete inactivation of the NF2 gene in the majority of sporadic meningiomas*". Nat. Genet. 6, 180–184, 1994.
- Salvador-Barbero B., Álvarez-Fernández M., Zapatero-Solana E., El Bakkali A., Ménendez M. C., López-Casas P. P. et al. "*CDK4/6 inhibitors impair recovery from cytotoxic chemotherapy in pancreatic adenocarcinoma*". Cancer Cell 37, 340-353, 2020.
- Sato T. and Sekido Y. "*NF2/Merlin inactivation and potential therapeutic targets in mesothelioma*". Int. J. Mol. Sci., 19,988, 2018.
- Sawai C. M., Freund J., Oh P., Ndiaye-Lobry D., Bretz J. C., Strikoudis A. et al. "*Therapeutic targeting of the cyclin D3-CDK4/6 complex in T cell leukemia*". Cancer Cell, 22:452-465, 2012.
- Scagliotti G. V., Gaafar R., Nowak A. K., Nakano T., van Meerbeeck J., Popat S., Vogelzang N. J., Grosso F. et al. "*Nintendanib in combination with pemetrexed and cisplatin for chemotherapy-naive patients with advanced malignant pleural mesothelioma (LUME-Meso): a double-blind, randomised, placebo-controlled phase 3 trial*". Lancet Respir Med, 7:569-80, 2019.
- Scholz A., Oellerich T., Hussain A., Lindner S., Luecking U., Walter A. O. et al. "*BAY 1143572, a first-in-class, highly selective, potent and orally available inhibitor of PTEFb/CDK9 currently in phase I shows convincing anti-tumor activity in preclinical models of acute myeloid leukemia (AML)*". Cancer Res 76: abstract 3022, 2016.
- Sekido Y. *"Molecular pathogenesis of malignant mesothelioma*". Carcinogenesis, 34(7):1413-1419, 2013.
- Sekido Y., Pass H. I., Bader S., Mew D. J., Christman M. F., Gazdar A. F. and Minna J. D. "*Neurofibromatosis type 2 (NF2) gene is somatically mutated in mesothelioma but not in lung cancer*". Cancer Res. 55, 1227–1231, 1995.
- Semenza G. L. "*Regulation of oxygen homeostasis by hypoxia-inducicble factor 1*". Physiology (Bethesda), 24:97-106, 2009.

- Semenza G. L. "*Defining the role of hypoxia-inducicble factor 1 in cancer biology and therapeutics*". Oncogene 29:625-634, 2010.
- Shih C., Gossett L., Gate S. et al. *"LY231514 and its polyglutamates exhibit potent inhibition against both human dihydrofolate reductase (DHFR) and thymidylate synthase (TS): multiple folate enzymes inhibition"*. NCI EORTC Symp New Drugs Cancer Ther, 289a, 1996.
- Shintani T. and Klionsky D. J. "*Autophagy in health and diseases: a double-edged sword*". Science 306(5698):990-5, 2004.
- Shore S. M., Byers S. A., Maury W. and Price D. H. "*Identification of a novel isoform of cdk9*". Gene, 307:175-182, 2003.
- Sikora E., Bielak-Zmijewska A. and Mosieniak G. "*Targeting normal and cancer senescent cells as a strategy of senotherapy*". Ageing Res Rev 55:100941, 2019.
- Sneddon S., Dick I., Lee Y. C. G., Bill Musk A. V., Patch A. M., Pearson J. V., Waddell N., Allcock R. J. N. et al. "*Malignant cells from pleural fluids in malignant mesothelioma patients reveal novel mutations*". Lung Cancer, 119,64-70, 2018.
- Soffritti M., Minardi F., Bua L., Degli Esposti D. and Belpoggi F. *"First experimental evidence of peritoneal and pleural mesotheliomas induced by fluoro-edenite fibres present in Etnean volcanic material from Biancavilla (Sicily, Italy)"*. Eur J Oncol, 9(3): 169-175, 2004.
- Stahel R. A., Riesterer O., Xyrafas A., Opitz I., Beyeler M., Ochsenbein A. et al. *"Neoadjuvant chemotherapy and extrapleural pneumonectomy of malignant pleural mesothelioma with or without hemithoracic radiotherapy (SAKK 17/04): a randomised, international, multicentre phase II trial"*. Lancet Oncol, 16:1651-58, 2015.
- Stamenkovic I. and Yu Q. "*Merlin, a "magic" linker between extracellular cues and intracellular signaling pathways that regulate cell motility, proliferation and survival*". Curr. Protein Pept. Sci, 11:471-484, 2010.
- Stemmer-Rachamimov A. O., Xu L., Gonzalez-Agosti C., Burwick J.A., Pinney D. et al. "*Universal absence of merlin, but not other ERM family members, in schwannomas*". Am. J. Pathol. 151, 1649–1654, 1997.
- Strepkos D., Markouli M., Klonou A., Papavassiliou A. G. and Piperi C. "*Histone methyltransferase SETDB1: a common denominator of tumorigenesis with therapeutic potential*". Cancer Res. 1;81(3): 525-534, 2021.

- Tarangelo A., Lo N., Teng R., Kim E., Le L., Watson D. et al. "*Recruitment of Pontin/Reptin by E2f1 transcriptional response during cancer progression*". Nat Commun 6:10028, 2015.
- Tarrado-Castellarnau M., de Atauri P. and Cascante M. "*Oncogenic regulation of tumor metabolic reprogramming*". Oncotarget, 38:62726-62753, 2016.
- Tas J. and Westerneng G. "*Fundamental aspects of the interaction of propidium diiodide with nuclei acids studied in a model system of polyacrylamide films*". 29(8):929-36, 1981.
- Taylor E. C. and Patel H. H. *"Synthesis of pyrazolo(3,4,-d)pyrimidine analogues of the potent antitumor agent n-{4-(2-(2-amino-4(3h)- oxo-7h-pyrrolo(2,3-d)pyrimidin-5-yl)ethyl)benzoyl}-l-glutamic acid (LY231514)"*. Tetrahedron Lett, 48:8089-8100,1992.
- Tchakarska G., Roussel M., Troussard X. and Sola B. "*Cyclin D1 inhibits mitochondrial activity in B cells*". Cancer Res 71 (5):1690-1699, 2011.
- Teo Z. L., Versaci S., Dushyanthen S., Carami F., Savas P., Mintoff C. P. et al. "*Combined CDK4/6 and PI3Kalpha inhibition is synergistic and immunogenic in triple-negative breast cancer*". Cancer Res 77 (22):6340-6352, 2017.
- Torres-Guzman R., Calsina B., Hermoso A., Baquero C., Alvarez B., Amat J. Et al. "*Preclinical characterization of abemaciclib in hormone receptor positive breast cancer*", Oncotarget 8(41): 69493-69507, 2017.
- Tranchant R., Quetel L., Tallet A., Meiller C., Renier A., de Koning L., de Reynies A., Le-Pimpec-Barthes F. et al. "*C0-occurring mutations of tumor suppressor genes, LATS2 and NF2, in malignant pleural mesothelioma"*. Clin. Cancer Res., 23,3191-3202, 2017.
- Treasure T., Lang-Lazdunski L., Waller D., Bliss J. M., Entwisle J. et al. *"Extra-pleural pneumonectomy versus no extra-pleural pneumonectomy for patients with malignant pleural mesothelioma: clinical outcomes of the Mesothelioma and Radical Surgery (MARS) randomised feasibility study"*. Lancet Oncol, 12:763-72, 2011.
- Tripathy D., Bardia A. and Sellers W. R. "*Ribociclib (LEE011): mechanism of action and clinical impact of this selective cyclin-dependent kinase 4/6 inhibitor in various solid tumors*". Clin Cancer Res. 23:3251-3262, 2017.

- Urso L., Cavallari I., Sharova E., Ciccarese F., Pasello G. and Ciminale V. "*Metabolic rewiring and redox alterations in malignant pleural mesothelioma*". Br. J. Cancer 122:52-61, 2020.
- Valenzuela C. A., Vargas L. Martinez V., Bravo S. and Brown E. N. "*Palbociclib-induced autophagy and senescence in gastric cancer cells*". Exp Cell Res 360 (2), 390-396, 2017.
- van Brummelen E. M. J., Levchenko E., Dómine M., Fennel D. A., Kindler H. L., Viteri S., Gadgeel S. et al. "*A phase Ib study of GSK3052230, an FGF ligand trap in combination with pemetrexed and cisplatin in patients with malignant pleural mesothelioma*". Invest. New Drugs, 38(2):457-467, 2020.
- Vander-Heiden M. G. and DeBerardinis R. J. "*Understanding the intersections between metabolism and cancer biology*". Cell, 09, 168(4):657-669, 2017.
- Vidula N. and Rugo H. S. "*Cyclin-dependent kinase 4/6 inhibitors for the treatment of breast cancer: a review of preclinical and clinical data*". Clin. Breast Cancer 16, 8-17, 2016.
- Vimercati L., Cavone D., Caputi A., Delfino M. C., De Maria L., Ferri G. M. and Serio G. *"Malignant mesothelioma in construction workers: the Apulia regional mesothelioma register, Southern Italy"*. BMC Res Notes, 12:636, 2019.
- Vogelzang N. J., Rusthoven J., Symanowski C., Denham E., Kaukel P., Ruffie U., Gatzemeier M. et al. "*Phase III sttudy of pemetrexed in combination with cisplatin versus cisplatin alone in patients with malignant pleural mesothelioma*". J. Clin. Oncol. 21(14):2636-2644, 2003.
- Wang Z., Fan M., Candas D., Zhang T. Q., Qin L., Eldridge A. et al. "*Cyclin B1/Cdk1 coordinates mitochondrial respiration for cell-cycle G2/M progression*". Dev. Cell 29, 217–232, 2014.
- Wang L. Y., Hung C. L., Chen Y. R., Yang J. C., Wang J., Campbell M. et al. "*KDMA4 coactivates E2F1 to regulate the PDK-dependent metabolic switch between mitochondrial oxidation and glycolysis*". Cell Rep 16(11): 3016-27, 2016.
- Wang C., Li Z., Lu Y., Du R., Katiyar S., Yang J., Fu M., Leader J. E. et al. "*Cyclin D1 repression of nuclear respiratory factor 1 integrates nuclear DNA synthesis and mitochondrial function*". Proc. Natl. Acad. Sci U.S.A. 103 (31), 2006.

- Wang H. Nicolay B. N., Chick J. M., Gao X., Geng Y., Ren H., Gao H. et al. "*The metabolic fuction of cyclin D3-CDK6 kinase in cancer cell survival*". Nature, 546:426-430, 2017.
- Warburg O., Wind F. and Negelein E. "*The metabolism of tumor in the body*". J. Gen Physiol. 8,519-530, 1927.
- Witkiewicz A. K. and Knudsen E. S. "*Retinoblastoma tumor suppressor pathway in breast cancer: prognosis, precision medicine and therapeutic interventions*". Breast Cancer Res, 16:207, 2014.
- Wood D.J. & Endicott J. A. "*Structural insights into the functional diversity of the CDK–cyclin family*". Open Biol. 8, 2018.
- Xu A., Huang X., Lien Y. C., Bao L., Yu Z. and Hei T. K. "*Genotoxic mechanisms of asbestos fibers: role of extranuclear targets.*" Chem Res Toxicol, 20(5):724-33, 2007.
- Xue J., Patergnani S., Giorgi C., Suarez J., Goto K., Bononi A., Tanji M., Novelli F., Pastorino S. et al. *"Asbestos induces mesothelial cell transformation via HMGB1-driven autophagy"*. Proc Natl Acad Sci USA, 117(41):25543-25552, 2020.
- Xue W., Zender L., Miething C., Dickins R. A., Hernando E., Krizhanovsky V. et al. "*Senescence and tumor clearance is triggered by p53 restoration in murine liver carcinomas*". Nature, 445:656-660, 2007.
- Xu J., Kadariya Y., Cheung M., Pei J., Talarchek J. et al. "*Germline mutation of Bap1 accelerates development of asbestos-induced malignant mesothelioma*". Cancer Res, 74:4388-97, 2014.
- Yang H., Bocchetta M., Kroczynska B., Elmishad A.G., Chen Y., Liu Z. et al. *"TNF-alpha inhibits asbestos—induced cytotoxicity via a NF-kappaB-dependent pathway, a possible mechanism for asbestos-induced oncogenesis*". Proc Natl Acad Sci USA, 103(27):10397-402, 2006.
- Yang H., Rivera Z., Jube S., Nasu M., Bertino P., Goparaju C. et al. *"Programmed necrosis induced by asbestos in human mesothelial cells causes high-mobility group box 1 protein release and resultant inflammation"*. Proc Natl Acad sci USA, 107(28):12611-6, 2010.
- Yap T. A., Aerts J. G., Popat S. and Fennel D. A. *"Novel insights into mesothelioma biology and implications for therapy"*. Nature Reviews Cancer, vol 17: 475-488, 2017.

- Yu H., Mashtalir N., Daou S., Hammond-Martel I., Ross J. Sui G. et al. "*The ubiquitin carboxyl hydrolase BAP1 forms a ternary complex with YY1 and HCF-1 and is a critical regulator of gene expression"*. Mol Cell Biol, 30:5071-85, 2010.
- Yu H., Pak H., Hammond-Martel I., Ghram M., Rodrigue A., Daou S. et al. "*Tumor suppressor and deubiquitinase BAP1 promotes DNA double-strand break repair*". Proc Natl Acad Sci USA, 111:285-90, 2014.
- Zhang J., Bu X., Wang H., Zhu Y., Geng Y., Nihira N. T., Tan Y., Ci Y., Wu F. et al. "*Cyclin D-CDK4 kinase destabilizes PD-L1 via cullin 3-SPOP to control cancer immune surveillance*". Nature, 553:91-95, 2018.
- Zhang Y., Shi J., Liu X., Feng L., Gong Z., Koppula P. et al. "*BAP1 links metabolic regulation of ferroptosis to tumor suppression*". Nat Cell Biol, 20:1181-92, 2018.
- Zhang J., Xu K., Liu P., Geng Y., Wang B., Gan W., Guo J., Wu F. et al. *"Inhibition of Rb phosphorylation leads to mTORC2-mediated activation of Akt",* Molecular Cell 62: 929-942, 2016.
- Zhang J., Zhou L., Zhao S., Dicker D. T. and El-Deiry W. S. "*The CDK4/6 inhibitor palbociclib synergizes with irinotecan to promote colorectal cancer cell death under hypoxia*". Cell Cycle 16, 1193-1200, 2017.
- Zhou Q., Li T. and Price D. H. "*RNA Polymerase II elongation control*". Annu. Rev. Biochem. 81:119-143, 2012.
- Zotti T., Scudiero I., Vito P. and Stilo R. "*The emerging role of TRAF7 in tumor development*". J. Cell. Physiol. 232:1233-1238, 2017.

Ringraziamenti

A conclusione di questo elaborato, vorrei ringraziare tutte le persone che hanno contribuito alla realizzazione del mio percorso di dottorato.

Un ringraziamento speciale va al Professor Pier Giorgio Petronini e alla Professoressa Roberta Alfieri per avermi dato l'opportunità di svolgere il mio percorso di dottorato presso il Laboratorio di Oncologia Sperimentale del Dipartimento di Medicina e Chirurgia dell'Università di Parma. Ci tengo a ringraziare di cuore la professoressa Mara Bonelli per il suo impegno e per la sua disponibilità. Ringrazio inoltre il professor Andrea Cavazzoni, la dottoressa Silvia La Monica, la dottoressa Claudia Fumarola, la dottoressa Maricla Galetti, il dottor Daniele Cretella, la dottoressa Graziana Digiacomo e il dottor Francesco Volta per i loro insegnamenti e i loro consigli. Infine, ringrazio la dottoressa Silvia Zoppi e il dottor Kamal Eltayeb per il loro prezioso sostegno.

Vorrei dedicare qualche riga anche alla mia famiglia per ringraziarla di cuore della fiducia che mi ha sempre dimostrato. Ringrazio mio padre Maurizio per avemi insegnato a mettere passione nel proprio lavoro, mia madre Stefania e mio fratello Stefano per aver sempre appoggiato le mie scelte. Vorrei ringraziare anche mia nonna Romana per avermi sempre spronato a proseguire il mio percorso. Ringrazio Alessandro per aver condiviso con me un pezzo di vita. Infine ringrazio mio nipote Lorenzo per averci reso la vita più bella.